ดุลน้ำบาดาลและปริมาณการใช้ที่ปลอดภัยของชั้นหินให้น้ำโคราชตอนกลาง ในลุ่มน้ำสาขาแควหนุมาน จังหวัดปราจีนบุรี

นายณรงค์ศักดิ์ แก้วดำ

วิทยานิพนธ์นี้เป็นส่วนหนึ่งของการศึกษาตามหลักสูตรปริญญาวิทยาศาสตรมหาบัณฑิต
สาขาวิชาธรณีวิทยา ภาควิชาธรณีวิทยา
คณะวิทยาศาสตร์ จุฬาลงกรณ์มหาวิทยาลัย
ปีการศึกษา 2559

GROUNDWATER BALANCE AND SAFE YIELD OF MIDDLE KHORAT AQUIFER IN THE KHWAE HANUMAN SUB-BASIN, CHANGWAT PRACHINBURI

Mr. Narongsak Kaewdum

A Thesis Submitted in Partial Fulfillment of the Requirements
for the Degree of Master of Science Program in Geology
Department of Geology
Faculty of Science
Chulalongkorn University
Academic Year 2016

Thesis Title	GROUNDWATER BALANCE AND SAFE YIELD OF MIDDLE KHORAT AQUIFER IN THE KHWAE HANUMAN SUB-BASIN, CHANGWAT PRACHINBURI
By	Mr. Narongsak Kaewdum
Field of Study	Geology
Thesis Advisor	Associate Professor Srilert Chotpantarat, Ph.D.

Accepted by the Faculty of Science, Chulalongkorn University in Partial Fulfillment of the Requirements for the Master's Degree

.....Dean of the Faculty of Science
(Associate Professor Polkit Sangvanich, Ph.D.)

THESIS COMMITTEE

.....Chairman
(Professor Montri Choowong, Ph.D.)

.....Thesis Advisor
(Associate Professor Srilert Chotpantarat, Ph.D.)

.....Examiner
(Assistant Professor Thanop Thitimakorn, Ph.D.)

.....External Examiner
(Tussanee Nettasana, Ph.D.)

ณรงค์ศักดิ์ แก้วดำ : ดุลน้ำบาดาลและปริมาณการใช้ที่ปลอดภัยของชั้นหินให้น้ำโคราชตอนกลางในลุ่มน้ำสาขาแควหนุมาน จังหวัดปราจีนบุรี (GROUNDWATER BALANCE AND SAFE YIELD OF MIDDLE KHORAT AQUIFER IN THE KHWAE HANUMAN SUB-BASIN, CHANGWAT PRACHINBURI) อ.ที่ปรึกษาวิทยานิพนธ์หลัก: รศ. ดร.ศรีเลิศ โชติพันธรัตน์, 144 หน้า.

ลุ่มน้ำย่อยแควหนุมานตอนล่างครอบคลุมอำเภอนาดีและอำเภอกบินทร์บุรี จังหวัดปราจีนบุรี มีพื้นที่ทั้งหมด 900 ตารางกิโลเมตร โดยปัจจุบันมีการพัฒนาน้ำบาดาลจากชั้นน้ำมาใช้เพื่อกิจกรรมต่างๆ โดยเฉพาะในพื้นที่เกษตรกรรมและนิคมอุตสาหกรรม ซึ่งในอนาคตพื้นที่นี้จะมีความต้องการใช้น้ำบาดาลเพิ่มขึ้นร้อยละ 2 ต่อปี ซึ่งหากมีการสูบใช้ในปริมาณมากอาจทำให้ระดับน้ำบาดาลลดลงจนเสียสมดุลน้ำได้ ดังนั้นจึงควรศึกษาและประเมินศักยภาพการเติมน้ำ สมดุลน้ำบาดาลและปริมาณการใช้น้ำปลอดภัยในพื้นที่ โดยมีวัตถุประสงค์ของการศึกษาเพื่อประเมินศักยภาพการเติมน้ำลงสู่ชั้นน้ำบาดาล สมดุลน้ำและปริมาณการใช้น้ำที่ปลอดภัยของชั้นน้ำชุดหินโคราชตอนกลางในบริเวณลุ่มน้ำแควหนุมานส่วนล่าง โดยคำนวณศักยภาพการเติมน้ำด้วยวิธีการซ้อนทับข้อมูลที่เกี่ยวข้องกับการเติมน้ำ ได้แก่ ลักษณะธรณีวิทยา ชนิดดิน การใช้ที่ดิน ความลาดชันของพื้นที่ ความหนาแน่นของทางน้ำและรอยแตก แล้วคูณด้วยปริมาณน้ำฝนเฉลี่ย 30 ปี ด้วยซอฟแวร์ Arc GIS จากการออกภาคสนามพบว่า ชั้นให้น้ำบาดาลในพื้นที่แบ่งได้ 2 ชั้นคือ ชั้นให้น้ำตะกอนร่วนยุคควอเทอร์นารีและชั้นหินให้น้ำโคราชตอนกลาง มีระดับน้ำบาดาลอยู่ที่ระดับ -37 ถึง 35 เมตรเหนือระดับน้ำทะเลปานกลางและทิศทางการไหลของน้ำบาดาลไหลจากทิศเหนือลงสู่ทิศใต้ ศักยภาพการเติมน้ำบาดาลสูง (2.3%) พบบริเวณตอนกลางของพื้นที่ศึกษา โดยมีปริมาณน้ำฝนที่ซึมลงชั้นน้ำบาดาลประมาณ 12.8 % ของปริมาณฝนเฉลี่ย 30 ปี ผลการประเมินสมดุลน้ำบาดาลรายฤดูกาลพบว่าสมดุลน้ำบาดาลของชั้นหินให้น้ำชุดโคราชตอนกลางในฤดูแล้งและฤดูฝนปีพ.ศ.2558 และฤดูแล้งถัดมาในปีพ.ศ.2559 เท่ากับ 0.33, 0.32 และ 0.38 ล้านลูกบาศก์เมตรต่อวัน ตามลำดับ พื้นที่ลุ่มน้ำแควหนุมานส่วนล่างสามารถสูบน้ำบาดาลได้อีก 27,286 ลูกบาศก์เมตรต่อวัน หรือประมาณ 2 เท่าของอัตราการสูบน้ำในปัจจุบัน เมื่อทดสอบสูบน้ำบาดาลเพิ่มขึ้น 10-200% ทำให้บริเวณตรงกลางของพื้นที่ศึกษาเกิดระยะน้ำลด 2.5-4.0 เมตร ซึ่งผลการศึกษาเหล่านี้สามารถนำไปใช้ในการศึกษาต่อเพื่อการพัฒนาการสำรวจน้ำบาดาลเพื่อการเกษตร และประเมินอัตราการสูบน้ำที่เหมาะสมเพื่อใช้น้ำบาดาลอย่างยั่งยืนโดยไม่ส่งผลกระทบต่อสภาพแวดล้อม

ภาควิชา ธรณีวิทยา ลายมือชื่อนิสิต .....

สาขาวิชา ธรณีวิทยา ลายมือชื่อ อ.ที่ปรึกษาหลัก .....

ปีการศึกษา 2559

5672161123 : MAJOR GEOLOGY
KEYWORDS: LOWER KHWAE HANUMAN / GROUNDWATER RECHARGE / GROUNDWATER BALANCE / SAFE YIELD

NARONGSAK KAEWDUM: GROUNDWATER BALANCE AND SAFE YIELD OF MIDDLE KHORAT AQUIFER IN THE KHWAE HANUMAN SUB-BASIN, CHANGWAT PRACHINBURI. ADVISOR: ASSOC. PROF. SRILERT CHOTPANTARAT, Ph.D., 144 pp.

The lower Khwae Hanuman sub-basin covers about 900 km^2 in the Nadi and Kabinburi Districts, Prachinburi province. Recently, people have developed groundwater used for various activities, particularly in agricultural areas and industrial estates. In this area, the demand for groundwater usage tends to be gradually increased and may result in declining of groundwater levels in the future. The objectives of the study were to evaluate the groundwater recharge amount into the middle Khorat aquifer and to assess safe yield in the aquifer. The groundwater recharges potential was estimated by the overlay method for several thematic layers, consisting of lithology, soil, land use, slope, lineaments density and drainage density, and finally multiplied by the annual 30-year rainfall by the ArcGIS software. According to hydrogeological characteristics and field survey, the groundwater aquifers can be divided into two aquifers: the Quaternary sediment (Q) and the Middle Khorat aquifer (Jmk). The groundwater level ranged from -37 to 35 m amsl. and groundwater flow generally orients in the north-south direction. The high recharge potentiality was about 33.9 km^2 (2.3% of the area), located in the center of the area. Only 12.8% of the total precipitation infiltrates into the groundwater aquifer. As per the model results, the groundwater balance in Jmk aquifer of dry and rainy seasons in 2015, as well as the consecutive dry season in 2016 are 0.33, 0.32, and 0.38 Mm^3/day, respectively. The study area can pump groundwater up to 27,286 m^3/d or about 2 times the current pumping rate. Interestingly, when increasing pumping rate from 10 to 200%, drawdowns in the central of the study area around the industrial areas, appeared to be intensively increased in the range of 2.5-4.0 m. The first-hand recharge potential and safe yield information can be used to develop an effective groundwater exploration for agricultural purposes and to estimate suitable pumping rates in order to obtain long-term sustainable groundwater utilization without adversely affecting the environment.

Department: Geology Student's Signature .....
Field of Study: Geology Advisor's Signature .....
Academic Year: 2016

ACKNOWLEDGEMENTS

My special thank go to the Department of Geology, Faculty of Science, Chulalongkorn University for various equipment in pre-field and fieldwork. The Department of Groundwater Resources, the Department of Water Resources, the Department of Mineral Resources, the Thailand Meteorological Department, the Royal Irrigation Department, the Royal Thai Survey Department and The Land Development Department, I am very thankful for partially providing data.

I sincerely thank my advisor, Associate Professor Dr. Srilert Chotpantarat. In addition, appreciation is also done to thank Dr. Aranya Fuangswasdi, Dr. Tussanee Nettasana, Mr. Chareon Chuamthaisong, and Dr. Thanu Harnpattanapanich for their support, teaching, critically advice, thesis reviewing and methodologies in life. Furthermore, I also sincerely thank Thesis Evaluation Committee members for contribution and useful suggestions.

My special thank also go to the 90th Anniversary of Chulalongkorn University Fund (Ratchadapiseksomphot Endowment Fund) for research funding.

I would like to thank the Panyaconsultant Co., Ltd. provides the opportunity and support for studying at the master's degree level, throughout supporting some research data. I thank you Miss Chutinun Limpakanwech and Mr. Jaturon Kornkul for advice on the groundwater modeling, Mr. Wiboon Kaentao for advice on the classification of soils, Mr. Wisut Chunnet for provision and guidance on the use of the ArcGIS program, Miss Ponyaporn Prabjabok, Mr. Sangkom Nadee, and Mr. Thuwanont Jirakannukul for their field investigation supporters, Mr. Sumran Praphat for thesis grammar check. I would like to thank all of my friends in Chulalongkorn University and Mahidol University for their support.

Finally, I most gratefully acknowledge my parents for all their support, suggestion, foundation and encouragement throughout the period of this research.

CONTENTS

Page

Page

Page

LIST OF TABLE

Page

LIST OF FIGURE

Page

CHAPTER I
INTRODUCTION

1.1 Rationale

Water is an essential resource for agriculture and industry, especially in Thailand, where the major freshwater usage is surface water. Local community, agriculturists and industrial sector confront a surface water shortage problem due to the increasing in water demands, especially dry season. Therefore, groundwater resource gradually becomes an essential additional freshwater resource for such activities.

Groundwater recharge is defined as the entry of water from the unsaturated zone into the saturated zone below the water table surface, together with the associated flow away from the water table within the saturated zone (Freeze 1979). Groundwater is also often withdrawn for municipal, industrial and agricultural uses by constructing and operating extraction wells. The lower Khwae Hanuman sub-basin is one of the areas that suffer from the surface water shortage problem in the dry season, and this needs to be resolved urgently since groundwater has been developed and used for various activities. The study area is in the lower Khwae Hanuman sub-basin, covering Nadi and Kabin Buri district, Prachinburi province, approx. 900 square kilometers. This area includes Nong Ki subdistrict, Kabin Buri district where will be gradually developed as industrial area in the future. The industrial areas have grown up, which causes water demand in this area has increased. Water demand of Prachinburi province is increased 2% per year (DGR 2008). High rate of groundwater pumping in the future may cause declining of groundwater levels and groundwater unbalance. In order to maintain groundwater balance, the hydrogeological characteristics such as groundwater flow condition, hydraulic properties of aquifer and safe yield in the potential area need to be concerned.

In this study, safe yield refers to the quantities of groundwater which can be developed without consequences. Water level rebound is the main factor result in yield balanced by recharging of ground water (DWR 2012). Understanding safe yield leads to effective study areas with limited data and short term information. Three

periods of field data including March, 2015 and May, 2016 in dry season and rainy season in November, 2015 were collected. Field data and secondary data were used to design mathematical models for groundwater balance assessment. Results of this study leads to understanding of hydrogeologic system and quantity of safe yield. There also can be used to develop an effective groundwater exploration for agricultural and industrial purposes as well as to estimate suitable pumping rates in order to obtain the long-term sustainable groundwater utilization.

1.2 Objective

The purposes of this research are to delineate the zones of groundwater recharge, infiltrating into aquifers, and to assess groundwater balance and safe yield of the middle Khorat aquifer in the lower Khwae Hanuman sub-basin, Prachinburi Province.

1.3 Scope of Study

1.3.1 The study area is located in the lower Khwae Hanuman sub-basin in the North of Prachinburi province. The total area is approximately 900 square kilometers.

1.3.2 The groundwater recharge potential was estimated by using GIS overlay analysis of factors involved in the groundwater recharge, including lithology, land use, lineaments, drainage, slope and soil. The mean annual rainfall in the period 1977–2006 (30 years) is used as the method to assess the groundwater recharge. Then, the seasonal groundwater recharge potential was calculated by multiplying the mean annual rainfall of each season (period 2015-2016) by the groundwater recharge potential map.

1.3.3 This research is used groundwater wells (such as, hand pump wells) from field investigation, simulation and analysis model.

1.3.4 The primary data of groundwater levels from field investigation were collected in the year 2015-2016, including March and November, 2015 and May 2016.

1.4 Study Area

The study area is the lower Khwae Hanuman sub-basin (**Figure 1.1**), part of the Prachinburi basin, covering Nadi and Kabinburi Districts, Prachinburi province. The area is 900 square kilometers, and its elevation ranges from 1 to 548 meters above mean sea level (m amsl.), located between longitudes 101^{o} 38’ 15.86” to 102^{o} 6’ 13.37” E and latitudes 13^{o} 57’ 7.19” to 14^{o} 13’ 2.64” N. The topography varies from high mountains range in northern part (the Khao Yai and the Tub Lan national park), which is the origin of a large amount of rivers in this area. The center of the study area is plains with various rivers and its tributaries, including the Khwae Hanuman, Prapong, Huai Sai Noi, Huai Sai Yai, Huai Prayathan, and Huai Samong Rivers. The Khwae Hanuman River is 38.3 km long and flows southward to Bang Pakong River in the southern part of the study area. The mean annual rainfall in the period 1977–2006 was 1,415.37 millimeters per year, which is derived from the Thailand Meteorological Department. The major geological features, as determined from the geologic maps of 1:50,000 scales derived from the Department of Mineral Resources (DMR) are sandstone, siltstone and conglomeratic sandstone, which have a medium-thick bedded and cross-bedding as part of the middle Khorat group. The hydrogeological features are determined from the hydrogeological maps of 1:100,000 scales which derived from the Department of Groundwater Resources (DGR). The groundwater in the middle Khorat aquifer can be found in crack and fracture structure.

1.5 Expected Outputs

1.5.1 The groundwater recharge potential in the lower Khwae Hanuman sub-basin, Prachinburi Province

1.5.2 The cross-section and conceptual hydrogeological model in the lower Khwae Hanuman sub-basin, Prachinburi Province

1.5.3 The water balance and water safe yield of the middle Khorat aquifer in the lower Khwae Hanuman sub-basin, Prachinburi Province

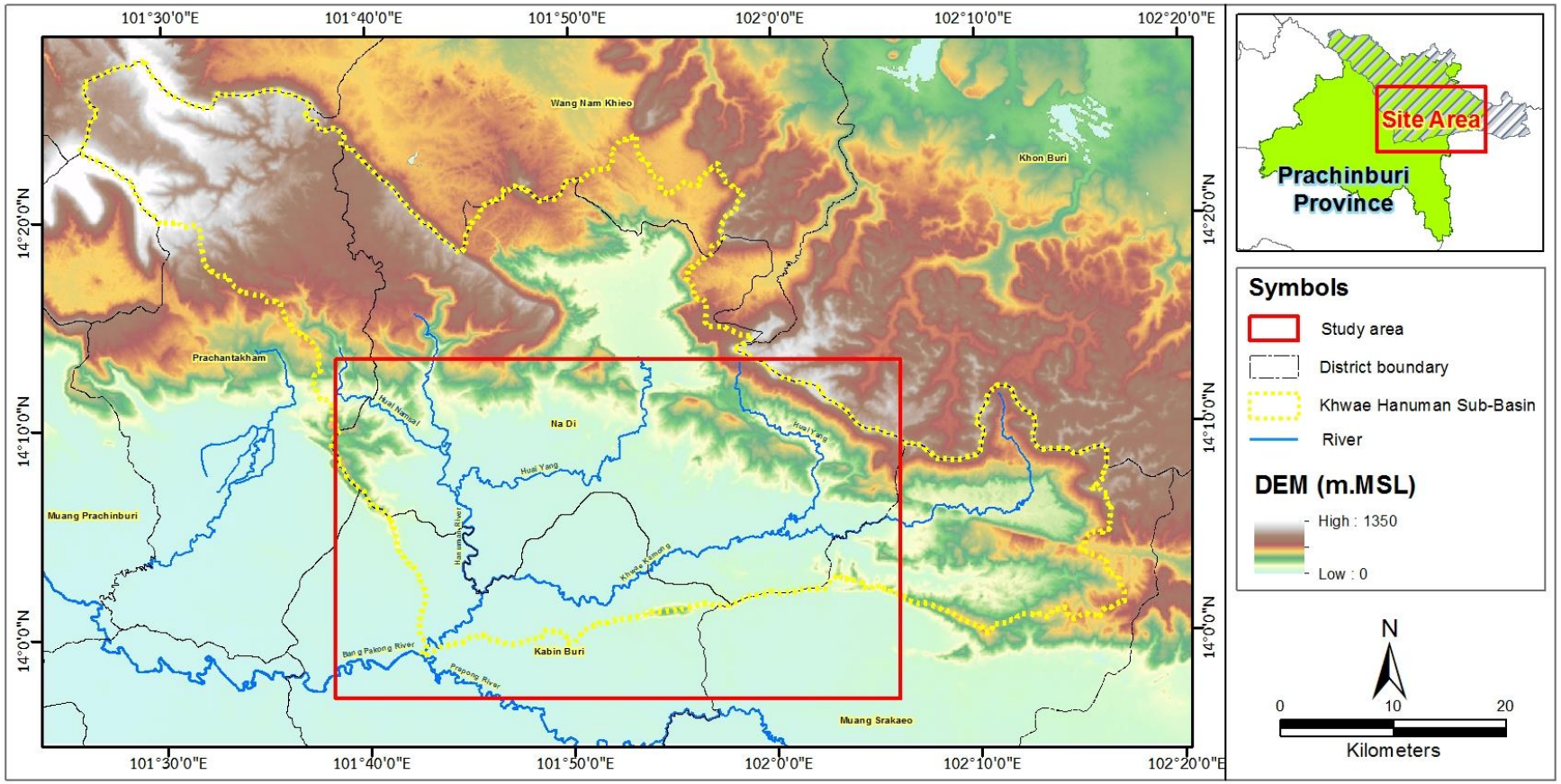

Figure 1. 1 Study area in the lower Khwae Hanuman sub-basin applied from DEM resolution 90x90 (Royal Thai Survey Department)

1.6 Research Methodology

In order to achieve the objectives of this study, the researcher divided the research methodology as shown in the diagram below (**Figure 1.2**):

1.6.1 Research study documents and secondary data collection

Local and national sources of safe yield processing theory and advanced assessment techniques were collected as research documents. The secondary data were compiled, including geology, hydrogeology, hydrology, pumping test, groundwater wells, geophysical survey, E-log, land use, soil properties, topography and hydraulic properties (i.e. hydraulic conductivity, transmissitivity and strorativity). These were used to determine the scope and study guidelines.

1.6.2 Cross section of hydrogeology

Hydrogeological cross-sections were created from groundwater wells (the layer, depth, thickness and type of aquifers rock unit data) by using ArcMap 10.1. The Visual-MODFLOW was used to stimulate a groundwater model in this area.

1.6.3 Conceptual model

Conceptual modeling was created by using secondary data including geology, hydrology (recharged rainfall and river), topography, groundwater wells and hydrogeology (aquifers, water levels and etc.) to study the relationship between surface water and groundwater, groundwater balance and geological characteristics associated with the hydrological characteristics of area.

1.6.4 Field investigation

Planning and field working were used hydrogeological data and locations of groundwater wells from the Pasutara database of DGR. Wells selections were a single screen of aquifer layer and distribution of groundwater wells. Groundwater table measurement is divided into 3 ranges, include March, 2015 (dry season), November 2015 (rainy season), and May 2016 (dry season).

1.6.5 Application of mathematical models

A grid of mathematical model is a square. Period and scope of area were assigned and installed the primary variable to set up the simulation. For instance, top-bottom, aquifer type, hydraulic properties, initial head, pumping well, observation well, recharge and river. The simulation and calibration models for model are similar to observing data which measured in field survey. The modeling was started from the

steady state conditions and transient state condition, and was then carried out analysis of the sensitivity and prediction, respectively.

1.6.6 Groundwater balance and safe yield analysis

Groundwater balance and safe yield were analyzed for the groundwater potential and an appropriate amount for pumping rate.

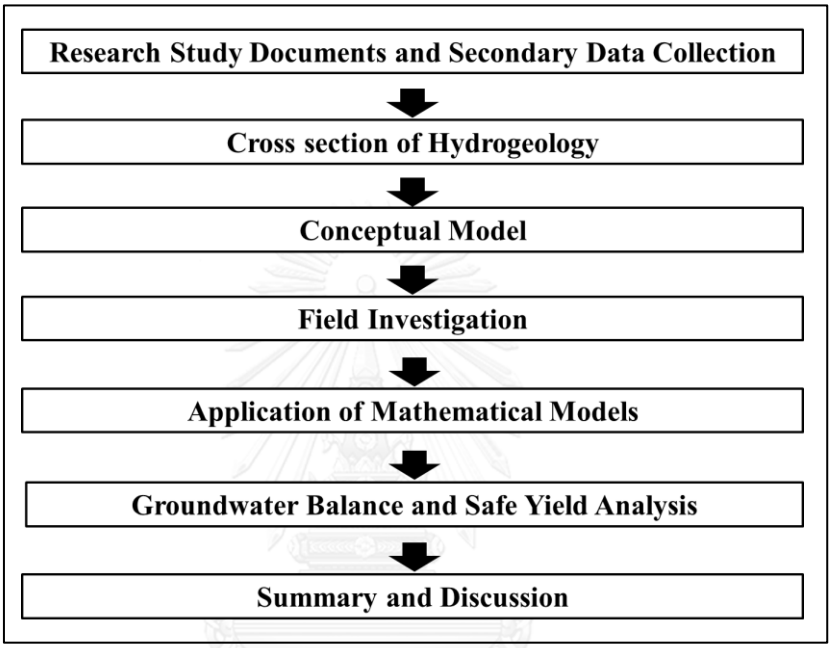

Figure 1. 2 Schematic diagrams of the research methodology

1.6.7 Summary and discussion

This study is summarized and discussed for the results, then thesis writing and articles.

CHAPTER II
LITERATURE REVIEW

Literature and research related to the study of groundwater balance and safe yield of the middle Khorat aquifer (Jmk) in the lower Khwae Hanuman sub-basin, Prachinburi province. It is about a groundwater flow, groundwater flow equation, groundwater aquifer, hydraulic properties, mathematical models, groundwater balance, and safe yield.

Groundwater flow equation is necessary to apply the groundwater flow model through porous media. This equation can explain by two basic principles: Darcy's law and principle of mass conservation.

2.1 Groundwater System

The term groundwater refers to all water which is below the surface of the ground in the saturated zone and which is in direct contact with the ground or subsoil. The saturated zone is where all the cracks in the rock and all the spaces between the grains of rock or within the soil are filled with water (**Figure 2.1**). The upper limit of the saturated zone may be considered as the water table. The zone above the water table, where pore spaces contain both air and water, is known as the unsaturated zone.

Groundwater flows through the spaces and cracks in the rock, being pulled by gravity and pushed by the force of the water above and behind it. The water moves from an area where water enters the aquifer (a recharge zone) to an area where water exits the aquifer (a discharge zone) as shown in **Figure 2.2**. The slope of the water table, or potentiometric surface, which is termed the hydraulic gradient, will dictate the direction of groundwater flow. Groundwater generally flows much more slowly than surface water.

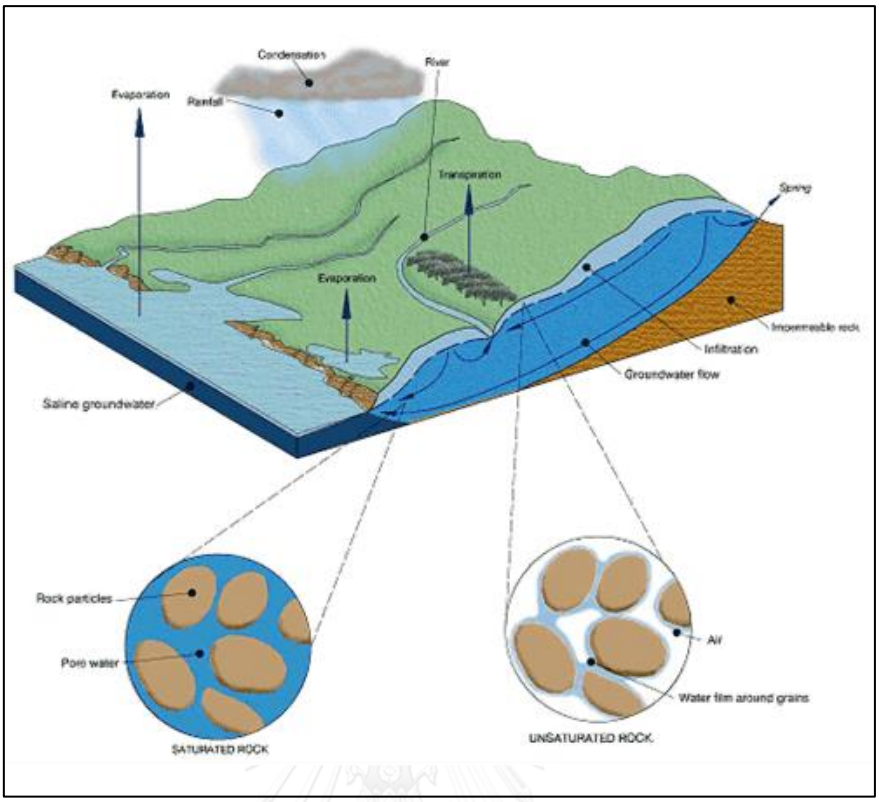

Figure 2. 1 The spaces between the grains of soil are filled with water (Nebraska–Lincoln)

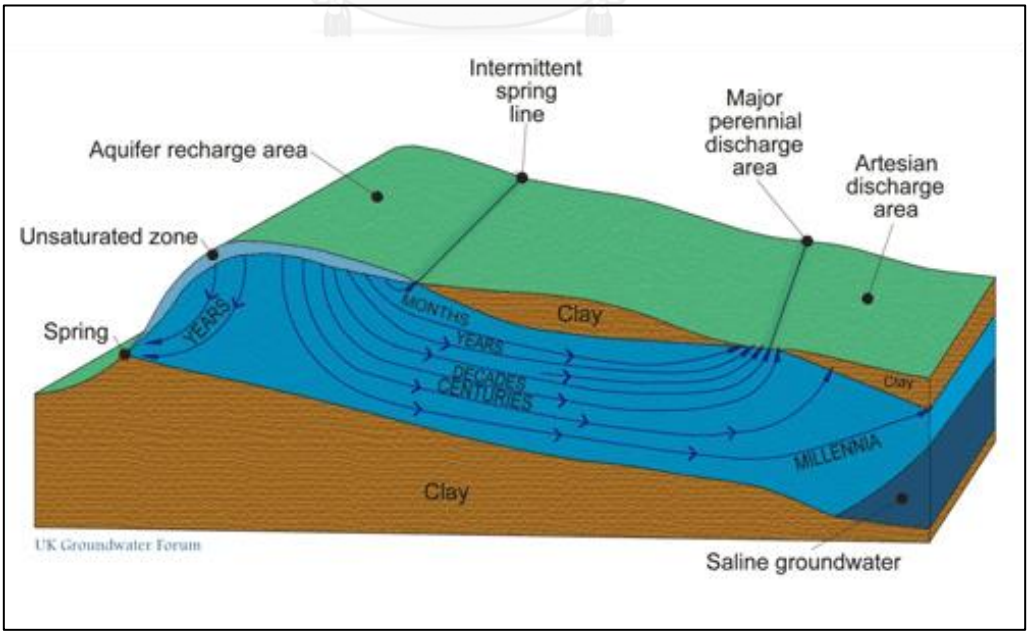

Figure 2. 2 Location of recharge and discharge point (Nebraska–Lincoln)

2.2 Aquifer Types

A groundwater aquifer refers to soil or rock layers saturated with water, moderate to high hydraulic conductivity and transmissivity under the natural hydraulic gradient conditions: layer of sand, not coagulation gravel, sandstone, limestone, high porous and fracture rocks (volcanic rocks). This aquifer can produce a production bore and also classified as follows:

1) Unconfined aquifer is non-pressure aquifer or no confining layer over top. Groundwater levels are equal to or lower than the aquifer layer (**Figure 2.3**).

2) Confined aquifer is pressure aquifer or confining layer over top. Groundwater level is higher than the aquifer layer. If the groundwater level is higher than the ground surface, it will be an artesian (**Figure 2.3**).

3) Semi-unconfined aquifer is non-pressure aquifer or no confining layer over top. Groundwater levels are equal to or lower than the aquifer layer (similar to unconfined aquifer).

4) Semi-confined aquifer is pressure aquifer or some confining layer over top. Groundwater level is higher than the aquifer layer in some area.

5) Perched aquifer is not width aquifer and insert in the unconfined aquifer, some confining layer over top (**Figure 2.3**). Groundwater levels are higher than or lower than the aquifer such as sand and gravel.

6) Aquitard refers to low hydraulic conductivity soil or rock, and very low transmissivity under the natural hydraulic gradient conditions. Groundwater is not enough for consumption and consumption such as clay, shale, and dense crystalline rocks.

7) Aquiclude refers to soil or rock layers saturated with water, no transmissivity under the natural hydraulic gradient conditions but it can slowly absorb water into it. Groundwater is not enough for consumption and consumption such as claystone.

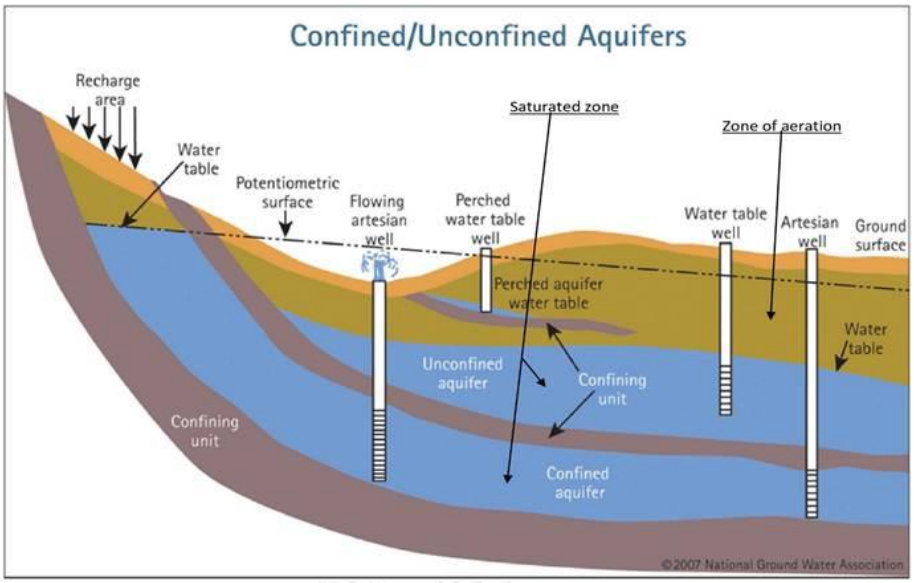

Figure 2. 3 Groundwater aquifer (Society)

2.3 Hydraulic Properties

Groundwater aquifer has many important hydraulic parameters such as hydraulic conductivity, transmissivity, storativity, specific storage, specific yield, and porosity as follows:

1) Hydraulic conductivity: K is a measure of a material's capacity to transmit water. It is defined as a constant of proportionality relating the specific discharge of a porous medium under a unit hydraulic gradient in Darcy's law:

$$V = -K \times i \qquad (2\text{-}1)$$

Where V is specific discharge, L/T

K is hydraulic conductivity, L/T

i is hydraulic gradient, (-)

2) Transmissivity: T is the rate of flow under a unit hydraulic gradient through a unit width of aquifer of given saturated thickness. The transmissivity of an aquifer is related to its hydraulic conductivity as follows:

$$T = K \times b \qquad (2\text{-}2)$$

Where T is transmissivity, L^2/T

b is aquifer thickness, L

3) Storativity: S is defined as the volume of water released from storage per unit surface area of the aquifer or aquitard per unit decline in hydraulic head. Storativity is also known by the terms coefficient of storage and storage coefficient. Pumping a well in a confined aquifer releases water from aquifer storage by two mechanisms: compression of the aquifer and expansion of water. In a confined aquifer, storativity is defined as:

$$S = S_s \times b \quad (2\text{-}3)$$

Where S is storativity, (-)

S_s is specific storage, L^{-1}

b is aquifer thickness, L

The typical storativity of a confined aquifer, which varies with specific storage and aquifer thickness, ranges from 5×10^{-5} to 5×10^{-3} (Todd 1980).

4) Specific storage: S_s refer to the volume of water that a unit volume of aquifer releases from storage under a unit decline in the head. The storativity of an unconfined aquifer includes its specific yield or drainable porosity:

$$S = S_y + (S_s \times b) \quad (2\text{-}4)$$

Where S_y is specific yield, (-)

Lowering of the water table in an unconfined aquifer leads to the release of water stored in interstitial openings by gravity drainage. The storativity in unconfined aquifers typically ranges from 0.1 to 0.3 (Lohman 1972).

5) Specific yield: S_y refers to the volume of water released from storage by an unconfined aquifer per unit surface area of aquifer per unit decline of the water table. (Bear 1979) relates specific yield to total porosity as follows:

$$n = S_y + S_r \quad (2\text{-}5)$$

Where n is total porosity, (-)

S_y is specific yield, (-)

S_r is specific retention, (-)

6) Porosity: n is defined as the void space of sediments or rock texture:

$$n = V_v / V_t \quad (2\text{-}6)$$

Where
- n is porosity, (-)
- V_v is void volume, L^3
- V_t is total volume, L^3

2.4 Groundwater Flow

In the natural state, groundwater is stored in fracture of rock or porous media. Groundwater can flow from one place to another, when there is a difference in hydraulic pressure or hydraulic head, groundwater flows through the continuous porous rock and slow flow. In addition, the groundwater flow is quite complex and it is occurs under the surface, so cannot observe. Therefore, it makes easy to study groundwater flows, should be understood as follow:

2.4.1 Darcy's Law

In 1856, Henry Darcy (French hydraulic engineer) study and experiment to determine the flow rate of water through porous media, found that volume discharge rate through cross-section area (A), is directly proportional to head drop $(h_2 - h_1)$ but is inversely proportional to length different $(l_1 - l_2)$, (Anderson and Wang 1982).

Henry Darcy has investigated the flow of the water through horizontal beds of sand to be used for water filtration (**Figure 2.4**). Experiment can be written as the equation. It is Darcy's Law. (Freeze 1979) as follow:

$$q_x = \frac{Q}{A} = -K\frac{dh}{dl} \quad (2\text{-}7)$$

$$Q = -K\frac{dh}{dl}A = -KiA \quad (2\text{-}8)$$

Where
- Q is discharge, L^3/T
- q_x is Darcy velocity, L/T
- K is hydraulic conductivity, L/T
- dh/dl is hydraulic gradient, (-)

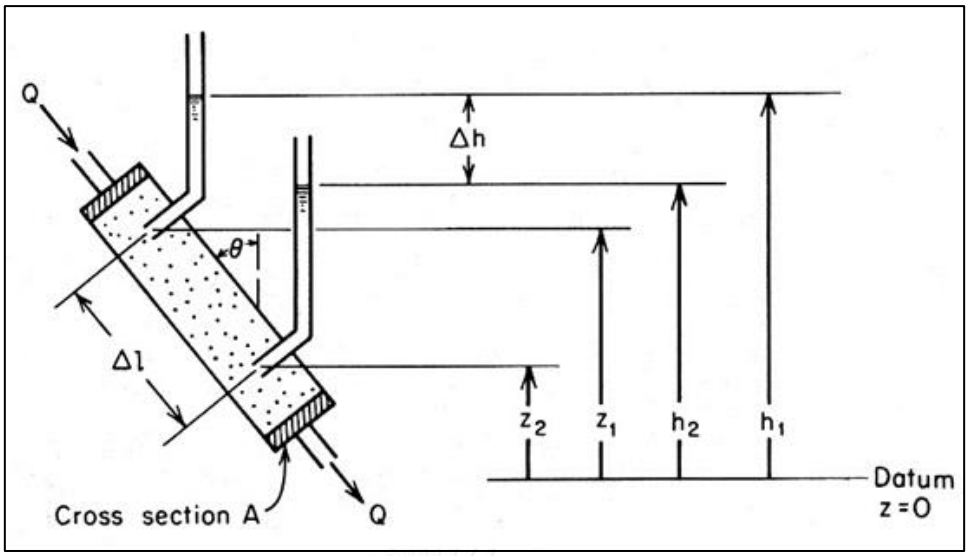

Figure 2. 4 The experiment of Darcy (Freeze 1979)

When K is hydraulic conductivity, unique properties of porous media, units are velocity (L/T). Minus sign means groundwater flows from a high to lower pressure head.

The above equation can write in terms of flow rate per area include specific discharge or Darcy velocity, which flow velocity is directly proportional to a hydraulic gradient (i) or difference of pressure head per distance. The equation can write as:

$$V = -K (dh/dx) \quad (2\text{-}9)$$

Where
- v = Flow velocity of water in porous media, L/T
- K = Hydraulic conductivity, L/T
- h = Pressure head, L
- x = Distance, L

This equation is use in the laminar flow case. It is not the actual flow velocity because they need to use seepage velocity in the calculation. The seepage velocity is average velocity of water flowing through a porous media in the aquifer. The porosity is very small, so the flow velocity calculated from Darcy's law is lower than the actual flow velocity. The relationship between actual flow velocity and Darcy's velocity, write the equation as follows:

$$V_{real} = V_{darcy} / n_e \quad (2\text{-}10)$$

Where V_{real} = Actual flow velocity, L/T

V_{darcy} = Darcy's velocity, L/T

n_e = Effective porosity, (-)

The hydraulic gradient in the direction of groundwater flow is the difference between the confined aquifers and unconfined aquifers because unconfined aquifers will flow both horizontal and vertical flow. So groundwater flow is a calculation in the unconfined aquifers, (Dupuit 1863) proposed the Dupuit assumption as follows:

1. Horizontal flow and uniform are every point in vertical section.
2. Hydraulic gradient equal to free surface and does not change by depth.

These assumptions can be said, (Verruijt 1982) vertical head is constant and not calculate, and can apply to steady state calculations. Although the groundwater level calculation is not correct at all points, but the flow rate is still valid.

2.4.2 Principle of Mass Conservation

The continuity equation is mass flow rate in one unit volume of porous media minus the outflow rate, which equal change in storage. The equation can write as:

$$\text{Inflow} - \text{Outflow} = \text{Change in storage} \quad (2\text{-}11)$$

The storage volume in the aquifer is different between the confined aquifer and unconfined aquifer, for understand the mechanism of water storage, should consider the following:

The confined aquifer is pressure aquifer or confining layer over top. In nature, there is no authentic confining layer due to most aquitard are low to very low hydraulic conductivity. Groundwater levels in the aquifer are a higher pressure than atmospheric pressure. So, water is adding or releasing from the aquifer by a pressure change process. This condition will cause compression of the rock and expansion in Space, when the water head drops, the pressure of the water decreases, but the aquifer is saturated. Therefore, the volumetric water is release from one unit volume of an

aquifer, when water head drops one unit, this process called specific storage (S_s), which unit is L^{-1}.

In the unconfined aquifer, when the water is released from the aquifer, the groundwater level decrease due to the pressure head drop. Pressure head drop is another type of storage process; called specific yield (Sy). This means the volume of water released under the gravity from the aquifer when one unit head drops.

The above process is related to the volumetric behavior of the aquifers, which is related to the amount of water flow out of the total thickness of aquifer; storage coefficient (S). For aquifer with a thickness of b, the storage coefficients are as follows:

Confined aquifer: $S = S_s b$ (2-12)

Unconfined aquifer: $S = S_y + S_s b$ (2-13)

When $S_y > S_s$, so the unconfined aquifer will have an S value close to the S_y value.

2.4.3 Groundwater Flow Equation

Numerical analysis has been used to solve the problem of groundwater flow simulation, by major equations were the water balance equation and Darcy's law, to apply the groundwater flow equation with constant density through intermediaries that qualify as heterogeneous and anisotropic under transient state conditions, when

$$\frac{\partial}{\partial x}\left(K_x \frac{\partial h}{\partial x}\right) + \frac{\partial}{\partial y}\left(K_y \frac{\partial h}{\partial y}\right) + \frac{\partial}{\partial z}\left(K_z \frac{\partial h}{\partial z}\right) = S_s \frac{\partial h}{\partial t} \quad (2\text{-}14)$$

K_x, K_y, K_z = Hydraulic conductivity (x, y, and z direction), LT^{-1}

h = Potentiometric head, L

S_s = Specific storage, L^{-1}

t = Time, T

2.4.4 Groundwater Flow System

(Toth 1963) classified groundwater flow in the basin into three systems, can be analyzed from the hydraulic and chemical data of the water from the field observation wells, include local flow system, intermediate flow system, and regional flow system (**Figure 2.5**) as follow:

1) Local flow system is shallow and fast flow, but direction and flow rate are uncertain due to affected by recharge from surface water, rain, and evapotranspiration. The flow distance and flow times are short, groundwater quality is quite good. The local flow system is separated by a groundwater divide. There is a high change in vertical groundwater levels and may change the seasonal water level.

2) Intermediate flow system is deep, and medium flow velocity, horizontal flow direction. The flow distance and flow times are more than the local flow system. It is a few the seasonal water level changes.

3) Regional flow system is very deep, and slow flow velocity. The flow distance and flow times are very long time. It is very little or no seasonal water level changes. Water temperature is quite high.

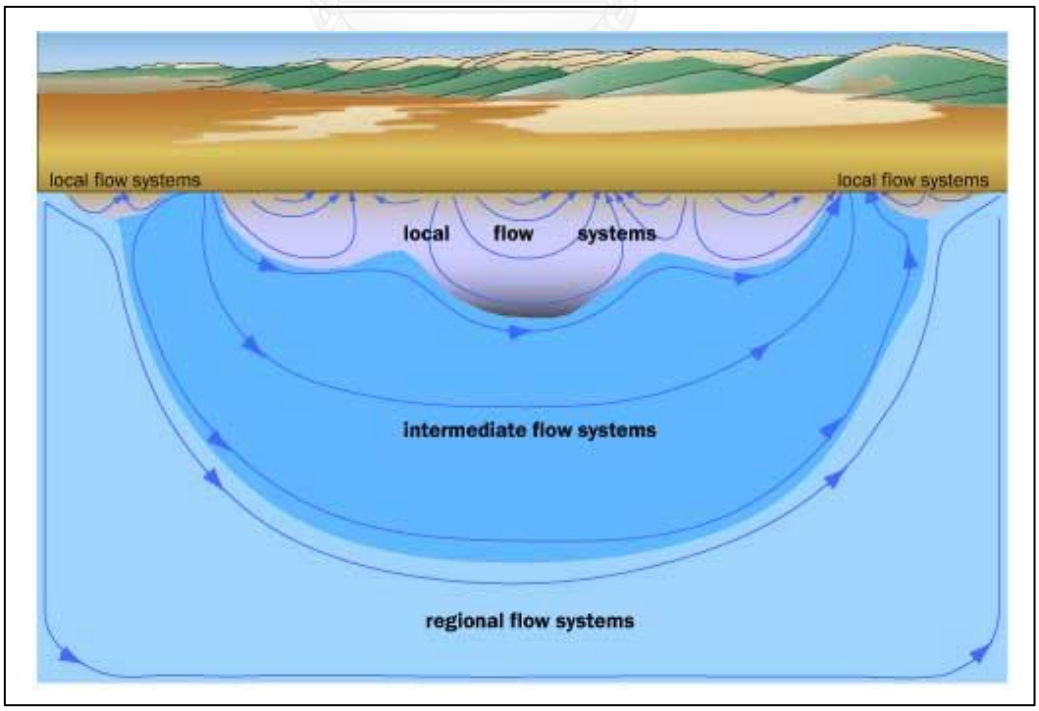

Figure 2. 5 Groundwater flow systems (Winter 1998) and (Toth 1963)

The groundwater flow system in the reservoir consists of three areas: recharge area (groundwater flows into storage in porous media), midline area (groundwater flows horizontal area), and discharge area (groundwater flows out of the porous media). The three areas are part of the groundwater flow system, may change the seasonal or time. This can be classified by install observation wells and analyze groundwater flow nets together with the chemical quality of groundwater.

2.5 Groundwater Flow Modeling

Model is tools or equipment use to represent actual conditions in nature. Groundwater models are tool use to evaluate and calculate the approximate results of field data or to simulate conditions that occur in nature, the experiments and predict events in the future.

The flow model is model shows the hydraulic head in various areas, both in map, cross-section or three-dimension. The flow model shows the direction of groundwater flow.

Mathematical models are applying mathematical methods to calculate and analyze groundwater systems. The advantages of the mathematical simulation are that they can simulate various conditions, both in natural condition, water use changes, and numerical or quantitative land use is fast. When the model of that area has been adjusted to a good variety, modeling can be used to plan water resources and predict or manage groundwater resources in future.

The mathematical models used in this study are Visual MODFLOW 2010.1, developed by Waterloo Hydrogeologic Inc, Canada. It is a program used to prepare pre-computed data and display calculated results. Modular Three-dimension Finite-Difference Groundwater Flow Model or MODFLOW is a program used to calculate the flow of groundwater, developed by U.S. Geological Survey (McDonald and Harbaugh 1988). It uses finite difference to compute by dividing the grid into Block-centered. This is the most widely applied and accepted in the simulation results at the moment. The basic equations used in the calculation are the Darcy equation and the Continuity equation.

2.5.1 Finite difference

Modeling by finite difference method divides the area of the domain that is clearly defined into a block. Therefore, the area is divided into quadrilateral or grid, square segments by grid lines may vary depending on the amount of data density. The width of the grid, the contact should not differ more than 1.5 times the grid side, for the results are not very accurate (Domenico and Schwartz 1998). The study area is divided into Y (Column), X axis (Row), and Z axis is the number of layers of the model (Layer), that shown in **Figure 2.6**.

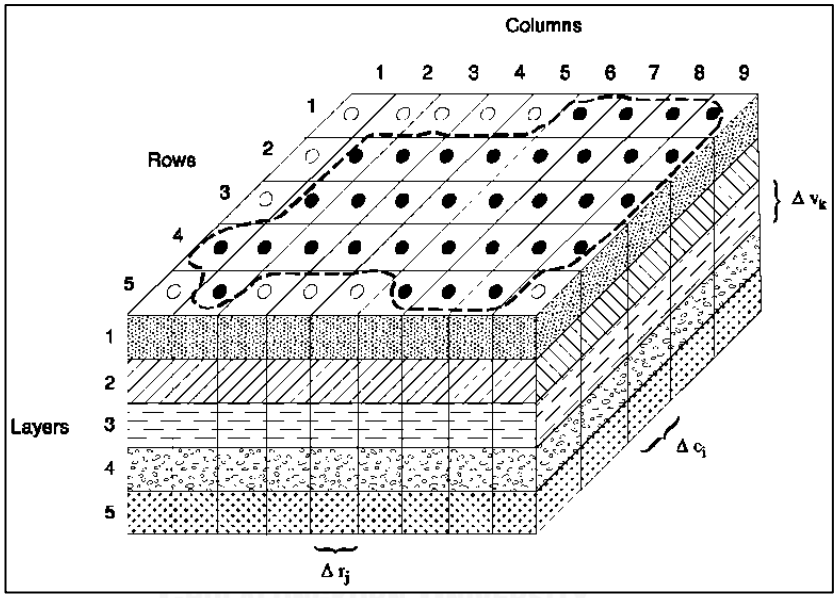

Figure 2. 6 Divide the area in the model (McDonald and Harbaugh 1988)

2.5.2 Groundwater flow modeling methods

The development of groundwater flow model aims to study the potential and equilibrium of groundwater resources consists of 7 steps as shown in **Figure 2.7** which can be described as follow:

1) Defining the purpose: The purpose of the model is to study the potential and equilibrium of groundwater resources, the effects of groundwater over-pumping and proposed mitigation measures.

2) Developing a conceptual model: The field data is required to understand the area characteristics which consume considerable of time. There

comprises of compiling data on geology, hydrogeology, groundwater flow condition, and groundwater aquifer boundaries, then simplifying the real problems in the field which are complicated to the format that can be analyzed and calculated.

3) Computer program selection: The Visual MODFLOW Version 2010.1 software was used to study groundwater flow modeling which developed by the Waterloo Hydrogeologic, Inc., Canada. The program comprises MODFLOW-200, MODPATH, MT3DMS, RT3D, Zone Budget, Stream Routing Package, WinPEST and VMOD 3D-Explorer programs, which are suitable for studying the potential and equilibrium of groundwater resources. However, the program should be suitable for the implementation of the objectives, widely used and reliable to develop efficiency groundwater modeling.

4) Model design: The conceptual overviews of the area and the simulation of physical characteristics of the aquifers will be conducted by dividing the study area (discretization) into small units or grid cells, defining boundary conditions, and selecting time steps and initial conditions to simulate the distribution patterns of groundwater hydraulic heads.

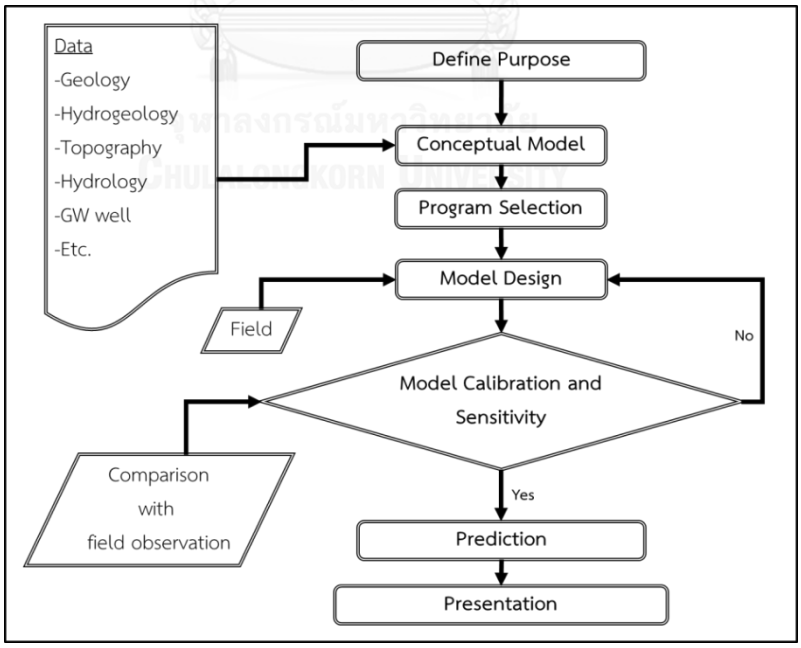

Figure 2. 7 Schematic diagrams of the development of groundwater flow model to study the potential and equilibrium of groundwater resource modified from (Anderson, Woessner et al. 2015)

5) Model calibration and sensitivity: The target of this step is to test the model and adjust some model parameters to simulate the study of groundwater flow phenomena. The model will be calibrated the results from model calculation. For instant, the values of hydraulic heads are close to the available field data at particular place and time. If the results of calculation do not correspond with the field data, it is necessary to adjust the values of the parameters that are uncertainly known, such as the hydraulic conductivity. This step is important because the results are representative of the groundwater aquifers study, which can be used in various simulating situations. The trial-and-error adjustment has to be used in some cases. The suitable ranges values of parameters have to be adjusted in model calibration. The model verification should be executed by using another set of field data that differ from the first set in order to confirm that the model is correct and applicable.

6) Prediction: The predictive values of model variables such as hydraulic heads can be generated base on carefully plan and consideration on the future situations. Moreover, the sensitivity analysis should be conducted. However, the sensitivity of model parameters is the characteristics of the particular area which will be displayed the possible range of the values of those parameters. The results will be useful in long-term monitoring preparation programs for model improvement. The suitable values of model parameters and other data, such as groundwater recharge rates, boundary conditions are decided. The model will be used to simulate the groundwater flow under various assuming scenarios. These scenarios may include the situations of groundwater use to reduce at some different percentages, or in case of groundwater aquifer recharge is implemented.

7) Presentation of results: Presentation of the model results is the last step of modeling work. This step will include communication to those who will use the model results in planning and management. The model results can be presented in digital or pictorial forms with some explanation and suggestion. The results obtained from sensitivity analysis and the values of model parameters, as well as the initial and boundary conditions and all the assumptions used in modeling should be provided.

2.6 Groundwater Balance

Groundwater balance refers to the balance of groundwater recharge and groundwater pumped and changes in groundwater storage.

The equilibrium of groundwater in a basin or any area during a time of interest can be explained by the general equation.

$$S_{gw} = Q_r - Q_d \quad (2\text{-}15)$$

Where S_{gw} is changes in the amount of water retained in the aquifer

Q_r is the amount of water recharge to the aquifer

Q_d is the amount of water lost from the aquifer

The above equation can be written recharge and a loss of water, as follow:

$$S_{gw} = W_s + W_r + W_c + GW_i - GW_b - GW_E - GW_{ET} - GW_c - GW_o \pm GW_n \quad (2\text{-}16)$$

Where S_{gw} = changes in the amount of water retained in the aquifer

W_s = additional water from the seepage of rainwater

W_r = additional water from the surface water

W_c = additional water from the seepage of irrigation system

GW_i = additional water from the groundwater inflow

GW_b = loss of water to surface water

GW_E = loss of water due to evaporations

GW_{ET} = loss of water due to dehydration of plants

GW_c = loss of water due to pumping

GW_o = loss of water due to groundwater outflow

GW_n = addition or loss of water in other cases

2.7 Groundwater Safe Yield

Many hydrogeologists have defined the groundwater safe yield include: the limit to the quantity of water which can be withdrawn regularly and permanently without dangerous depletion of the storage reserve (Lee 1915). Later, the maximum quantities of water which can be extracted from an underground reservoir, yet still maintain the supply unimpaired (Todd 1959). Next, the maximum pumpage for which the consequences are considered acceptable (Alley, Reilly et al. 1999). Then, the

amount of capture, and whether this amount can be accepted as a reasonable compromise between a policy of little or no use, on one extreme, and the sequestration of all natural discharge, on the other extreme (Ponce 2007). Afterward, all high pumping rate to ensure that the groundwater level of each aquifer will be decrease lower than 30 meters from the ground level in the next 20 years (DGR 2009). Finally, the quantities of groundwater that can be developed without consequences will be balanced with the recharge by water level rebound (DWR 2012).

Words with a similar meaning to the words that are safe yield: potential sustained yield (Freeze 1979), permissive sustained yield (American Society of Civil Engineers, 1961), and maximum basin yield (Freeze 1979). Including the above definitions of the hydrogeologist, safe yield refers to the amount of naturally occurring groundwater that can be pumping sustainably in both economic and legal terms, without having a negative impact on water quality and the environment (Nettasana, 2002).

In estimating the maximum amount of pumping should be acceptable criteria. Shibasaki and Research Group for Water Balance (1995) discusses the factors used to determine the maximum pumping volume, which consists of:

1) Recharge factor - maintain water balance.

2) Economic factor - the cost of developing the water used must be below the threshold limit.

3) Legal factor - not violate the Water Act or Law.

4) Geo-environmental factor - not cause land subsidence or encroachment of saline water.

5) Amenity factor – conservation of the environment and increasing people's livelihoods.

Although these factors are not currently guaranteed, but it is the starting point to find the maximum amount of pump and permissible critical groundwater level

2.8 Groundwater Recharge

Groundwater recharge is defined as the entry of water from the unsaturated zone into the saturated zone below the water table surface, together with the associated flow away from the water table within the saturated zone (Freeze 1979).

Many studies on the groundwater recharge potential have used remote sensing and GIS with different factors, such as the geology, geomorphology, and topography, including this study.

Although many researchers have used the GIS process to determine the groundwater recharge potential map ((Shaban 2003); (Shaban, Khawlie et al. 2006); (Yeh, Lee et al. 2009); (Adham, Jahan et al. 2010); (Patil and Mohite 2014); (Chotpantarat, Konkul et al. 2015); (Deepa, Venkateswaran et al. 2016); (Selvam, Dar et al. 2016)), the different weights and scores of the factors under various effects were evaluated based on the characteristics of the area, including the lithology, drainage density, lineament density and land use. Some other researchers have used the slope and soil factors that were related with the groundwater recharge.

Spatial analysis was used to integrate the GIS multilayer system to achieve the groundwater recharge potential map. Finally, the volume of water that could infiltrate into the groundwater aquifers was calculated using Eq. (9) (Adham, Jahan et al. 2010);

$$W = P \times \text{Recharge Ratio} \times \text{Percentage of Recharge Area} \qquad (2\text{-}17)$$

Where W is the recharge water volume (m^3/y) and P is the precipitated volume (m^3/y). The volume of water recharged was calculated as the percentage of groundwater potential maps, which were derived from the six weighted factors that affect the groundwater recharge, and are detailed as follows:

1) Lithology: (Su 2000) and (Shaban 2003) showed that rock rails have a direct relationship with the recharge, where each stone has a different water body, but the rate of water recharge is equal. According to (O'leary, Friedman et al. 1976), the type of rock exposed to the surface (outcrop) significantly affected the groundwater recharge. Lithology affects the groundwater recharge by controlling the infiltration of water into the saturated zone. Some investigations have ignored this factor by considering the lineaments and drainage characteristics as a secondary porosity (El-

Baz, Himida et al. 1995). The lithology reduces the uncertainty in defining the lineaments and drainage factors (Yeh, Lee et al. 2009).

2) Slope gradient: The slope gradient is one of the factors that directly influence the rate of infiltration of rainfall ((Selvam, Magesh et al. 2014); (Deepa, Venkateswaran et al. 2016)). At higher or steeper slopes, the volume of groundwater recharge is smaller because the water rapidly flows over the surface and has insufficient time to infiltrate into the saturated zone. The flatter plain areas can keep and drain the water into the ground, and increase the groundwater recharge, whereas steep slopes increase the surface runoff and decrease the infiltration of surface water into the saturated zone.

3) Drainage density: According to Ramingwong (2003), the characteristics of landforms and drainage are related to their hydrogeology and hydrology because the characteristics of drainage water may be either water recharge or discharge. The structural analysis of the drainage density helps to assess the characteristics of the groundwater recharge zone (Yeh, Lee et al. 2009), where the drainage networks are based on the lithology, which provides an important index of the infiltration rate. According to (Dinesh Kumar, Gopinath et al. 2007), areas with a high drainage density are not suitable for groundwater development because of the greater surface runoff. The groundwater occurrence and distribution depend on the density of the drainage (Murthy 2000). Furthermore, the topography is important. A low drainage density has a high void ratio, which indicates a high potential of groundwater recharge.

The area with a low density of water will result in a high recharge potential. In this study area, the drainage consists of rivers, both perennial and intermittent streams in a dendritic pattern. The length of drainage density, D_d (km^{-1}), was derived from the total length of drainage in a unit area (Greenbaum 1985), using Eq. (10);

$$D_d = \frac{\sum_{i=1}^{i=n} S_i}{A}, \tag{2-18}$$

where $\sum_{i=1}^{i=n} S_i$ denotes the total length of drainage in the watershed (km) and A denotes the unit area (km^2). The total length of drainage densities correlates with the

groundwater recharge, where a high drainage density zone has a high groundwater recharge volume. The weighting and rating of drainage-length density were classified into three types by the method of (Selvam, Dar et al. 2016).

4) Lineament density: (O'leary, Friedman et al. 1976) defined lineaments as simple and complex linear properties of structural geology, such as faults, joints, and fractures. The lineaments are arranged in a direct line or slight curve as detected by remote sensing. According to (Dinesh Kumar, Gopinath et al. 2007) and (Selvam, Magesh et al. 2014), in a hard rock landscape, the lineaments represent the fault and fracture zones that result in an increased secondary porosity and permeability. Accordingly, lineaments are good indicators of groundwater recharge and are generally referred to remote sensing analysis of fractures or structures (Yeh, Lee et al. 2009).

Areas with a lineament structure, such as faults, cracks, and fractures, have a high potential of water recharge because the water can seep into undersurface faster and deeper. Lineaments were mostly found in the north area. The length of the lineaments density, L_d (km^{-1}), was derived from the total length of lineaments in a unit area, as in Eq. (11);

$$L_d = \frac{\sum_{i=1}^{i=n} L_i}{A}, \tag{2-19}$$

Where $\sum_{i=1}^{i=n} L_i$ denotes the total length of lineaments (km) and A denotes the unit area (km^2). A high length of lineament refers to the high level of fractures, and so indicates a zone with a high groundwater potential. The weighting and rating of the lineament-length density were classified into four types by the method of (Selvam, Dar et al. 2016).

5) Land use**:** Land use is an important factor in groundwater recharge. (Leduc, Favreau et al. 2001) found that the difference in the volume of groundwater recharge mainly caused by changes in land utilization. (Shaban, Khawlie et al. 2006) concluded that vegetation cover benefited the groundwater recharge by three main routes, Firstly, biological decomposition of the roots helps water to flow easily under the surface. Secondly, vegetation prevents the direct evaporation of water in the soil,

while thirdly the roots of a plant can absorb water. According to (Patil and Mohite 2014), land use controls the occurrence of groundwater and also causes the recharge.

6) Soil: Soil is a significant factor in the groundwater recharge and runoff (Murthy 2000) as it is the medium through which water must penetrate to get into the water table. The water holding capacity of an area depends on the types and permeability of the soils. Groundwater recharge capacity is lower on hills due to the high degree of slope that results in a high runoff. Soils have the capacity to generate biomass and act as the filter between the atmosphere and the groundwater aquifer (Selvam, Dar et al. 2016). Soil types are more important and are the main factor in determining the groundwater recharge in agricultural production. Soils have an important role in supporting or resisting the groundwater recharge and determining the quality factors of groundwater (Lillesand, Kiefer et al. 2014). Soil media represents the uppermost weathered portion of the unsaturated zone, which then continues to the penetration area of plant roots and organic creature activities (Baghapour, Talebbeydokhti et al. 2014).

2.9 Overlay Technique

Overlay analysis is one of the spatial GIS operations which integrate spatial data with attribute data. (Attributes are information about each map feature.) Overlay analysis is combining information from one GIS layer with another GIS layer to derive or infer an attribute for one of the layers.

The key elements in feature overlay are the input layer, the overlay layer, and the output layer. The overlay function splits features in the input layer where they are overlapped by features in the overlay layer. New areas are created where polygons intersect. If the input layer contains lines, the lines are split where polygons cross them. These new features are stored in the output layer. The original input layer is not modified. The attributes of features in the overlay layer are assigned to the appropriate new features in the output layer, along with the original attributes from the input layer.

In raster overlay, each cell of each layer references the same geographic location. That makes it well suited to combine characteristics of numerous layers into a single layer. Usually, numeric values are assigned to each characteristic and be able

to mathematically combine the layers and assign a new value to each cell in the output layer (Resources).

2.10 The Previous Investigations for This Research Assessment

2.10.1 Groundwater balance and safe yield in the country

1) (Arlai, Lukjan et al. 2012) numerical investigation of the groundwater balance in the Mae Sai aquifer, Northern Thailand, for determining the groundwater balance in the Mae Sai aquifers. The Mae Sai aquifer is conceptualized as a multi-layer aquifer and groundwater flow is simulated by a fully 3D finite difference model. The numerical results show that (a) the top layer of the multi-aquifer system is the most productive aquifer with groundwater yields of about 186,000 cubic meter per day, whereas the 4th aquifer is the least productive, with a groundwater yield of only 14,000 cubic meter per day, (b) the rainfall recharge is the most influential inflow into the groundwater system, whereas the inflow from the bordering river (simulated through a general head boundary condition) plays only a small role, and (c) the most number of pumping wells are developed in the 3rd aquifer (2,400 cubic meter per day).

2) (Koch, Arlai et al. 2012) modeling investigation on the future permissible yield in upper Chiang Rai aquifers system, for the estimation of the future permissible groundwater yield. The result is a total permissible yield of 1.3 cubic meters per rai per day for the upper Chiang Rai aquifer system.

3) (Nettasana, Craig et al. 2012) conceptual and numerical models for sustainable groundwater management in the Thaphra area, Chi River Basin, Thailand, to predict the impacts of future pumping on hydraulic heads. Four scenarios of pumping and recharge were defined to evaluate the system response to future usage and climate conditions, uses the three-dimensional finite-difference flow models were developed with MODFLOW. Primary model simulations show that groundwater heads will continue to decrease by 4 –12 meters (2040) at the center of the highly exploited area, under conditions of both increasing pumping and drought. The uncertainty analysis results strongly support addressing conceptual model uncertainty

in the practice of groundwater management modeling. Doing so will better assist decision makers in selecting and implementing robust sustainable strategies.

2.10.2 Groundwater balance and safe yield in the abroad

1) (Zhou, Wang et al. 2012) create options of sustainable groundwater development in Beijing Plain, China, for achieving a long-term sustainable development of groundwater resources in Beijing Plain. Four options of groundwater development in Beijing Plain were formulated and assessed with a regional transient groundwater flow model. The combined scenario of the reduction of abstraction and the increase of recharge could bring the aquifer systems into a new equilibrium state in 50 years.

2) (Shi, Chi et al. 2012) identifying the sustainable groundwater yield in a Chinese semi-humid basin. To address this problem, an integrated evaluation model was constructed for a series of purposes including the maximal efficiency of water use, the integral benefit of development and utilization, the optimized environmental water demand and the minimal anthropogenic influence on groundwater system. Results indicated the optimized groundwater yield could be sustained by intensive reservoir supply and maintain suitable ecological water demand simultaneously. The work proposed a potential groundwater utilization strategy for economically developing countries across the worlds.

3) (Hugman, Stigter et al. 2013) the importance of temporal scale when optimizing abstraction volumes for sustainable aquifer exploitation: A case study in semi-arid South Portugal, to understand the effects and feasibility of varying the temporal scale at which groundwater abstraction is modified in order to maximum sustainable yield and minimum freshwater losses. To predicted seasonal changes in rainfall for Portugal will make taking the temporal scale of the system into account more important, as the concentration of recharge into a shorter period will lead to faster depletion.

2.11 Sensitivity Analysis

Sensitivity analysis refers to the analysis of the effects of adjusting parameters used in model calibration. If the results show which parameters are high sensitivity, that parameter is important to the model.

Monte Carlo method is the most commonly used method for model sensitivity analysis (Beven and Binley 1992). The method is a study of the relationship of each parameter in the model that affects the results from the model (Morgan, Henrion et al. 1992). The method is used the probability principle to determine the optimal parameters by replicating the event repeatedly, but with a certain number of times, to achieve different values of results (Karuchit 2002).

2.12 Uncertainty Analysis

Uncertainty is a representation of model reliability. There are three possible reasons (Helton 1993) as follows:

1) Scenario Uncertainty is caused by incomplete data, resulting in uncertainty in forecasts. In addition, there may be discrepancies in the preparation of the information or may result from inappropriate model selection.

2) Parameter Uncertainty is caused by data discrepancies, such as the amount of data is too small, error from measurement or sampling.

3) Model Uncertainty is caused by model constraints. In addition, uncertainty may be due to model structure, model detail, validation, or extrapolation.

CHAPTER III
AREA DESCRIPTION

3.1 Location and Topographic

The study area locates in lower Khwae Hanuman sub-basin, as part of the Prachinburi basin. This sub-basin consists of Nadi District and Kabinburi District, Prachinburi province, approximately 900 square kilometers. The area is in longitudes 101^{o} 38' 15.86" to 102^{o} 6' 13.37" E and latitudes 13^{o} 57' 7.19" to 14^{o} 13' 2.64" N (zone 47N at 785,000-835,000 East and 1,547,000-1,574,000 North). Topography details of lower Khwae Hanuman sub-basin (**Figure 3.1**) as follow:

1) Mountain Range – The northern side area covers Nadi District, which is source of rivers in this area such as Khwae Hanuman River, Prachantakham River and Huai Samong River. Ground levels in the range of 201-548 m amsl.

2) Hill and Intermountain basin – Most of area is northern side and central. The area between mountain and plain area cover part of Nadi District and Kabinburi District. Ground levels in the range of 51-200 m amsl.

3) Plain area – It covers a large of study area, covers central area adjacent to the southern area. The central area is flat and has several rivers and tributaries, including Khwae Hanuman River, Prapong River, Huai Sai Noi sub-river, Huai Sai Yai sub-river, Huai Prayathan sub-river, and Huai Samong sub-river. Ground levels in the range of 0-50 m amsl.

4) Khwae Hanuman River – Occurrence from Khao Yai mountain range, There has a length 38.3 kilometers and flows through Nadi District and Kabinburi District. These rivers merge with Bang Pakong River at Ban Sapan Hin.

3.2 Climate

Climate in study area (DGR 2008) is classified as tropical climate with influence from Southwest and Northeast Monsoons. Climatic feature in this region can be described below:

3.2.1 Season: Considering temperature and rainfall amount, climate in this region can be classified into three seasons as follow:

1) Summer – The summer starts from February until May. The temperature is rather high especially in April which the average monthly maximum temperatures reach 36.9 degrees Celsius.

2) Rainy - The rainy season starts from May until the end of October. During this period, the region is influenced by the Southwest Monsoon which brings moisture from the Indian Ocean. September is the month with highest rainfall.

3) Winter – The winter begins in November and ends at January. The area is influenced by the Northeast Monsoon which brings cool weather from Vietnam. The lowest temperature is in December with mean monthly minimum temperature 19.4 degrees Celsius.

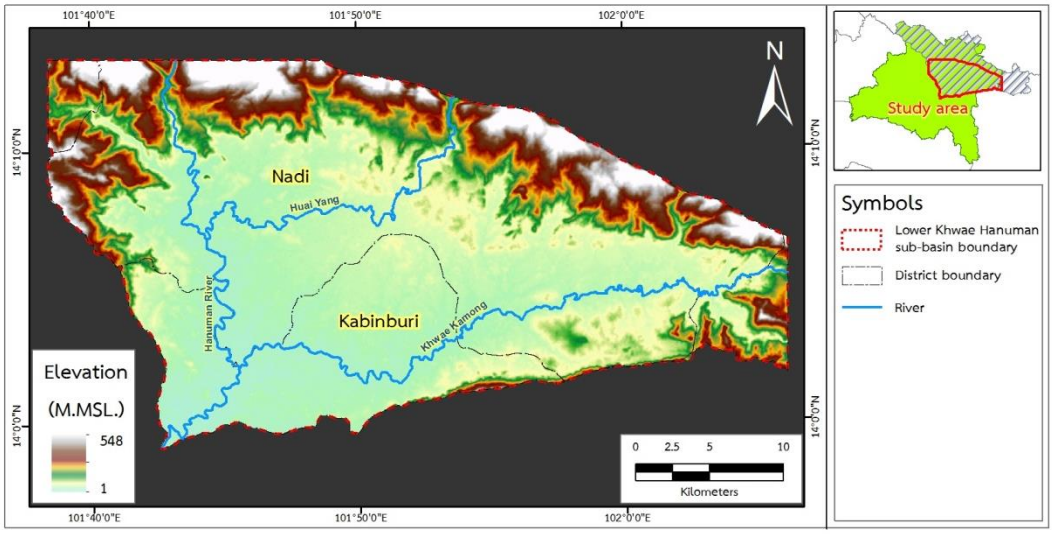

Figure 3. 1 Topography of lower Khwae Hanuman sub-basin

3.2.2 Temperature: Monthly mean temperature in Kabinburi District, Prachinburi province, rather high all year, range from 25.5 – 29.7 degrees Celsius. The mean maximum temperature is 36.9 degrees Celsius in April, whereas the mean minimum temperature is 19.4 degrees Celsius in December.

3.2.3 Relative Humidity: The relative humidity in Kabinburi District, Prachinburi province is rather high with 77% of annual value. The mean monthly value varies from 67% in December to 86% in August.

3.2.4 Evaporation: The evaporation rate (TMD 2015) is related to relative humidity and temperature. The average monthly evaporation in this region varies

from 117.7 millimeter in August to 161.9 millimeter in May. The annual evaporation is about 1,597.2 millimeter per year. In this study, evaporation rate data from 2 stations (ST.430201 and ST.430401) were collected. Details of the selected stations and recording periods are shown in Table 3.1. August has lowest evaporation rate while May has highest evaporation rate.

Table 3. 1 Evaporation and rainfall other stations

Month, 2015	**Rainfall (mm)**		**Evaporation (mm)**	
	ST.430007	**ST.430401**	**ST.430201**	**ST.430401**
January	Non	4.80	127.30	135.70
February	5.90	31.20	128.60	118.80
March	22.80	31.50	130.10	152.90
April	48.60	84.40	143.20	166.20
May	35.90	121.20	159.60	164.30
June	167.40	91.60	150.80	132.70
July	329.20	167.00	138.40	127.80
August	277.00	356.70	120.40	115.00
September	295.70	248.20	122.90	115.70
October	239.20	231.90	129.30	111.50
November	14.80	31.20	130.40	121.00
December	Non	Non	116.70	135.00
Total	**1,436.50**	**1,399.70**	**1,597.70**	**1,596.60**
Dry	**280.60**	**364.70**	**839.60**	**870.60**
Rainy	**1,155.90**	**1,035.00**	**758.10**	**726.00**
Avg.	**119.71**	**116.64**	**133.14**	**133.05**

* ST.430401 (Nadi station), ST.430007 (Kabinburi station), ST.430201 (Prachinburi station)

3.2.5 Wind: The prevailing wind in summer and rainy season is mostly southerly wind whereas the prevailing wind in winter is northerly and northeasterly wind. The mean monthly wind speed is about 1.0 to 3.1 knots.

3.2.6 Rainfall: The mean monthly rainfall (TMD 2015) varies from 5.4 millimeter in January to 316.9 millimeter in August. The annual rainfall is 1,418.1

millimeter. The total number of rainy day is 90 days in a year. In this study, rainfall data from 2 stations (ST.430007 and ST.430401) are collected. Details of the selected stations and recording periods are shown in Table 3.1. The highest rainfall is in August while January has the lowest rainfall.

3.3 Surface Water Sources

Lower Khwae Hanuman sub-basin includes of Nadi and Kabinburi Districts, Prachinburi province. The area is around 900 square kilometers. The boundary of area reach the upper Khwae Hanuman sub-basin (north), the lower Mae Nam Prachinburi sub-basin (south), the Mae Nam Phra Prong sub-basin (east) and the Lum Takhong sub-basin (west). The Khwae Hanuman River is 38.3 km long and flows into Bang Pakong River (DWR 2004).

Surface water table study has provided of surface water table data to use in modeling. This study collected surface water table data (Royal Irrigation Department) in the study area three spots namely; Khwae Hanuman (Kgt 34), Khwae Kamong (Kgt 15A) and Huai Yang (Kgt 14), details as show in **Table 3.2** and **Figure 3.2**

Table 3. 2 The details of rivers in lower Khwae Hanuman sub-basin area

Code	River Name	Coordinates		Riverbed (m amsl)	Average River Stage (m amsl.)			River Width m.
		E	N		Dry season 2015	Rainy season 2015	Dry season 2016	
KGT14	Huai Yang	810975	1567119	32.64	34.30	35.30	34.15	50
KGT15A	Khwae Kamong	816223	1556993	12.26	14.93	15.71	14.26	50
KGT34	Khwae Hanuman	796305	1561025	17.70	19.88	22.07	19.26	60

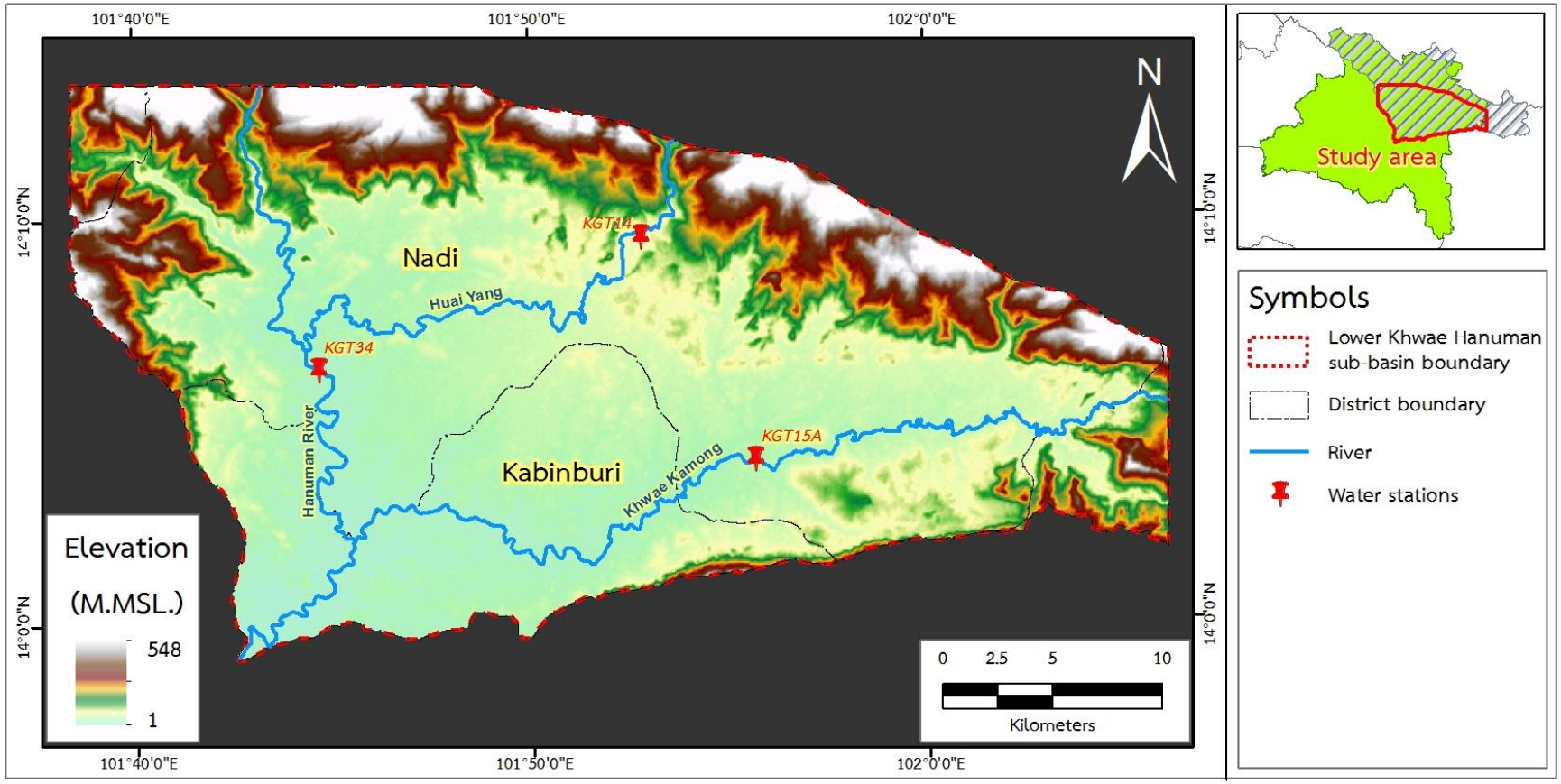

Figure 3. 2 The water stations of Lower Khwae Hanuman sub-basin area

3.4 Soil properties

The soil data in this study was based on the soil map which derived from Land Development Department. There can be divided soil group in this area to 17 groups, which the most area of soil group is unit 62 (36.88 % of area) and smallest area is unit 3 (0.05 % of area) as shown in **Table 3.3** and **Figure 3.3**.

Table 3. 3 Percentage of the soil group unit area

Soil Group Units	Area (Square Kilometers)	Percentage
3	0.48	0.05
4	37.95	4.22
6	12.45	1.39
17	234.24	26.06
18	2.40	0.27
21	0.95	0.11
24	13.05	1.45
25	10.38	1.15
35	164.26	18.28
38	16.84	1.87
40	5.83	0.65
46	4.43	0.49
48	84.29	9.38
56	9.47	1.05
59	9.62	1.07
60	17.83	1.98
62	274.32	30.52
Total	**898.79**	**100.00**

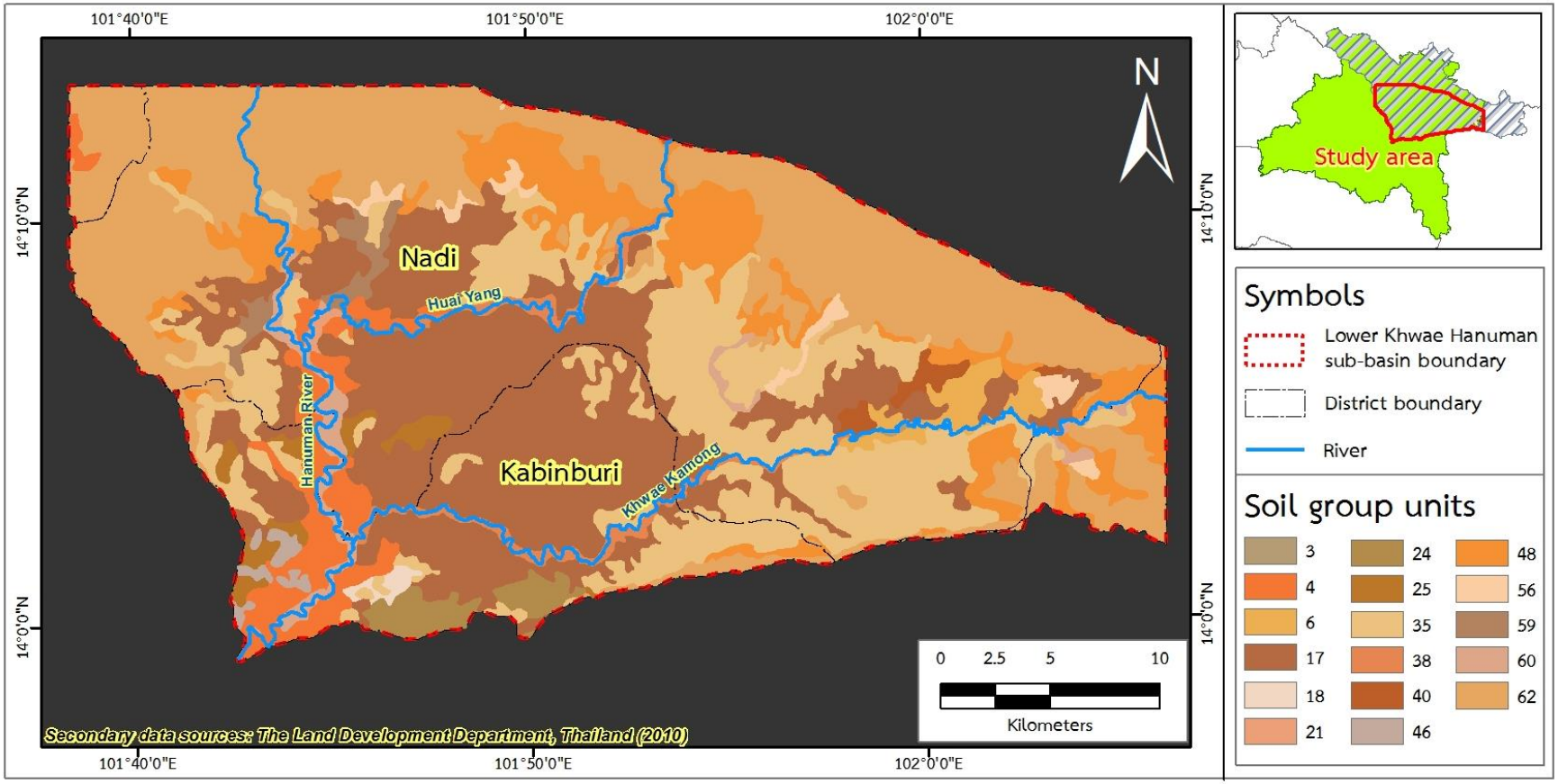

Figure 3. 3 Soil group unit map of lower Khwae Hanuman sub-basin area

3.5 Land use

The land use data in this study was based on the land use map derived from Land Development Department. The results display land use type including agricultural lands, forest area, meadow, local communities and houses and water resources. The land use percentage is 478.30 km^2 (47.17%), 383.54 km^2 (37.82%), 101.20 km^2 (9.98%), 44.98 km^2 (4.44%), and 5.20 km^2 (0.51%), respectively that shown in **Table 3.4** and **Figure 3.4**.

Table 3. 4 Percentage of land use unit area

Code	Type	Description		Area (km2)	%
A	A01	Transplanted paddy field		294.42	32.76
	A02	Corn/Mixed orchard		138.08	15.36
	A03	Eucalyptus		23.47	2.61
	A04	Mixed orchard-Corn		19.29	2.15
	A07	Poultry farm house		0.56	0.06
			Sum	475.82	52.94
F	F01	Disturbed evergreen forest		249.66	27.78
	F02	Disturbed deciduous forest		23.80	2.65
	F03	Mixed forest plantation		2.37	0.26
			Sum	275.83	30.69
M	M01	Grass		98.58	10.97
			Sum	98.58	10.97
U	U01	City, Town, Commercial and Service		0.46	0.05
	U02	Low land village-Mixed orchard		35.45	3.94
	U03	Institutional land		1.19	0.13
	U05	Factory		6.17	0.69
	U06	Golf course		0.73	0.08
			Sum	44.00	4.90
W	W01	Lake		4.14	0.46
	W02	Reservoir		0.41	0.05
			Sum	4.55	0.51

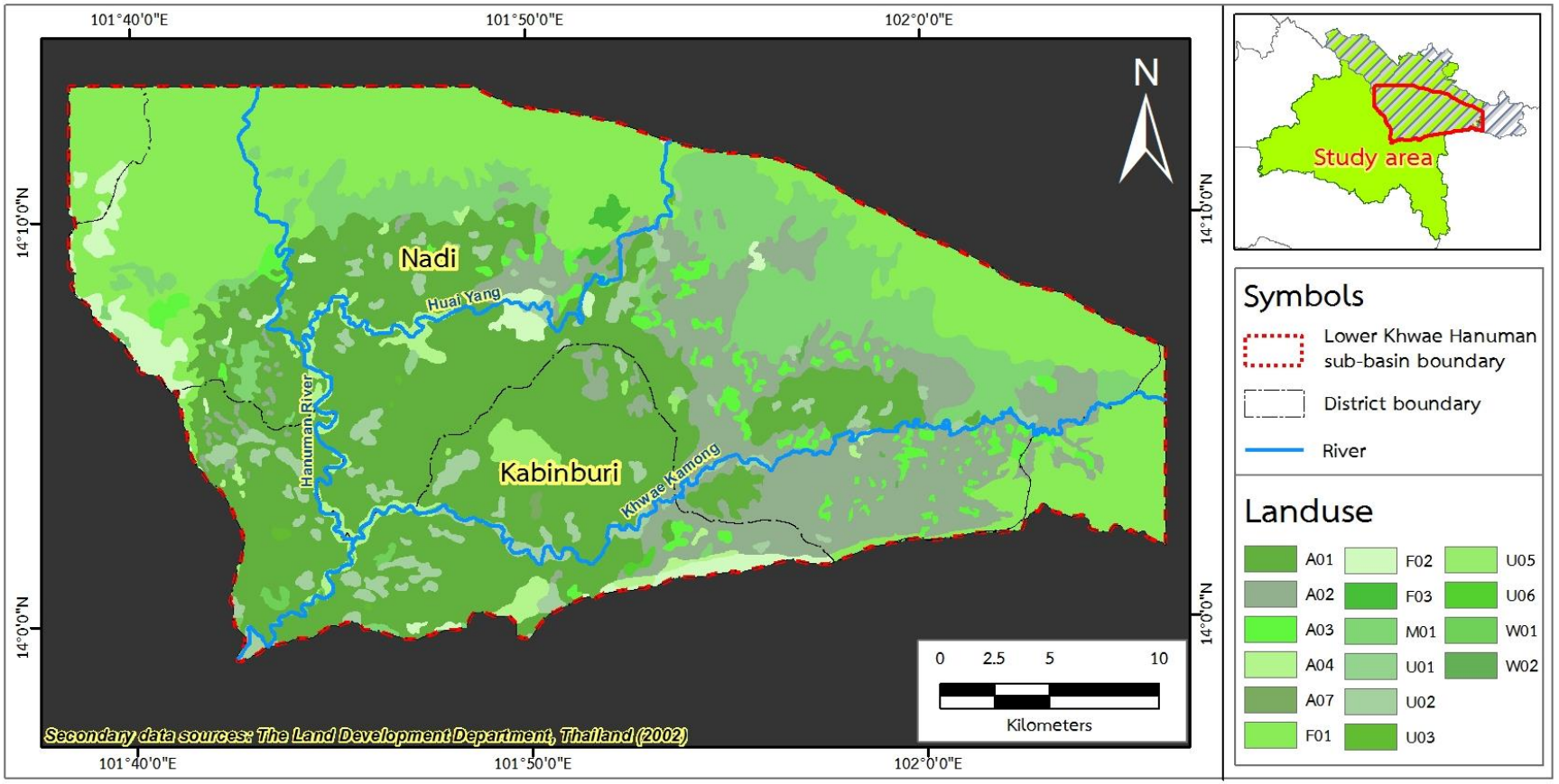

Figure 3. 4 Land use map of lower Khwae Hanuman sub-basin area

3.6 Geomorphology

From the geomorphology derived from the DMR, the study area is located in the river plains of Hanuman, as part of the Prachinburi River basin, which geomorphology characteristics was classified into five divisions as follow:

1) Alluvial Fans - there founds widespread in central to the south area and around the Khwae Hanuman River, with 5-20 m amsl.. The topography characteristic is slightly wavy slopes landscape which consists of clay, silt, gravel sandy mixed, mostly fine sand to coarse sand.

2) Alluvial – there can be found in central to the south area and around the alluvial fans geomorphic. The elevation is 8-30 m amsl.. The topography characteristic is slightly wavy slopes landscape which consists of clay, silt, gravel and sand.

3) Terraces – there expands in central area and near the Khwae Kamong River. The elevation is 20-30 m amsl.. The topography characteristic is slightly wavy slopes landscape which consists of terrace sediment, clay, silt, gravel and sand. The lower layer is bed of brownish red laterite, 10-20 cm size. Next layer (lower) is sandy clay, which has gone through weathering process for a long time.

4) Peneplain - the elevation of area is 10-50 m amsl.. Abundant laterite cover on surfaces, caused by weathering process of metamorphic rocks (3-4 mm thickness) and granite (4-5 mm thickness), consisting of quartz and feldspars.

5) Mountains and hills – there can be found in several areas in north, east and west. The significant characteristic mountains are the height and continuous. The elevation ranges from 51-500 m amsl.. A few mountains may be higher than 500 m. This geomorphology consists of sandstone and shale (Jurassic - Cretaceous Era) and igneous rocks (Triassic Era).

3.7 Geology

The geology data from the 1:50,000 scale geological maps derived from Department of Mineral Resources, the study area is mainly composed of sandstone, siltstone and conglomerate of the middle Khorat group, along with units of

sedimentary rock, such as alluvial and fluvial deposits that shown in **Figure 3.5**. There can be summarized by sorting from youngest to oldest age as follows:

1) Alluvial deposits (Qa) - the units aged in Quaternary period consisting of gravel, sand, silt and clay. The deposit characteristic is along river. Sediments are very sorted and rounded.

2) Terrace deposits (Qt) - the units aged in Quaternary period including gravel, sand, silt, clay and laterite. The deposit characteristic is plains causing by flood.

3) Fluvial deposits (Qff) - the units aged in Quaternary period including gravel, sand, silt and clay. The deposit characteristic of sediment is alluvial fan.

4) Colluvial deposits (Qc) - the units aged in Quaternary period consist of rock fragments in clayey sand or sand matrix. On the surface is found that horizontal sand, the next layer (lower) is commonly laterite. The deposit is occurred by residual weathering process.

5) Phu Phan Formation (Kpp) - the rock unit is in the middle Khorat group including gray and medium to coarse grained conglomeratic sandstone, pebbles of quartz, chert, jasper and volcanic rock. The sedimentary feature can be classified as poor to moderate sorted, sub rounded and silica cement. Rocks bedding are medium to very thick with cross bedding.

6) Sao Khua Formation (Ksk) - the rock unit is in the middle Khorat group which consist of reddish brown, purplish red and purple siltstone and some mixed calcareous, intercalated with brownish red and fine to medium grained sandstone and micaceous campsites. The special characteristics of this unit are small to medium scaled cross-bedding and paleosol.

7) Phra Wihan Formation (JKpw) - the rock unit is in the middle Khorat group consist of brownish white and reddish brown, medium to coarse grained sandstone and conglomeratic sandstone. Sedimentary feature can be classified as moderately to well sorted. Rock beddings are medium to very thick. Special characteristic is planar cross-bedding. This formation is very hard rock and low erosion. Thickness is around 56 to 136 meters.

8) Phu Kradung Formation (Jpk) - the rock unit is in the lower Khorat group which consist of maroon and reddish brown siltstone, brown, gray and yellow micaceous sandstone and micaceous shale. The special characteristics of this unit are small scaled cross-bedding and limestone nodules. This formation exposes some Permian formation with unconformity pattern. The formation thickness is around 1,001 meters.

9) Unknown Formation Triassic Era (Tr) - the units is in the Triassic era including gray and yellowish brown sandstone, greenish gray greywacke, conglomerate and limestone lens. There can be found in a small area southward of study area.

10) Sap Bon Formation (Ps) - the unit is in the Triassic era consisting of chert, shale interbedded with limestone lens, greywacke, tuff and agglomerate. There can be found fossils of fusulinid and radiolaria. The formation thickness is around 1,103 meters.

3.8 Structural geology

Following the geology of Thailand book (Ridd, Barber et al. 2011), there can be concluded that the structural geology in Prachinburi province has mainly northwest - southeast direction of bedrock, which is consistent with direction of Kho Look Chang and Kho Mai Kaew. The limestone group at Baan Kho Poon was found the intruding of quartz vein dike (N40W direction) which parallel to the axis of large syncline of Khorat group. Syncline was appeared in the Permian and Permo-Triassic period which have axis direction in northwest - southeast. Folding was occurred in late Triassic to early Jurassic period, as a result of Indosinian Orogeny and granite intrusion. Faults and fractures have mainly direction in northwest – southeast, and a couple fractures in the northeast - southwest and east – west direction.

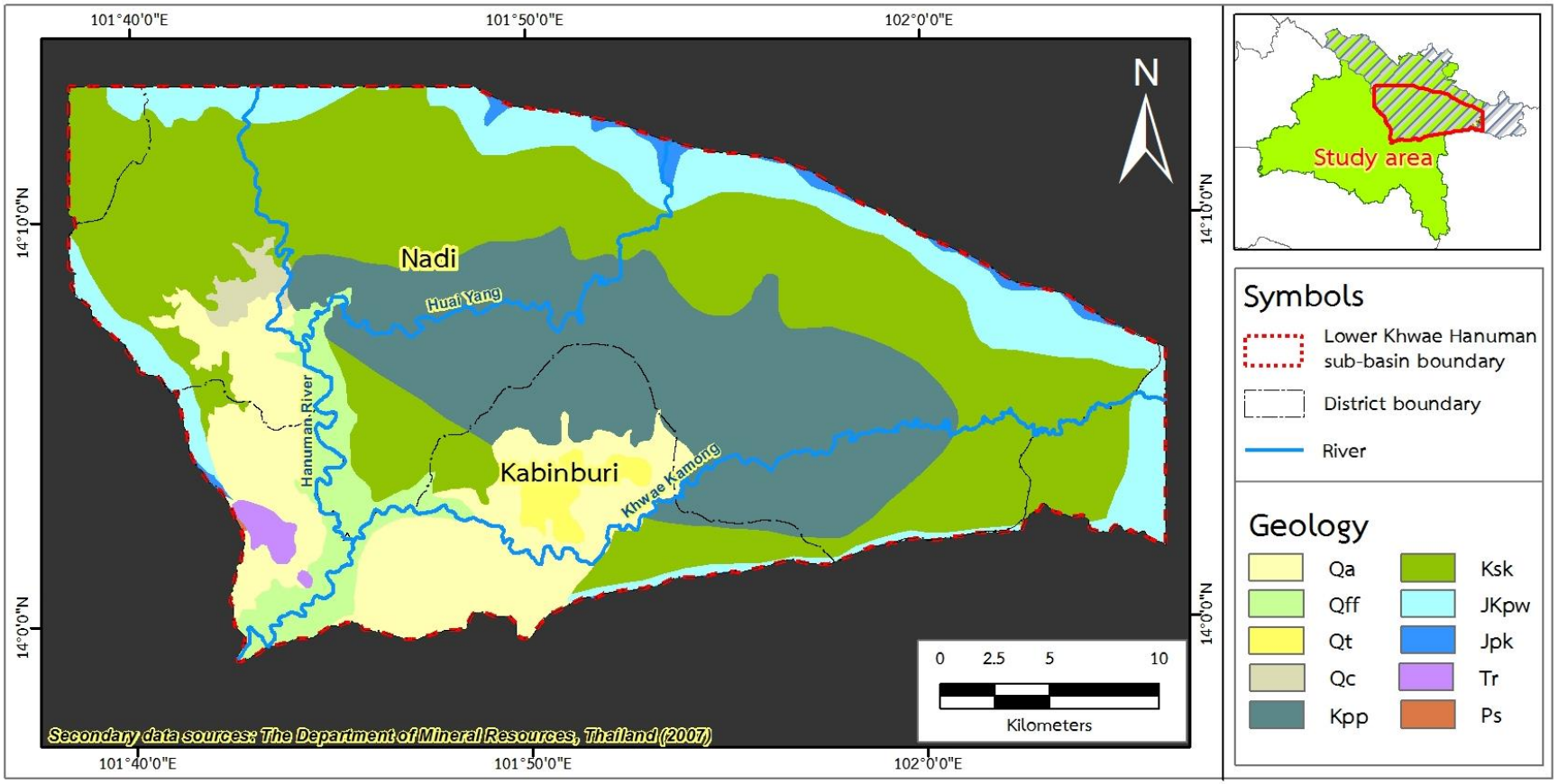

Figure 3. 5 Geological maps of lower Khwae Hanuman sub-basin area

3.9 Geological history

According to the geology of Thailand book (Ridd, Barber et al. 2011), the study area was submerged sea in early Triassic period. In late Triassic period, there has suffered pressure from igneous intrusion in Northeastern, as a result to ground shifting. The uplifting ground level lead to the deposition of sediment changes from the marine deposit to continental deposit (sandstone and shale of the Khorat group). In early Tertiary period, there has a tremendous tectonics occurred which result to northern and middle plateau collapsed into large basin, called the Chao Phraya basin. As a result of the Tectonic events, the study area became the contract between the Korat Plateau and the Chao Phraya Basin. It was part of the Tectonic Chan - Thailand and Indochina (Bunopas and Vella 1983).

3.10 Hydrogeology

The hydrogeology data from the 1:100,000 scale hydrogeological maps derived from the DGR. There can be summarized that the most hydrogeological formation of study area is in middle Khorat aquifer that shown in **Figure 3.6**. The groundwater can be found in the fractures of rock. In addition, the hydrogeology in this area which is consist of Permian carboniferous metasediments aquifer (PCms) and volcanic aquifer (Vc), the details are as below:

1) Middle Khorat aquifer (Jmk) - the aquifer unit is in Khorat aquifer which Jurassic aquifer consist of white, gray and yellowish brown sandstone, cemented by silica, very low weathered. Groundwater can be found in fractures of rock. The depth of groundwater aquifer is about 5 to 10 m. The rate of water is 2 to more than 10 m^3/hr and good water quality.

2) Permo-Carboniferous metasediments aquifer (PCms) - the aquifer unit is in Permo-Carboniferous aquifer which consist of sandstone, shale, slate interbedded with limestone lens, quartz-schist, phyllite and gneiss. Groundwater can be found in the fractures of rock. The average depth of groundwater aquifer is about 24 to 42 m. The rate of water is 2 to less than 10 m^3/hr and good water quality.

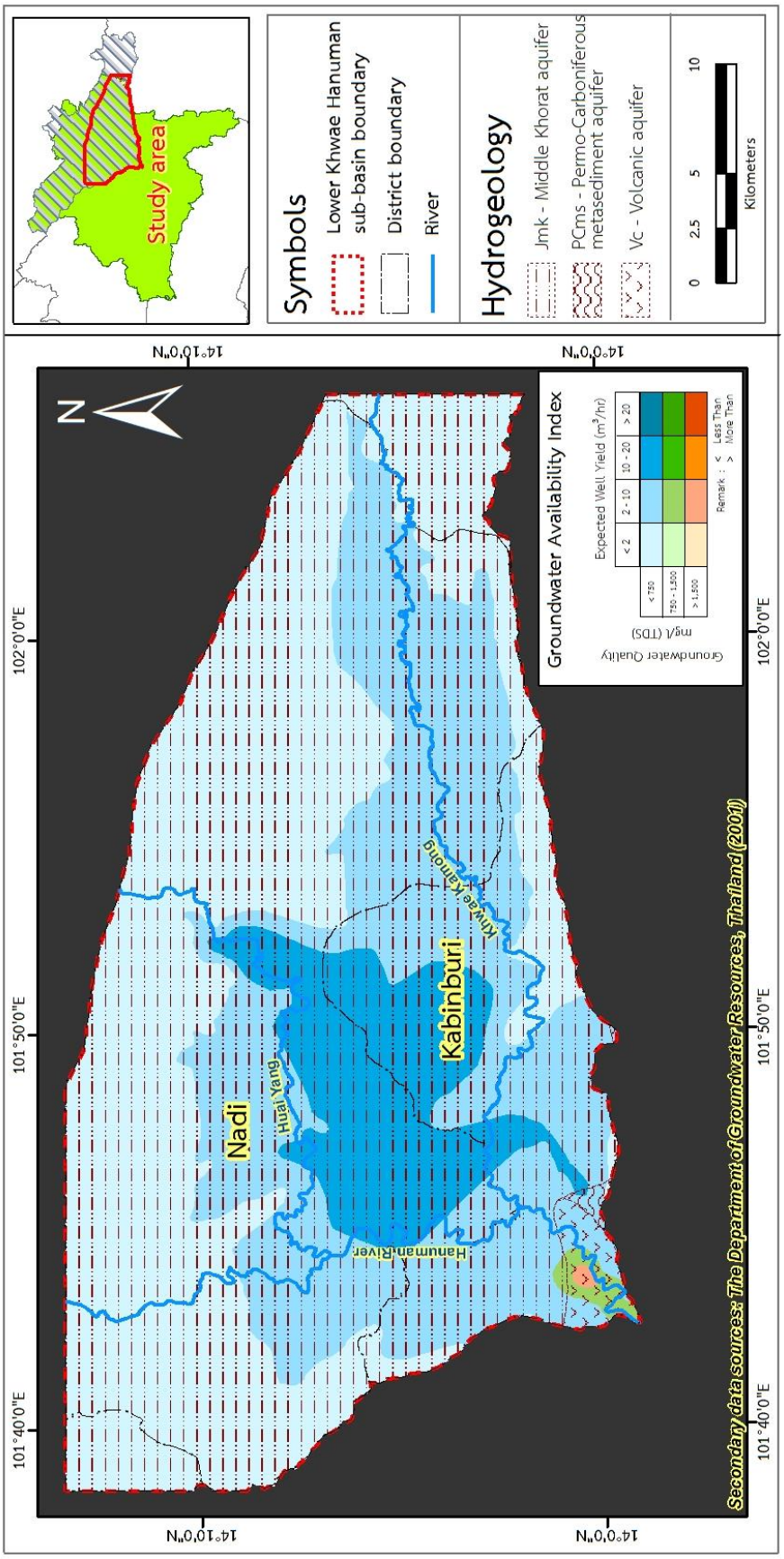

Figure 3. 6 Hydrogeological maps of lower Khwae Hanuman sub-basin area

3) Volcanic aquifer (Vc) - the aquifer unit is in volcanic rock aquifer which consist of rhyolite, andesite and tuff. The groundwater can be found in the fractures of rock. The average depth of groundwater aquifer is around 24 to 60 m. The rate of water is 1 to less than 10 m^3/hr and good water quality.

3.11 Hydrogeology cross section

The geological maps 1:50,000 in scale which derived from the Department of Mineral Resources shown that the study area is located in Quaternary deposits of the central part of lower Khwae Hanuman sub-basin. The Quaternary deposits can be divided into 4 groups namely; alluvial deposits of Khwae Hanuman River, terrace deposits, fluvial deposits and colluvial deposits. The alluvial deposit of Khwae Hanuman River consists of clay, silt and sand.

The lithologic logs data of 91 wells were recorded by the Pasutara database of Department of Groundwater Resources. The details of these wells are shown in **Table 3.5** and **Figure 3.7**. The study results can be stratified aquifers into two sequences: quaternary sediment aquifer is a sequence A with depth 0-35 m and sequence B is weathered rock aquifer with depth 55-120 m The sequence A is aquifer of all sediments in study area which consist of gravel, sand, silt, clay and laterite. The sequence B is hard rock aquifer which consists of mostly sandstone and shale. The stratigraphic correlation of hydrogeologic cross-section are 8 line; A-A', B-B', C-C', D-D', E-E', F-F', G-G' and H-H', as shown in **Figures 3.8** to **3.11**. The sequences details as below:

3.11.1 Sequence A

This sequence was found that all sediments thickness ranges from 1.5 to 27 m There can be divided in 4 sediment sequences following by geological maps 1:50,000 in (Department of Mineral Resources, 2008), four sequences can be primary divided in 10 sedimentary facies. These facies mainly consist of gravel, sand, silt and clay, as follow:

Clay - composed of clay, yellowish brown, brown, light brownish gray color, with white mottled, non-plastic to high plastic and compacted textures, some

area is highly calcareous, limonitic massive and sandy slightly. Thickness ranges from 1.5 to 15 m.

Clayey sand - composed of clay and sand, brownish orange, yellowish and white color, grains sizes are very fine sand to coarse sand. Grain properties are sub-angular to sub-rounded and poorly sorted to well sorted. There are contained of quartz, feldspars, some dark minerals, iron oxide, and sandstone fragments. Thickness ranges from 2.5 to 13 m.

Clayey gravel - composed of clay and gravel, various colors. Grains sizes are very fine gravel to fine gravel. Grain properties are sub-rounded and moderately sorted. There are composed of quartz, feldspars and sandstone fragments. Thickness ranges from 1 to 3 m.

Silt - composed of silt, reddish gray and light orangish brown color. There is composed of quartz. Thickness ranges from 1.5 to 9 m.

Silty clay - composed of silt and clay, brownish orange color, plastic textures. Thickness ranges from 2 to 5 m.

Sand - composed of sand, light brownish orange, light reddish brown and light brownish pink color. Grains sizes are fine sand to very coarse sand. Grain properties are sub-angular to sub-rounded and moderately sorted to well sorted. There are composed of quartz and some iron oxide. Thickness ranges from 2 to 9 m and good aquifer.

Sandy gravel - composed of sand and gravel, white color. Grains sizes are very fine gravel to fine gravel. Grain properties are sub-rounded to rounded and moderately sorted. There are composed of quartz and sandstone fragments. Thickness ranges from 2 to 6 m.

Sandy clay - composed of sand and clay, orange, yellowish brown and reddish brown color, non-plastic to slightly plastic textures. Grain sizes are very fine sand to medium sand. Thickness ranges from 1.5 to 5 m.

Sandy silt - composed of sand and silt, greenish green color. There are composed of quartz and feldspars. Thickness ranges from 3 to 6 m.

Gravelly clay - composed of gravel and clay, brown, brownish orange and greenish gray color, slightly plastic textures. Grains sizes are very fine gravel to

fine gravel. Grain properties are poorly sorted with some slate fragments. Thickness ranges from 2.5 to 27 m.

3.11.2 Sequence B

This sequence was identified as high weathered rock, thickness ranges from 10 to more than 30 m There can be primary divided in 9 sedimentary facies. These facies mainly consist of sandstone and shale, as follow:

Sandstone 1 is composed of weathered sandstone, dark gray, yellowish brown to yellow and light reddish brown. Grains sizes are very fine sand to medium sand. Grain properties are angular to sub-rounded and moderately to well sorted, hard and compacted, siliceous cemented. There are slightly to moderately weathered, composed of quartz and white weathered feldspar. Thickness is around 28 m, good aquifer.

Sandstone 2 is composed of sandstone, purplish gray and light gray color. Grains sizes are fine sand. There are slightly weathered to fresh rock, calcareous, brittle, composed of quartz, muscovite, and dark minerals. Thickness is more than 18 m.

Siltstone 1 is composed of weathered siltstone, gray, brown and brownish pink color. Grains sizes are fine sand to coarse sand. Grain properties are sub-angular to rounded and moderately to well sorted, siliceous cemented. There are weathered moderately to high, composed of quartz and iron oxide. Thickness is about 20 m.

Siltstone 2 is composed of siltstone, reddish brown to purplish brown and purplish red. Grains sizes are very fine to fine sand. Grain properties are angular and well sorted, strong calcareous, hard and compacted. There are slightly weathered, composed mostly of quartz. Thickness is more than 25 m.

Shale 1 is composed of weathered shale, brown and reddish brown color. There are moderately weathered, calcareous cemented, hard and brittle. Thickness is around 27 m, with good aquifer.

Shale 2 is composed of shale, reddish brown, dark purplish brown and grayish red color, compacted and massive. There are slightly weathered, brittle and dense, and interbedded with calcareous, very indurated. Thickness is more than 45 m.

Andesite is composed of andesite, red to purplish red color, hard and massive, porphyritic texture, phenocrysts in feldspar and quartz matrix. There are composed of feldspar and amphibole. Thickness ranges 17 to 29 m.

Tuff is composed of tuff and tuffaceous sandstone, purple and reddish brown color. Grains sizes are very fine sand to medium sand, hard. Grain properties are sub-angular to sub-rounded and well sorted. There are weathered slightly to moderately, composed of feldspars, dark minerals, and calcite vein in places. Thickness is around 8 to 27 m.

Limestone is composed of carbonate rock, light gray and dark reddish brown color, massive and hard rock, non-plastic, ferruginous. Thickness is around 10 to 28 m.

Table 3. 5 The location of hydrogeologic log wells

Name	Coordinate		Elev.	Name	Coordinate		Elev.
	North	East	m amsl.		North	East	m amsl.
5503H008	792814	1544891	20.19	MF302	795148	1558783	25.12
5503H046	805828	1563638	34.03	MF312	810518	1564521	58.53
5603H003	810195	1545163	31.76	MF345	788642	1553968	24.98
5703H054	822407	1554349	46.28	MF385	802167	1560888	30.43
5803H002	821883	1553636	52.37	MF388	812196	1573915	80.62
5803H006	826432	1554772	50.00	MF389	811525	1561149	41.00
5803H007	824263	1554409	65.55	MF419	810927	1553607	27.93
C779	800688	1564990	32.53	MF422	818653	1558460	35.63
C792	793047	1548493	10.73	MF460	791565	1552785	22.56
CTV101PB20	802199	1557608	23.88	MF481	800828	1546606	20.00
CTV104PB23	798762	1546371	16.00	MF497	822457	1551258	44.00
DH268	804464	1563837	31.00	MF508	802595	1566638	37.10
DH275	791920	1554660	33.31	MF509	800371	1553251	17.98
DH328	810433	1564289	57.59	MF510	816632	1559519	27.02
DH329	796259	1554144	21.19	MF529	818163	1553522	47.71
DH330	791909	1556058	40.40	MF553	810063	1553439	21.93
DH338	806623	1548686	28.67	MF554	802714	1567803	35.90
DH339	817101	1548211	31.00	MF642	801362	1562068	40.00
DH343	812831	1547969	34.60	MF680	792892	1564373	30.17
DH362	790172	1553336	23.40	MF681	793096	1557479	29.80

Table 3.5 the location of hydrogeologic log wells (continuous)

Name	Coordinate		Elev. m amsl.	Name	Coordinate		Elev. m amsl.
	North	East			North	East	
DH389	788066	1554323	22.40	MF689	806576	1565144	49.79
DH390	786424	1554214	24.93	MF690	820777	1558774	38.00
DH397	809897	1564643	45.60	MF691	821385	1558520	33.50
DH460	809897	1564643	45.60	MF694	813208	1554385	29.39
DJ307	789732	1548327	18.77	MF695	813389	1571922	80.77
DJ309	796422	1564509	29.00	MF707	794398	1564593	24.53
DJ310	798904	1558693	22.29	MF767	800821	1551992	19.83
DJ312	799690	1559704	24.00	MF776	786140	1559062	35.87
MA145	810926	1565783	66.20	MF833	793283	1557772	27.34
MA146	811697	1567072	55.98	MF837	795503	1565098	22.77
MA153	799136	1547273	18.40	MF841	801810	1564425	33.72
MF1025	806533	1552873	21.54	MF856	819290	1550045	48.00
MF119	793162	1563563	22.09	MF884	807145	1565081	50.20
MF124	795849	1548685	17.00	MF908	796399	1559038	20.12
MF1288	815881	1553151	50.93	MF912	808621	1558237	31.06
MF1328	811809	1562733	45.40	MF914	818629	1561518	36.74
MF135	790681	1563838	31.00	MF915	818891	1553689	72.37
MF145	824760	1548548	35.11	MF932	827832	1548501	43.30
MF152	810948	1556380	25.49	MF944	792411	1562399	27.21
MF155	791695	1558368	36.00	PW7956	822204	1548866	35.96
MF156	809630	1544238	27.28	Q102	801204	1563549	26.42
MF197	793254	1561546	36.00	Q117	805216	1547096	22.89
MF264	816087	1559966	35.57	X39	792570	1550185	19.94
MF265	817955	1559173	31.00	X42	793341	1545435	22.87
MF270	799002	1564081	27.47	X43	816250	1544300	21.50
MF276	785170	1550103	16.04				

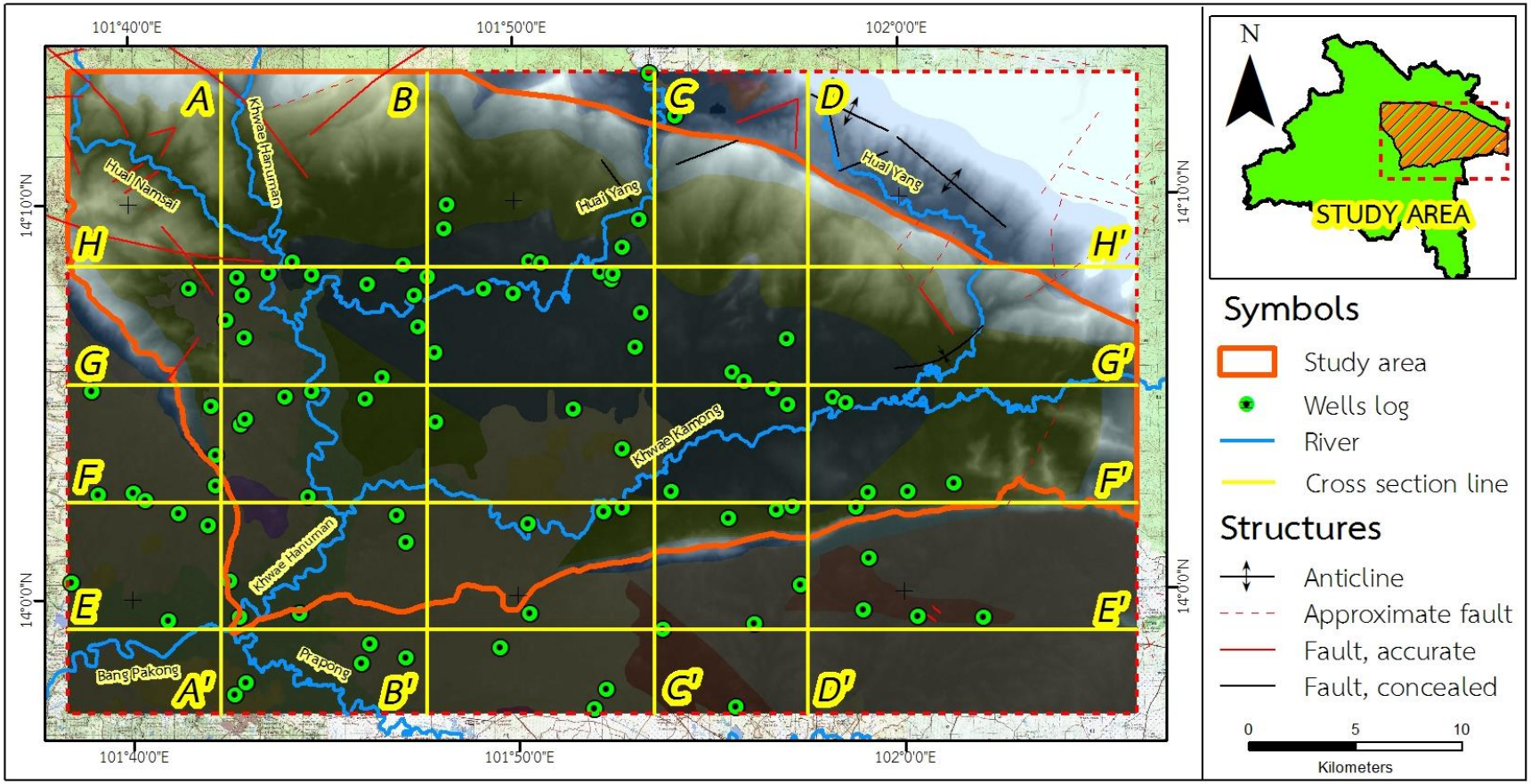

Figure 3. 7 Location of wells and hydrogeologic cross sections line

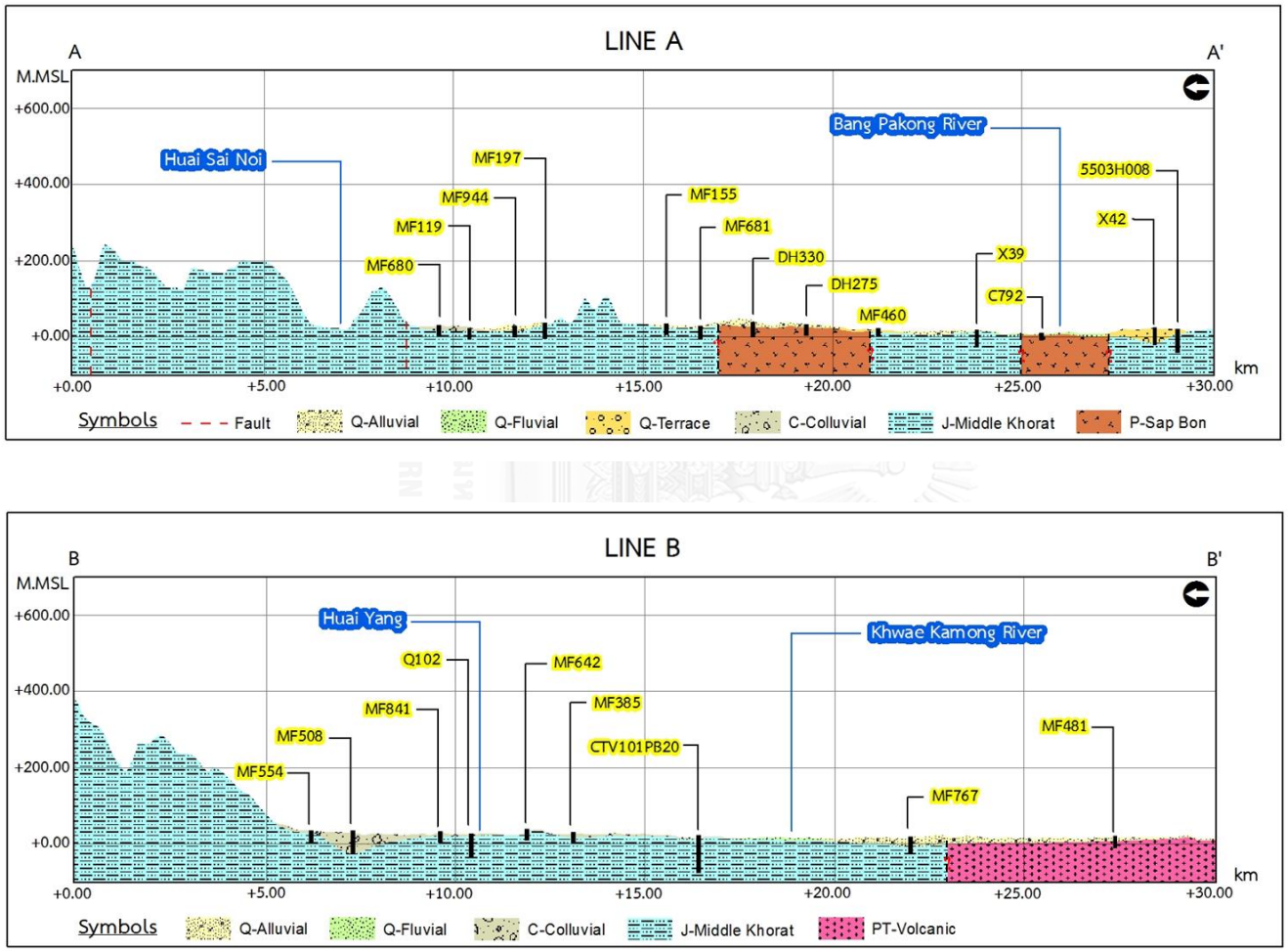

Figure 3. 8 The hydrogeologic cross-section of line A-A'(up) and line B-B' (down)

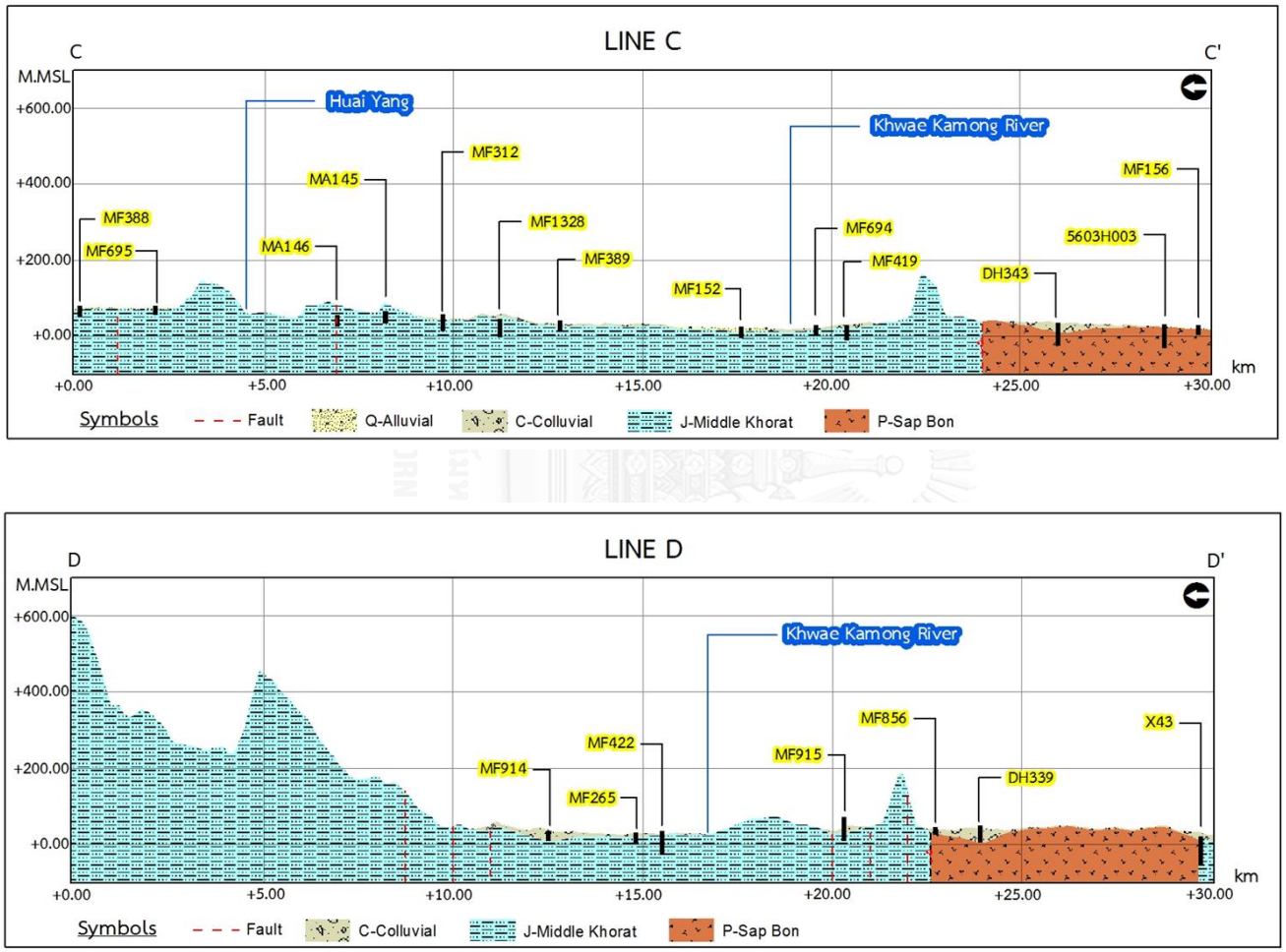

Figure 3. 9 The hydrogeologic cross-section of line C-C’ (up) and line D-D’ (down)

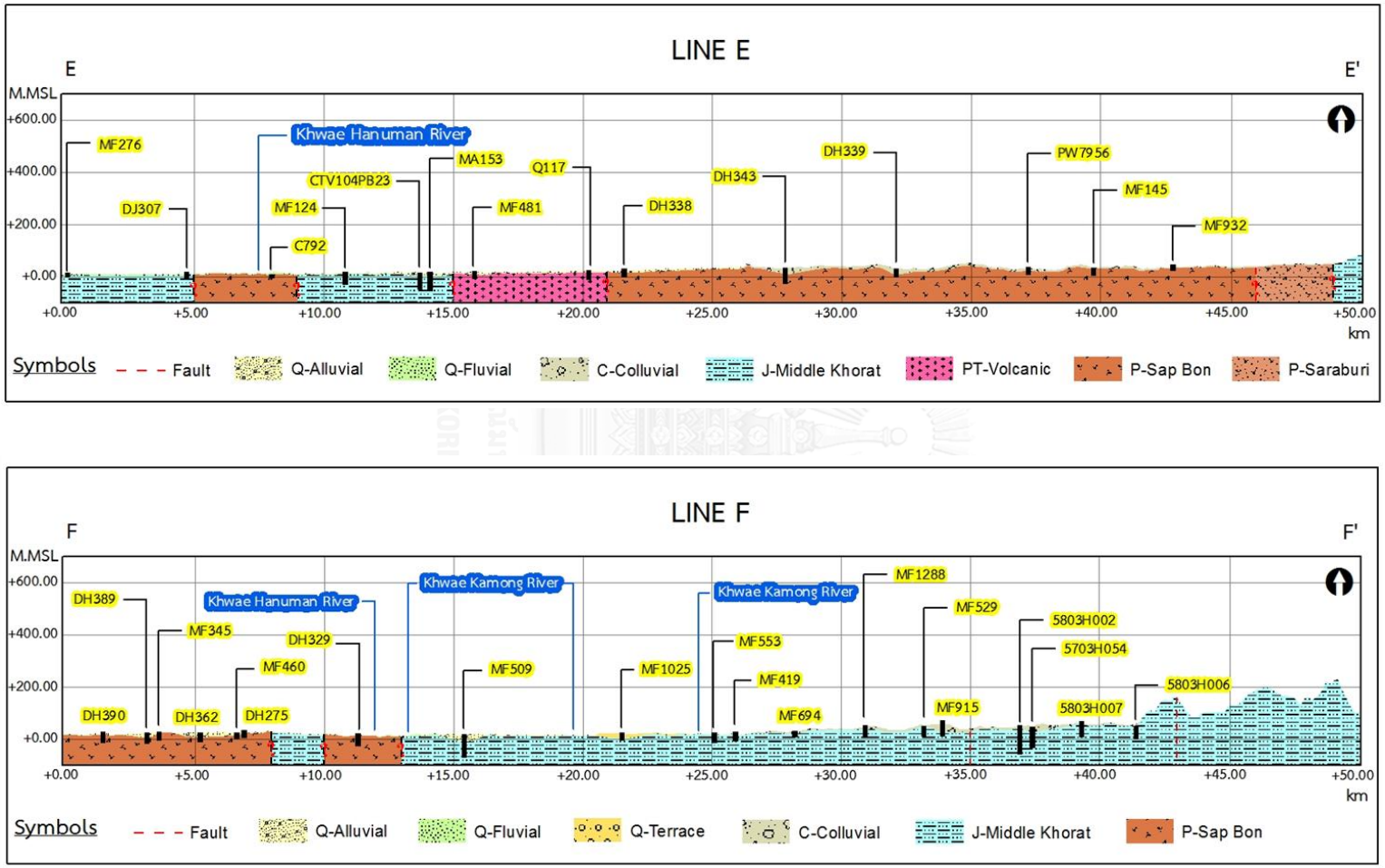

Figure 3. 10 The hydrogeologic cross-section of line E-E’ (up) and line F-F’ (down)

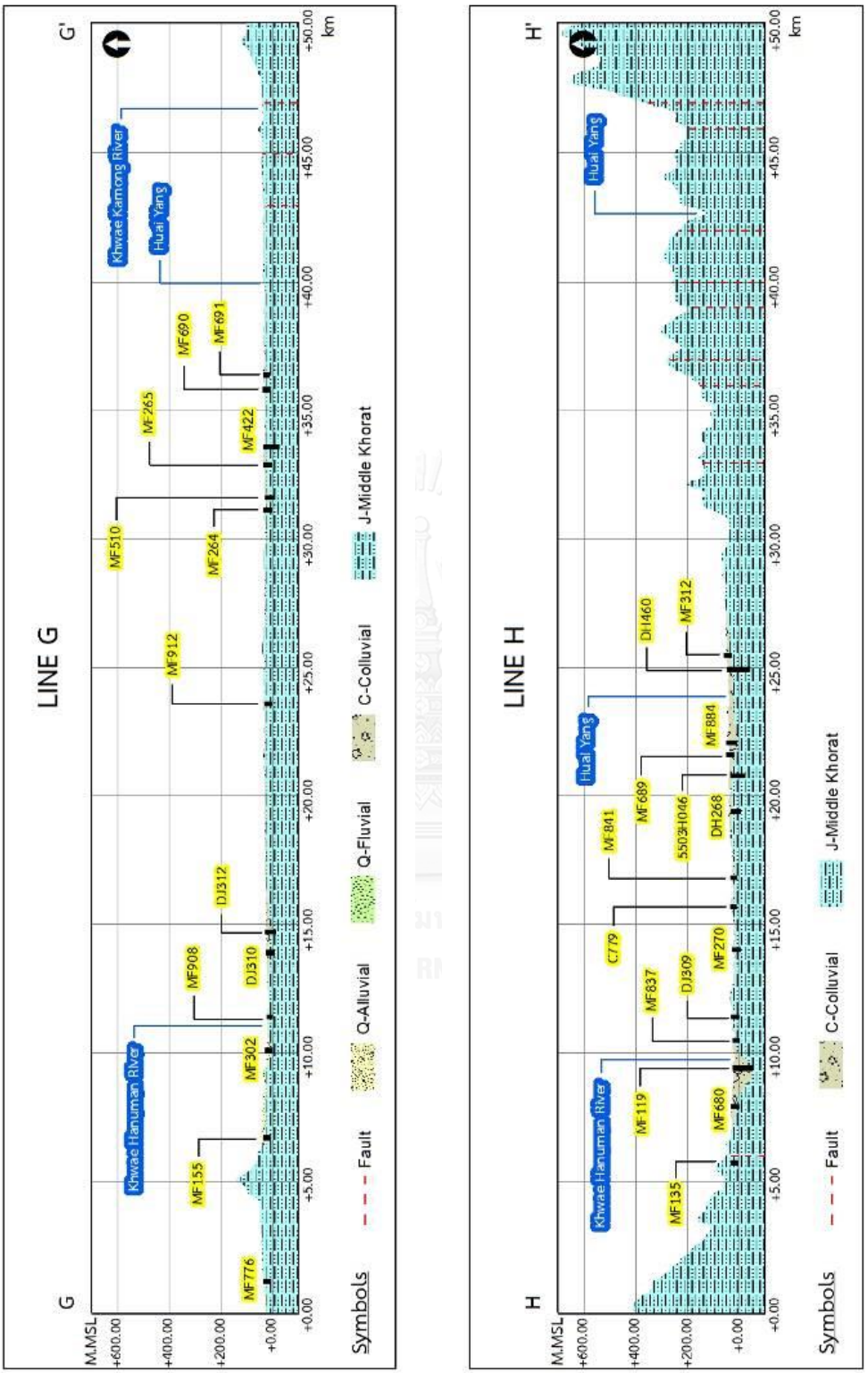

Figure 3. 11 The hydrogeologic cross-section of line G-G' (up) and line H-H' (down)

CHAPTER IV
FIELD INVESTIGATION AND GROUNDWATER RECHARGE

4.1 Field investigation

Field data collection including geological, hydrogeological and hydrological data was conducted during 2015 to 2016. Field investigation of this study had 4 times; the site reconnaissance, the first time collect groundwater level data and surface water level data during the dry season (March, 2015), the second time during the rainy season (November 2015) and the third time during the dry season (May 2016).

4.1.1 Collection of data

1) Site reconnaissance: In November 2014, we conducted site reconnaissance in the study area to see an overview of the area and primary survey data including, geological survey for lithological and structural identification, hydrogeological survey for observing groundwater monitoring wells by following location data from the Department of Groundwater Resources., and hydrological survey for studying characteristics of river and measuring surface water levels. The survey photos are shown in **Figure 4.1**

2) Geology investigation: Based on geology investigation in November 2015, outcrops in the area are mostly white sandstone and white and purplish red siltstone that shown in **Figure 4.2**. Comparing to geological map of the Department of Mineral Resources, the Phra Wihan Formation, Sao Khua Formation, Phu Phan Formation, and unknown formation were characterized in details as **Table 4.1**:

The Phra Wihan Formation - white sandstone, medium to coarse grained, moderately to well sorted, medium to thick bedded with cross-bedding. The bedding of rock in area is northwest-southeast and 6 southwest dip directions, and direction of joints such as 350/72 E, 250/70 NW, 40/70 SE, 320/90, and 350/70 E.

The Sao Khua Formation – reddish brown, purplish red and purple siltstone, intercalated with brownish red sandstone, fine to medium grained, small scaled cross-bedding. The bedding of rock in area is northwest-southeast and 10 East dip directions, and direction of joints such as 320/90 and 25/80 SE.

The Phu Phan Formation - white sandstone and gray conglomeratic sandstone, medium to coarse grained, pebbles of quartz, poor to moderate sorted, sub-rounded, silica cement, and medium to very thick bedded. The bedding of rock in area is northwest-southeast and 5 northeast dip directions, and direction of joints such as 335/90 and 190/85 SE.

Unknown Formation – white and gray sandstone, fine to medium grained, moderately to well sorted, some iron oxide. The bedding of rock in area is northeast-southwest and 30 southeast dip directions, and direction of joints such as 95/45 NE, 70/75 SE, and 100/80 SW.

Figure 4. 1 The site reconnaissance in the study area

Table 4. 1 Details of lithology and structural geology in the area

Coordinates		Rock	Bedding	Joint	Formation
North	East	name	direction	direction	
1552868	795002	Sandstone	35/30SE	30 SE	Unknown
			95/45NE	45 NE	
			70/75SE	75 SE	
			100/80SW	80 SW	
1568306	804536	Sandstone	135/6 SW	6 SW	Phra Wihan
			350/72 E	72 E	
			250/70 NW	70 NW	
			40/70 SE	70 SE	
			320/90	90.00	
			350/70 E	70 E	
1563761	792888	Siltstone	95/10E	10 E	Sao Khua
			320/90	90.00	
			25/80 SE	80 SE	
1565061	807758	Sandstone	335/90	90.00	Phu Phan
1556848	819486	Sandstone	310/5 NE	5 NE	Phu Phan
			190/85 SE	85 SE	

3) Hydrogeology investigation

The hydrogeologicaly survey is finding observation wells by following groundwater well location data from the Department of Groundwater Resources. Since there was no observation well in the area, we considered using hand pump wells, inactive groundwater wells and shallow wells instead. Eighteen selected observation wells in the area are showed in **Figures 4.3** to **4.4**. Groundwater level measuring was done by using slack probe of water level in the wells, when the probe touched water inside the hole, it will sound signals and notes the depth. The ground water level measurements were done for three periods which represent groundwater levels of each season such as the dry season in March (2015), the rainy season in November (2015) and the dry season in May (2016), the one hole of shallow

groundwater level data is varies of 6-12 meters (during dry season to rainy season) and deep groundwater level data in **Table 4.2**.

4) Hydrology investigation: The study characteristic of river and finding staff gage of each river in area found that staff gage and telemetry of the Royal Irrigation Department can be collect data 3 spots consist of Khwae Hanuman River Bridge, Khwae Kamong River Bridge and Huai Yang River Bridge, as shown in **Figure 4.5**. The details are show in **Table 3.2** of **Chapter 3**.

Figure 4. 2 Lithology and structural geology in the area

Table 4. 2 The details of the deep groundwater level

Name	Coordinates		Elevation	Groundwater level (m)		
	North	East	(m amsl.)	Mar 2015	Nov 2015	May 2016
5503H006	814620	1561279	49.20	16.58	12.04	17.20
5803H002	821883	1553636	52.37	15.02	11.41	17.90
5803H003	823245	1553894	52.00	5.22	3.21	6.69
DCD12310	793058	1563837	28.17	6.33	3.11	7.16
MA148	797932	1556505	20.24	5.96	4.48	6.65
MF1026	808626	1558456	30.65	14.65	15.24	15.90
MF1098	800733	1567078	36.08	5.80	4.18	6.87
MF1174	798190	1565929	42.09	14.00	9.01	16.44
MF151	804505	1568303	34.33	2.90	0.60	3.43
MF823	818457	1561266	34.01	1.00	0.00	2.19
MF944	792153	1562436	34.94	6.11	3.89	7.57
MW1	793307	1557903	31.00	4.22	2.03	5.28
MW2	797704	1550066	20.30	5.76	5.69	7.67
MW4	800784	1552272	19.94	4.05	2.43	4.89
Obs1	818562	1556549	49.45	16.58	15.92	18.52
PB294	798132	1562563	24.47	7.60	4.20	8.41
PW22955	795674	1559482	18.34	6.12	4.88	7.00
PW29276	810774	1563532	48.73	10.52	7.34	11.39
งฒ0209	799535	1565951	31.80	6.65	3.58	8.50

Figure 4. 3 Groundwater data levels collection

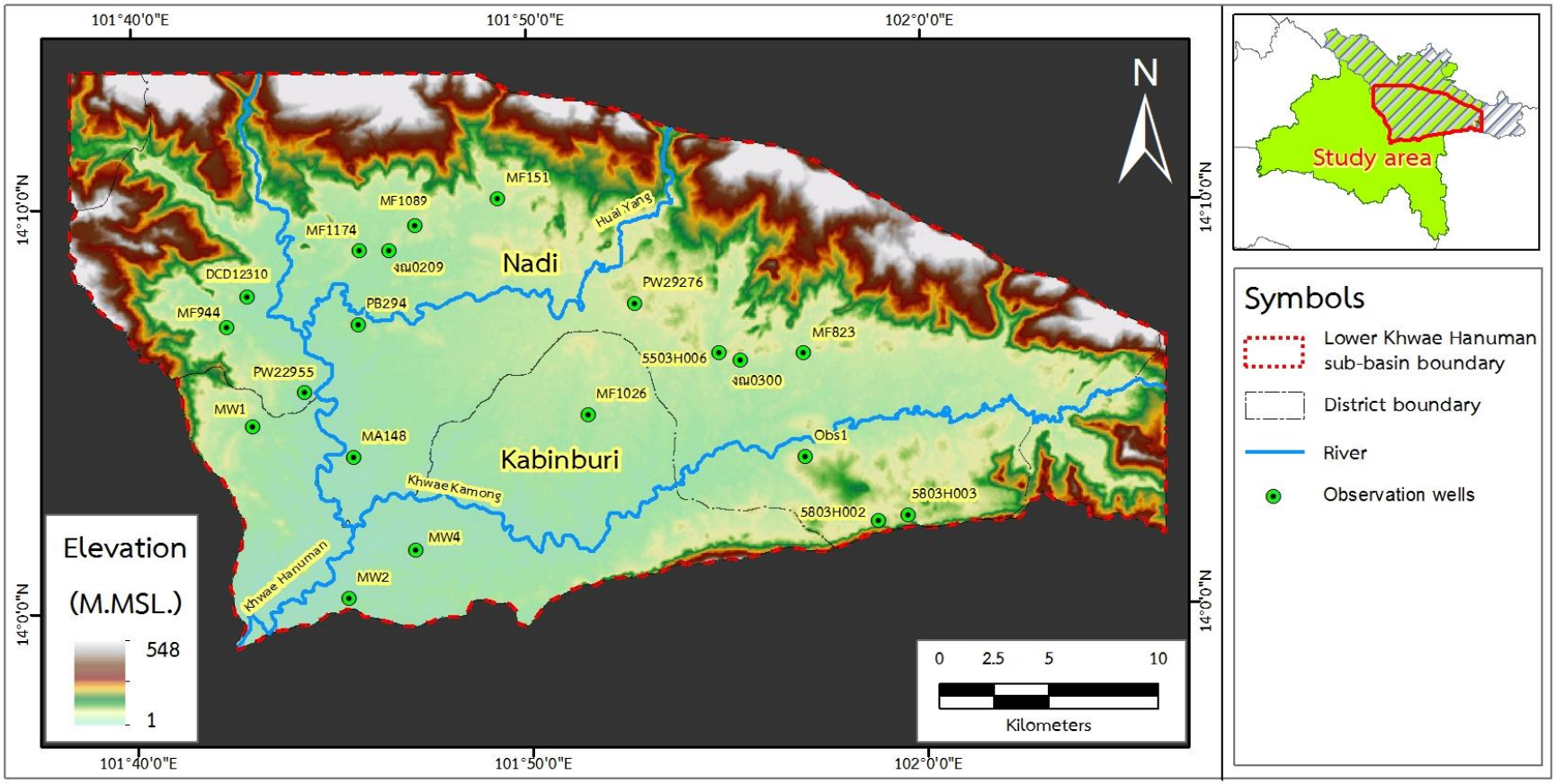

Figure 4. 4 Groundwater wells in the study area

Figure 4. 5 Telemetry in the study area

4.1.2 Groundwater levels and flow directions

The groundwater levels were collected from 14 wells (**Table 4.2**). The data can be used to create groundwater flow pattern, which were measured in dry season (2015, March and 2016, May) and rainy season (2015, November). The shallow groundwater levels ranged from 6 to 12 m, and 1 to 18 m of deep groundwater levels. The directions of deep groundwater flow in both dry season and rainy season flow toward the central parts of the study area, as shown in **Figures 4.6**.

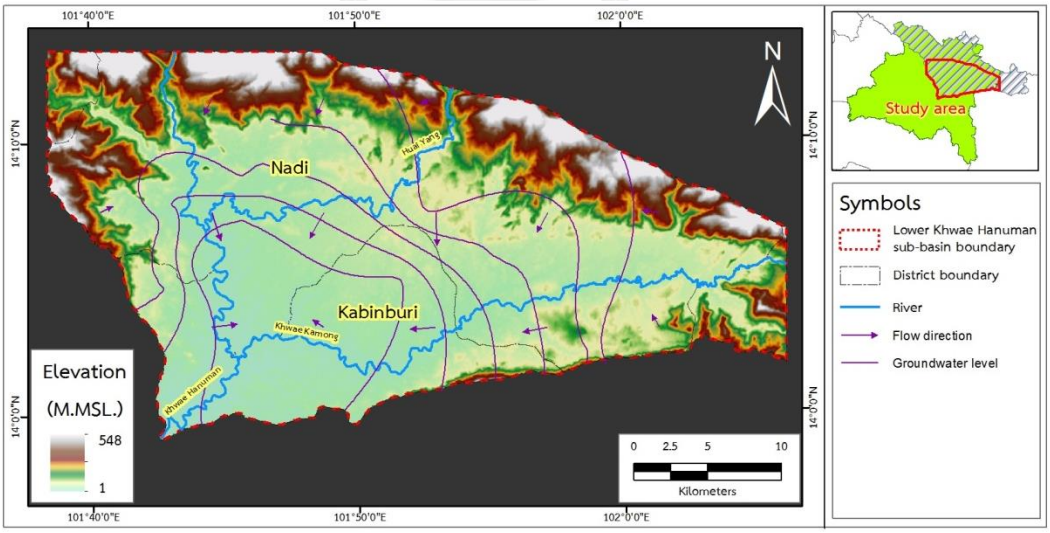

Figure 4. 6 Groundwater levels and flow directions of deep groundwater aquifer

4.2 Groundwater Recharge Potential

Groundwater recharge is defined as the entry of water from the unsaturated zone into the saturated zone below the water table surface, together with the associated flow away from the water table within the saturated zone (Freeze 1979). Recharge of water occurs when water flows pass the groundwater level and infiltrates into the aquifer and then is trapped in the groundwater aquifer. Factors affecting the groundwater recharge include the rainfall volume, characteristic of stream or river, fracture of rocks and porosity of soils, slope, rock type and land use or land cover. The groundwater recharge potential has method as follows.

4.2.1 Methodology

Remote sensing technology was used to identify the terrain and the distribution of rivers in the region, as well as to find the factors that influence the groundwater recharge and the interrelationship between the effects of each factor. By integrating within the GIS, the distribution of the potential groundwater recharge zones is represented as a potential map, and this approach is shown as a flowchart in **Figure 4.7**.

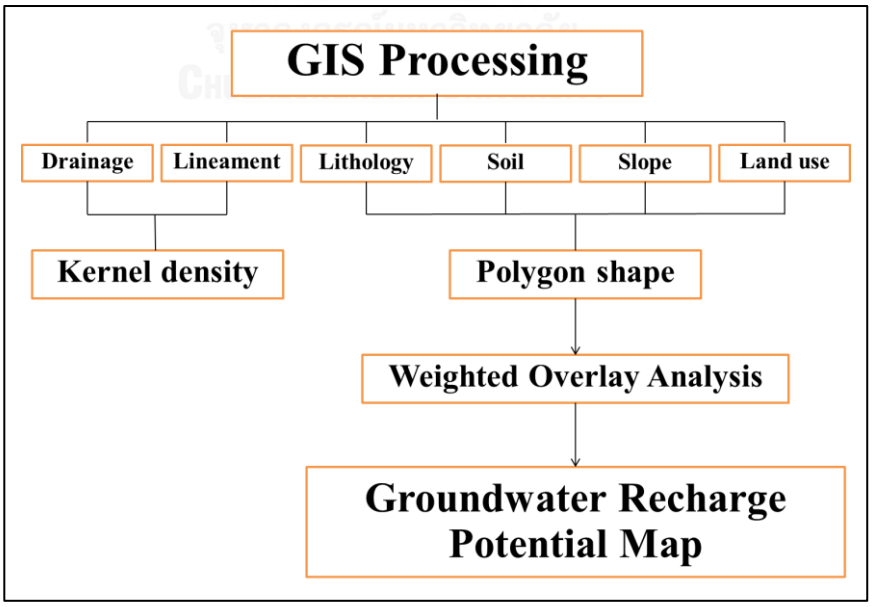

Figure 4. 7 Flowchart of groundwater recharge potential processing using GIS technique; modified from (Selvam, Dar et al. 2016)

Although many researchers have used the GIS process to determine the groundwater recharge potential map ((Shaban 2003); (Shaban, Khawlie et al. 2006); (Yeh, Lee et al. 2009); (Adham, Jahan et al. 2010); (Patil and Mohite 2014); (Chotpantarat, Konkul et al. 2015); (Deepa, Venkateswaran et al. 2016); (Selvam, Dar et al. 2016)), the groundwater recharge potential map has not been evaluated in the Khwae Hanuman sub-basin, especially at the mountain in the north side of the sub-basin. In this study, the different weights and scores of the factors under various effects were evaluated based on the characteristics of the lower Khwae Hanuman sub-basin, including the lithology, drainage density, lineament density and land use. Some other research has used the slope and soil factors that were related with the groundwater recharge, so they were also added in this study. The weight and score of these six factors on the groundwater recharge were categorized according to their values (Selvam, Dar et al. 2016). **Table 4.3** shows the sources of data used and their categorization.

Table 4. 3 Factors that affect the groundwater recharge potential

Data	Basics of categorization	Source[a]	File type
Lithology	Rock type, weathering	DMR	Shape
	characteristic, fracture	DGR	Shape
Land use	Type, area extent, associated vegetation	LDD	Shape
Lineaments	Lineaments density value	DMR	Shape
Drainage	Drainage density value	DWR	Shape
Slope	Slope gradient	RTSD	Shape
Soil	Soil types	LDD	Shape
Rainfall	Average precipitations volume	TMD	Excel

a DMR: Department of Mineral Resources, LDD: The Land Development Department, DWR: Department of Water Resources, RTSD: The Royal Thai Survey Department, TMD: Thailand Meteorological Department, DGR: Department of Groundwater Resources.

The determination of the rating was related to the volume of the groundwater recharge potential factors, where the interrelationship between two factors was determined from the major and minor effects, as shown schematically in **Figure 4.8**

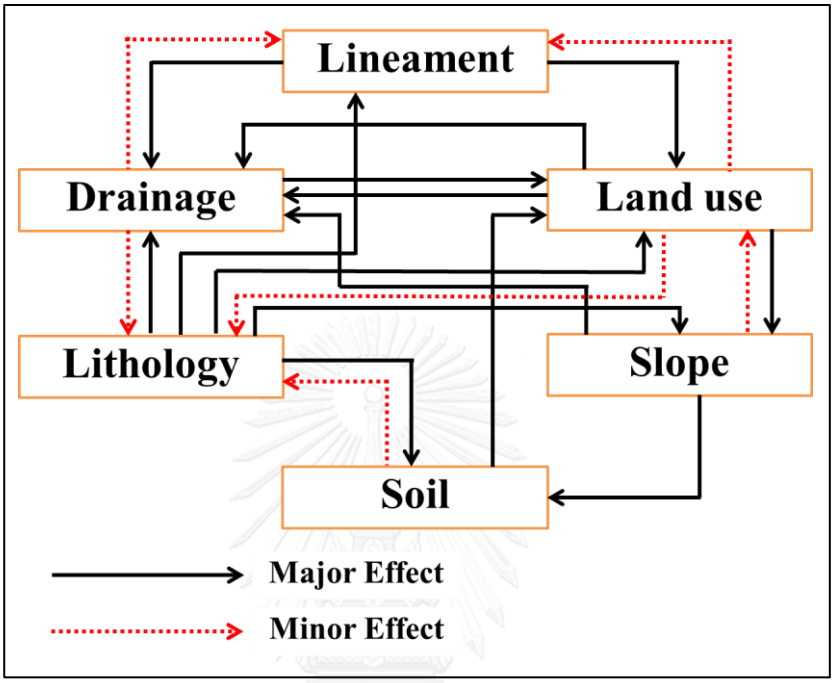

Figure 4. 8 Interaction of factors that affect the recharge property modified from (Selvam, Dar et al. 2016)

Spatial analysis was used to integrate the GIS multilayer system to achieve the groundwater recharge potential map. Finally, the volume of water that could infiltrate into the groundwater aquifers was calculated using Eq. (4-1) (Adham, Jahan et al. 2010);

$$W = \text{P} \times \text{Recharge Ratio} \times \text{Percentage of Recharge Area} \qquad (4\text{-}1)$$

where W is the recharged water volume (m^3/y) and P is the precipitated volume (m^3/y). The volume of water recharged was calculated as the percentage of groundwater potential maps, which were derived from the six weighted factors that affect the groundwater recharge, and is detailed as follows:

1) Lithology: (Su 2000) and (Shaban 2003) showed that rock rails have a direct relationship with the recharge, where each stone has a different water body, but the rate of water recharge is equal. According to (O'leary, Friedman et al. 1976), the type of rock exposed to the surface (outcrop) significantly affected the groundwater recharge. Lithology affects the groundwater recharge by controlling the infiltration of water into the saturated zone. Some investigations have ignored this factor by considering the lineaments and drainage characteristics as a secondary porosity (El-Baz, Himida et al. 1995). The lithology to reduce the uncertainty in defining the lineaments and drainage factors (Yeh, Lee et al. 2009).

2) Slope gradient: The slope gradient is one of the factors that directly influences the rate of infiltration of rainfall ((Selvam, Magesh et al. 2014); (Deepa, Venkateswaran et al. 2016). At higher or steeper slopes, the volume of groundwater recharge is smaller because the water rapidly flows over the surface and has insufficient time to infiltrate into the saturated zone. The flatter plain areas can keep and drain the water inside the ground, and so increase the groundwater recharge, whereas steep slopes increase the surface runoff and decrease the infiltration of surface water into the saturated zone.

3) Drainage density: According to (Ramingwong 2003), the characteristics of landforms and drainage are related to their hydrogeology and hydrology because the characteristics of drainage water may be either water recharge or discharge. The structural analysis of the drainage density helps to assess the characteristics of the groundwater recharge zone (Yeh, Lee et al. 2009), where the drainage networks are based on the lithology, which provides an important index of the infiltration rate. According to (Dinesh Kumar, Gopinath et al. 2007), areas with a high drainage density are not suitable for groundwater development because of the greater surface runoff. The groundwater occurrence and distribution depend on the density of the drainage (Murthy 2000). Furthermore, the topography is important. A low drainage density has a high void ratio, which indicates a high potential of groundwater recharge.

The area with a low density of water will result in a high recharge potential. In this study area, the drainage consists of rivers, and perennial and intermittent streams in a dendritic pattern. The length of drainage density, Dd (km^{-1}),

was derived from the total length of drainage in a unit area (Greenbaum 1985), using Eq. (4-2);

$$D_d = \frac{\sum_{i=1}^{i=n} S_i}{A} \tag{4-2}$$

where $\sum_{i=1}^{i=n} S_i$ denotes the total length of drainage in the watershed (km) and A denotes the unit area (km^2). The total length of drainage densities correlate with the groundwater recharge, where a high drainage density zone has a high groundwater recharge volume. The weighting and rating of drainage-length density were classified into three types by method of (Selvam, Dar et al. 2016).

4) Lineament density: (O'leary, Friedman et al. 1976) defined lineaments as simple and complex linear properties of structural geology, such as faults, joints and fractures. The lineaments are arranged in a direct line or slight curve as detected by remote sensing. According to (Dinesh Kumar, Gopinath et al. 2007) and (Selvam, Magesh et al. 2014), in a hard rock landscape the lineaments represent the fault and fracture zones that result in an increased secondary porosity and permeability. Accordingly, lineaments are good indicators of groundwater recharge, and are generally referred to remote sensing analysis of fractures or structures (Yeh, Lee et al. 2009).

Areas with a lineament structure, such as faults, cracks and fractures, have a high potential of water recharge because the water can seep into undersurface faster and deeper. Lineaments were mostly found in the north area. The length of the lineaments density, Ld (km^{-1}), was derived from the total length of lineaments in a unit area, as in Eq. (4-3);

$$L_d = \frac{\sum_{i=1}^{i=n} L_i}{A} \tag{4-3}$$

where $\sum_{i=1}^{i=n} L_i$ denotes the total length of lineaments (km) and A denotes the unit area (km^2). A high length of lineament refers to high level of fractures, and so indicates a zone with a high groundwater potential. The weighting and rating of the lineament-length density was classified into four types by the method of (Selvam, Dar et al. 2016).

5) Land use: Land use is an important factor in groundwater recharge. (Leduc, Favreau et al. 2001) found that the difference in the volume of groundwater recharge mainly caused from changes in land utilization. (Shaban, Khawlie et al. 2006) concluded that vegetation cover benefited the groundwater recharge by three main routes, Firstly, biological decomposition of the roots helps water to flow easily under the surface. Secondly, vegetation prevents the direct evaporation of water in soil, while thirdly the roots of a plant can absorb water. According to (Patil and Mohite 2014), land use controls the occurrence of groundwater and also causes the recharge.

6) Soil: Soil is a significant factor in the groundwater recharge and runoff (Murthy 2000) as it is the medium through which water must penetrate to get into the water table. The water holding capacity of an area depends on the types and permeability of the soils. Groundwater recharge capacity is lower on hills due to the high degree of slope that results in a high runoff. Soils have the capacity to generate biomass and act as the filter between the atmosphere and the groundwater aquifer (Selvam, Dar et al. 2016). Soil types are more important and are the main factor in determining the groundwater recharge in agricultural production. Soils have an important role in supporting or resisting the groundwater recharge and determining the quality factors of groundwater (Lillesand, Kiefer et al. 2014). Soil media represents the uppermost weathered portion of the unsaturated zone, which then continues to the penetration area of plant roots and organic creature activities (Baghapour, Talebbeydokhti et al. 2014).

7) Overlay Analysis and Recharge Water Volumes: Overlay analysis map is a decision-making tool developed for the multi-criteria analysis of complex problems. The overlay analysis process used to determine the rate (score) and the weight of each factor is shown in **Figure 4.9** All the thematic maps were converted into raster format and superimposed by a weighted overlay method, which consisted of the GIS rate and weight thematic maps.

Each recharge potential factor may influence the groundwater recharge process to a different degree. Determination of their rating was related to their volume of the groundwater recharge potential factors. The six factors were plotted over a range from very low to very high, where very high was assigned as 10 points and very

low as 1 point. All of these factors were then integrated to obtain the recharge potential map. A major interrelationship between two factors was assigned a weight of 2.0, while a minor interrelationship was assigned a weight of 1.0 (Selvam, Dar et al. 2016). For example, lithology had major interrelationships with five factors (lineaments, drainage, slope, soil and land use), and so its evaluated weight was 10.0. The process for determining the relative rate of each factor is show in **Table 4.4**.

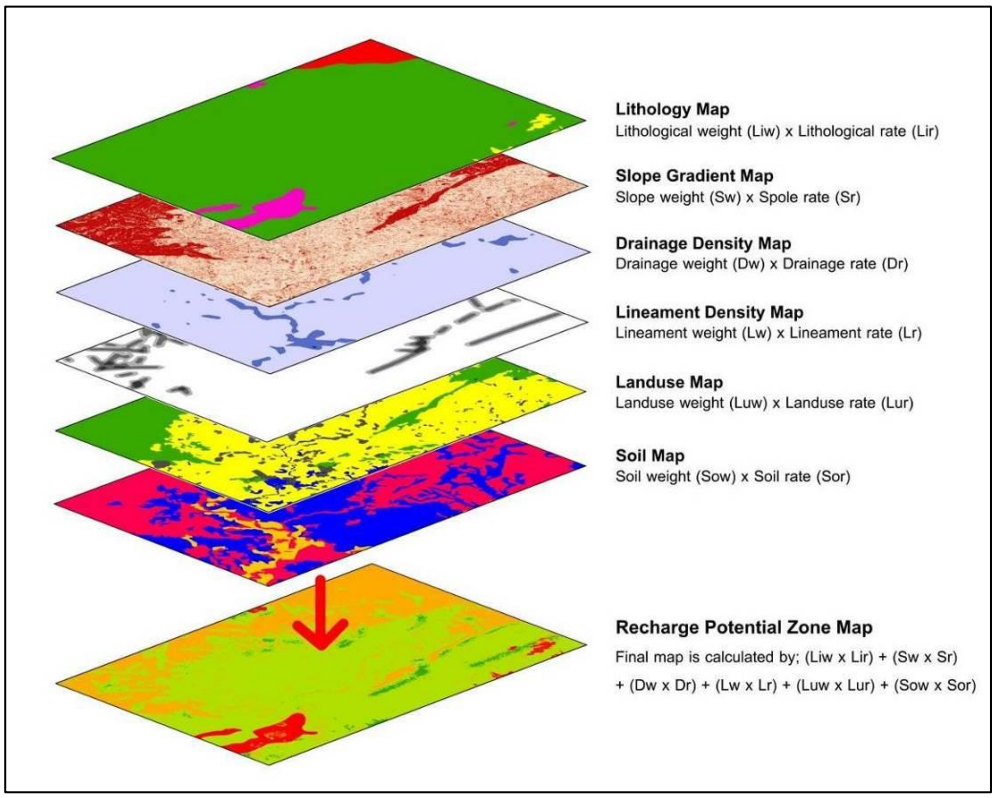

Figure 4. 9 Process of groundwater recharge potential zone analysis

Table 4. 4 The process of determining the relative rate of each factor; modified from (Selvam, Dar et al. 2016)

Factor	Major effect (A)	Minor effect (B)	Calculation process	Relative rate (A + B)
Lineaments	2 + 2	0	4 + 0 = 4.0	4.0
Land use	2 + 2 + 2	1 + 1	6 + 2 = 8.0	8.0
Lithology	2 + 2 + 2 + 2 + 2	0	10 + 0 = 10.0	10.0
Drainage	2	1 + 1	2 + 2 = 4.0	4.0
Slope	2 + 2	1	4 + 1 = 5.0	5.0
Soil	2	1	2 + 1 = 3.0	3.0
			Total	**34.0**

*2.0: Major effect, 1.0: Minor effect

The polygon area was used to quantify the score of each recharge potential factor based on the characteristics of six factors in the study area. The relative rates and score of each corresponding recharge potential factor were set as shown in **Table 4.5**, and then were integrated and the obtained total weighting assessment was used to obtain the recharge potential factor (Khawlie 1986); (Shaban 2003). The grand total weight (GTW) was calculated from Eq. (4-4) (Selvam, Dar et al. 2016),

$$GTW = (WLIT \times RLIT) + (WLU \times RLU) + (WS \times RS) + (WLIN \times RLIN) + (WD \times RD) + (WSLP \times RSLP) \quad (4\text{-}4)$$

The results from Eq. (4-4) were then used to calculate the percentage of recharge potential factor following (Selvam, Dar et al. 2016) by Eq. (4-5);

$$\frac{\sum(X \times Y)}{\sum\left(\sum(X \times Y)\right)} \times 100 \quad (4\text{-}5)$$

where X is the weight and Y is the rate. The percentage recharge potential factors are shown in **Table 4.5**. Finally, the recharge potential zones map was created**,** and a quantitative estimation of the recharged water volume (W) was calculated using Eq. (4-1).

Table 4. 5 Recharge potential factors scores (modified from (Selvam, Dar et al. 2016).

Factor	Domain of effect	Descriptive level	Weight (A)	Rate (B)	(A×B)	Total Σ(A×B)	(%)
Lithology	Sandstone, siltstone, shale, limestone	High	8.5	10	85	190	28.11
	Quartzite	Good	6.5		65		
	Colluvium	Moderate	2.5		25		
	Granite, volcanic	Low	1.5		15		
Land Use	Surface water bodies	Very High	8.0	8	64	192	28.40
	Cultivated land	High	6.0		48		
	Forests	High-Moderate	5.5		44		
	Settlements	Good	4.5		36		
Lineaments density	1.2–2.0	High	10.0	4	40	84	12.43
	0.8–1.2	Good	6.0		24		
	0.3–0.8	Moderate	3.5		14		
	0.0–0.3	Low	1.5		6		
Drainage density	0–3	High	9.0	4	36	76	11.24
	3–6	Good	6.5		26		
	6–8	Moderate	3.5		14		
Slope gradient	0–1^{o}	High	7.5	5	37.5	110	16.27
	1–2^{o}	High-moderate	5.5		27.5		
	2–3^{o}	Moderate	4.0		20		
	3–4^{o}	Moderate-low	2.5		12.5		
	4–5^{o}	Low	1.5		7.5		
	> 5^{o}	Very low	1.0		5		
Soil	Fine sandy silt, silty sand	High	4.5	3	13.5	24	3.55
	Silty gravel, poorly graded gravel	Moderate	2.5		7		
	Clay, silty clay	Low	1.0		3		
		Total				**676**	**100.0**

4.2.2 Results of groundwater recharge potential

The lithology data from the 1:50,000 scale geological maps derived from the DMR and 1:100,000 scale hydrogeological maps derived from the DGR of Prachinburi and Srakeaw provinces revealed the study area is mainly composed of sandstone, siltstone and conglomeratic sandstone of the middle Khorat group, along with units of sedimentary rock, such as alluvial and fluvial deposits. Some areas were composed of limestone of Saraburi group. This study assigned the percolation values of the lithological units based on the infiltration rate. The lithological weighting and rating of rock units in the study area were classified into sediments and sedimentary, metamorphic and igneous rocks (Selvam, Dar et al. 2016). Sedimentary rocks were considered as having a high potential for groundwater penetration due to their high porosity and permeability, while igneous rocks were considered as having the lowest groundwater potential due to their low porosity, as shown in the geological map in **Figure 4.10**.

The slope was represented in percentage based on the digital elevation model (DEM) raster information (90 × 90 m resolution) derived from the RTSD. Slope gradient values were calculated by the opposite angle (rise) divided by the adjacent corner (run) and then multiplied by 100. The slope was classified into six degrees of slope gradient by the method of (Selvam, Dar et al. 2016). If the slope is greater than 50, the precipitation rapidly runs off and does not store water easily. On the other hand, if the slope is 0–10 (the plains) the precipitation easily infiltrates into saturated zone. **Figure 4.11** shows the distribution of slopes in the study area.

The calculation of the drainage density was based on the streams data derived from the DWR. The dendritic drainage pattern was distributed mostly in the north region of the study site (**Figure 4.12**). Most of the drainage density map ranged from 0–3 m^{-1}, which means a high recharge potential.

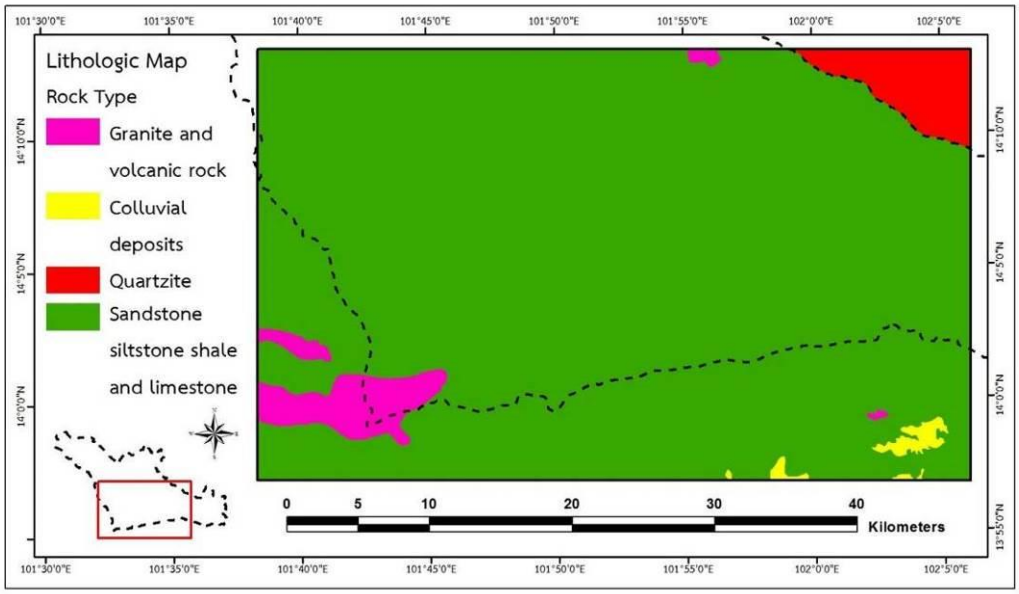

Figure 4. 10 Geological map of the lower Khwae Hanuman sub-basin

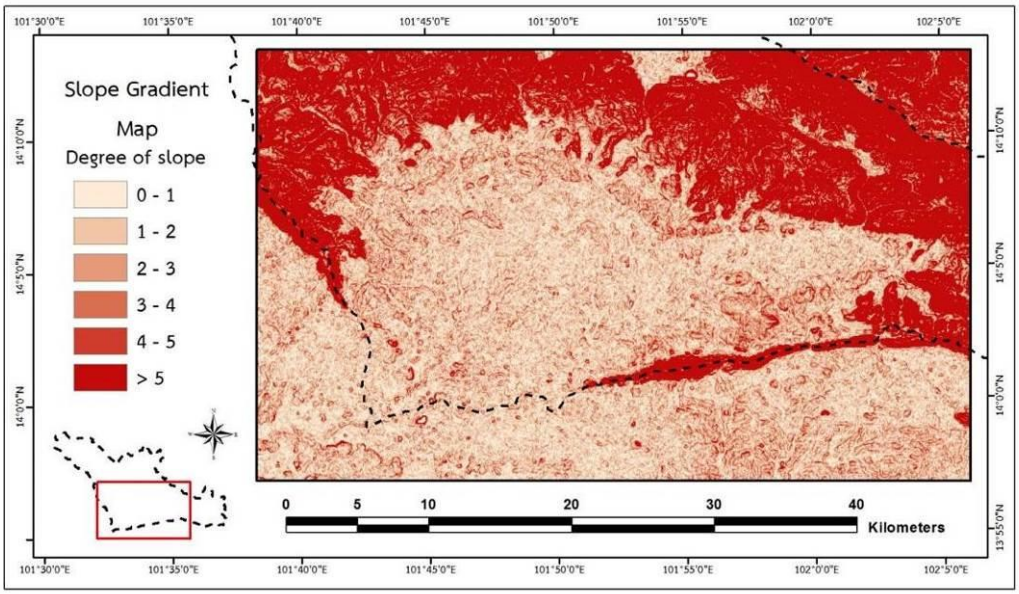

Figure 4. 11 Slope gradient map of the lower Khwae Hanuman sub-basin

The calculation of the lineaments density was based upon the structural data derived from the DMR. The lineaments of the sub-basin were distributed to upstream, with a high lineament-length density of approximately 1.2–2.0 km^{-1}, and so a high recharge potential due to the increased porosity and permeability. **Figure 4.13** shows the density lineament in the study area.

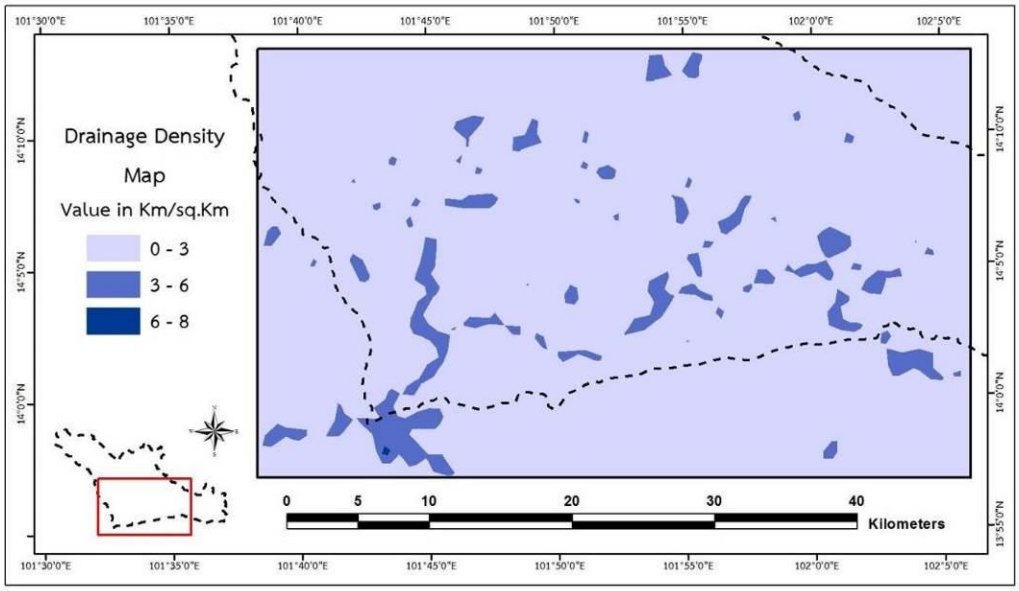

Figure 4. 12 Drainage density map of the lower Khwae Hanuman sub-basin

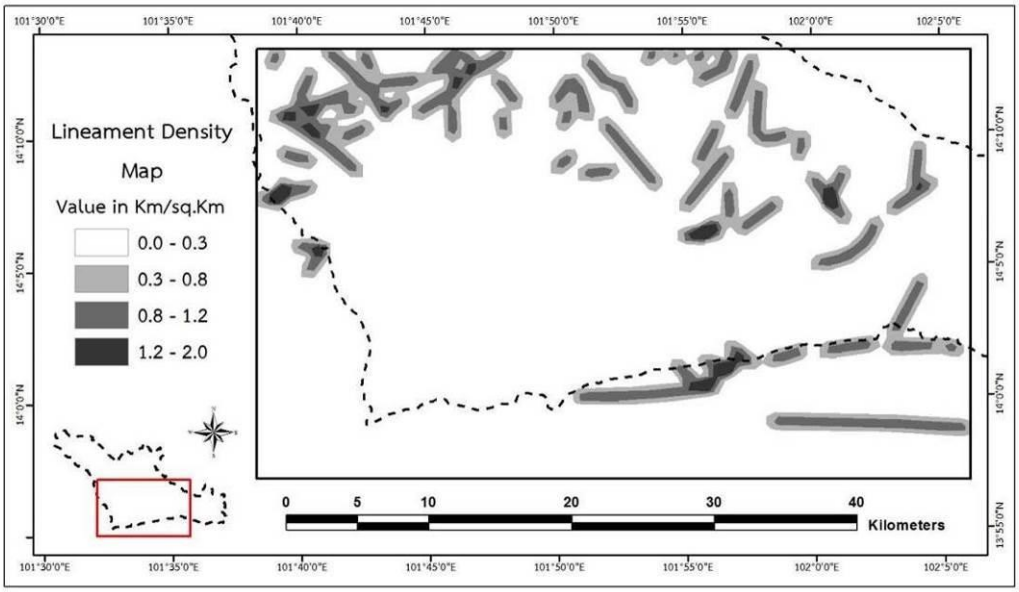

Figure 4. 13 Lineament density map of the lower Khwae Hanuman sub-basin

The land use data in this study was based on the land use map derived from the LDD. The weighting and rating of land use were classified into four types by the method of (Selvam, Dar et al. 2016). The main land use in this study area was cultivated land and then forest (**Figure 4.14**). The water body area has a high recharge potential because the water is present at all time.

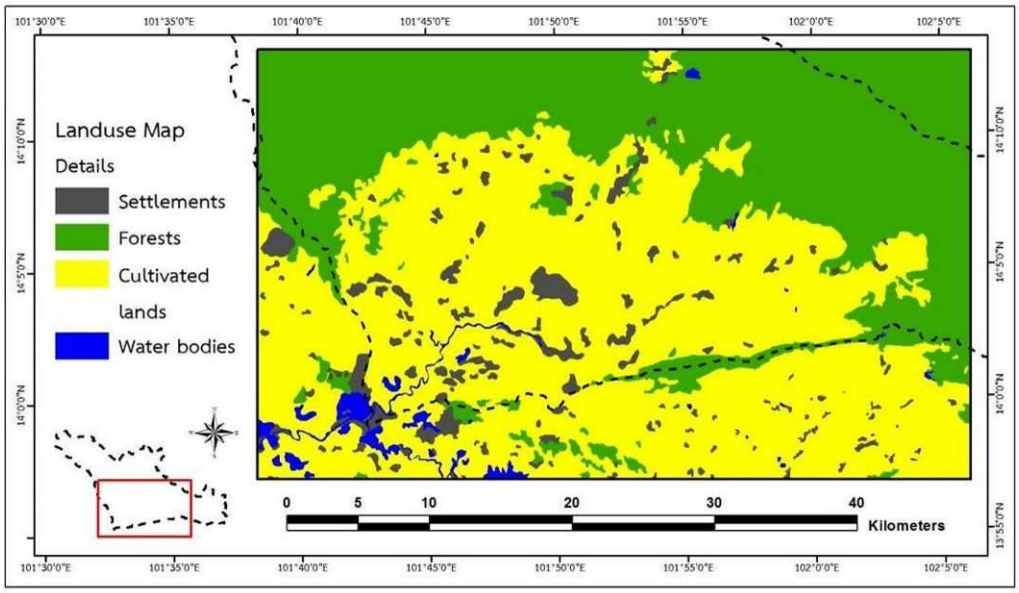

Figure 4. 14 Land use map of the lower Khwae Hanuman sub-basin

The soil data in this study was based on the soil map derived from the LDD. The weighting and rating of soil were classified into three types by the method of (Selvam, Dar et al. 2016). In this study area, soils with high water holding capacity consisted of fine sandy silt and silty sand, which were located at the center of the study area (**Figure 4.15**).

The lithology map ranged from low to high, depending on the type of sandstone, siltstone, shale and limestone. Land use map was analyzed based on the water bodies, cultivated lands, forests and settlements containing different values of water infiltration, and their values range from good to very high. The lineament density map ranged from low to high, where a high value indicates a very high recharge potential, but a low density does not indicate a low recharge potential. The drainage density map ranged from moderate to high, where a low drainage density corresponds to a high recharge potential zone. The soil map ranged from low to high, where a high soil value is defined as a high permeability and results in a high recharge. Lastly, the slope map ranged from very low to high.

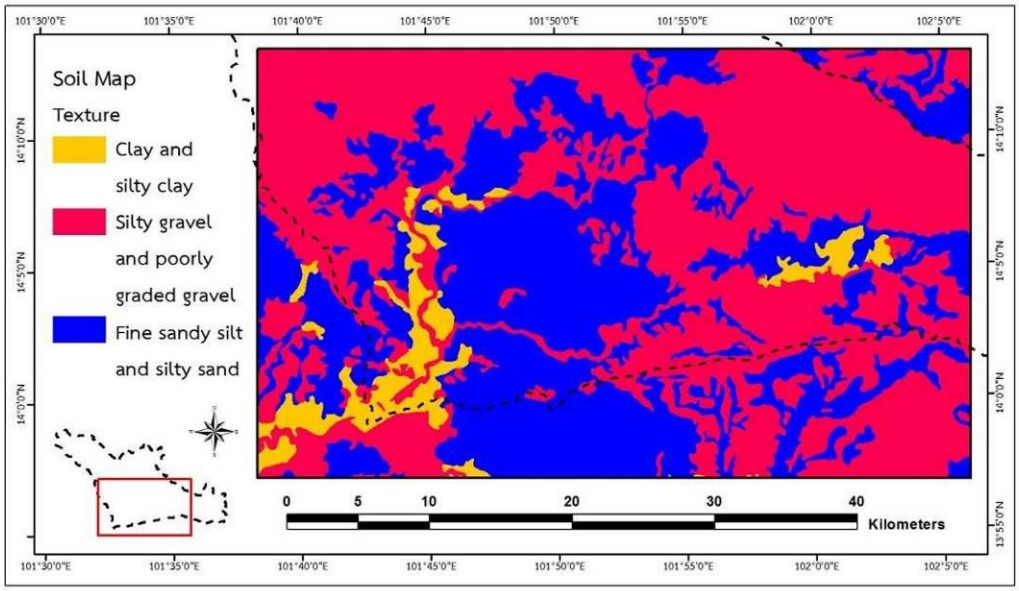

Figure 4. 15 The soil map of the lower Khwae Hanuman sub-basin

The results of the groundwater recharge potential zone were divided into the four classes of high, moderate, low and very low, based on the analysis of the six factors of groundwater recharge potential. The high groundwater recharge potential zone was concentrated at the central plains due to the distribution of the lithology, slope gradient and agricultural land with high infiltration ability. Moreover, the density of drainage also helped the stream-flow infiltrate into the groundwater aquifer. Especially, the density of lineament at the top of the study area allows water to recharge into the aquifer.

The recharge potential zone map (**Figure 4.16**) was described by the four levels of potential zones of high, moderate, low and very low and these occupied areas of 33.88 km^2 (2.3%), 971.73 km^2 (64.8%), 442.15 km^2 (29.5%) and 52.23 km^2 (3.5%), respectively. The maximum area was characterized by a moderate recharge potential zone that occupied 64.8% of the total area. The values of the recharge potential shown in the groundwater recharge potential map were compared with the standards from the UN (1967), and these levels were categorized as shown in **Table 4.6**. However, a quantitative estimation of the recharged water in this area was performed by a simplified calculation for the proposed recharges rates, as adapted from the UN (1967). The estimation of the recharged water volume (W) was

calculated from Eq. (1), where the precipitated volume (P) was 1,415.37 × 10^6 m/y, giving a recharged water volume of 180.5 × 10^6 m/y. This means that only 12.8% of the precipitated water in the study area was recharged into the groundwater, with the rest being lost due to evapotranspiration or surface runoff.

Table 4. 6 Recharge potential categories and their quantitative estimation modified from (Selvam, Dar et al. 2016)

Recharge potential category	**Estimate according to UN (1967)**	**Average (%)**	**Recharge ratio**	**Areal extent (km^2)**	**Percent of area**
Very high	45–50%	47.5	0.475	0.00	0.00
High	30–35%	32.5	0.325	33.9	2.3
Moderate	10–20%	15.0	0.150	971.7	64.8
Low	5–10%	7.5	0.075	442.2	29.5
Very low	< 5%	2.5	0.025	52.2	3.5

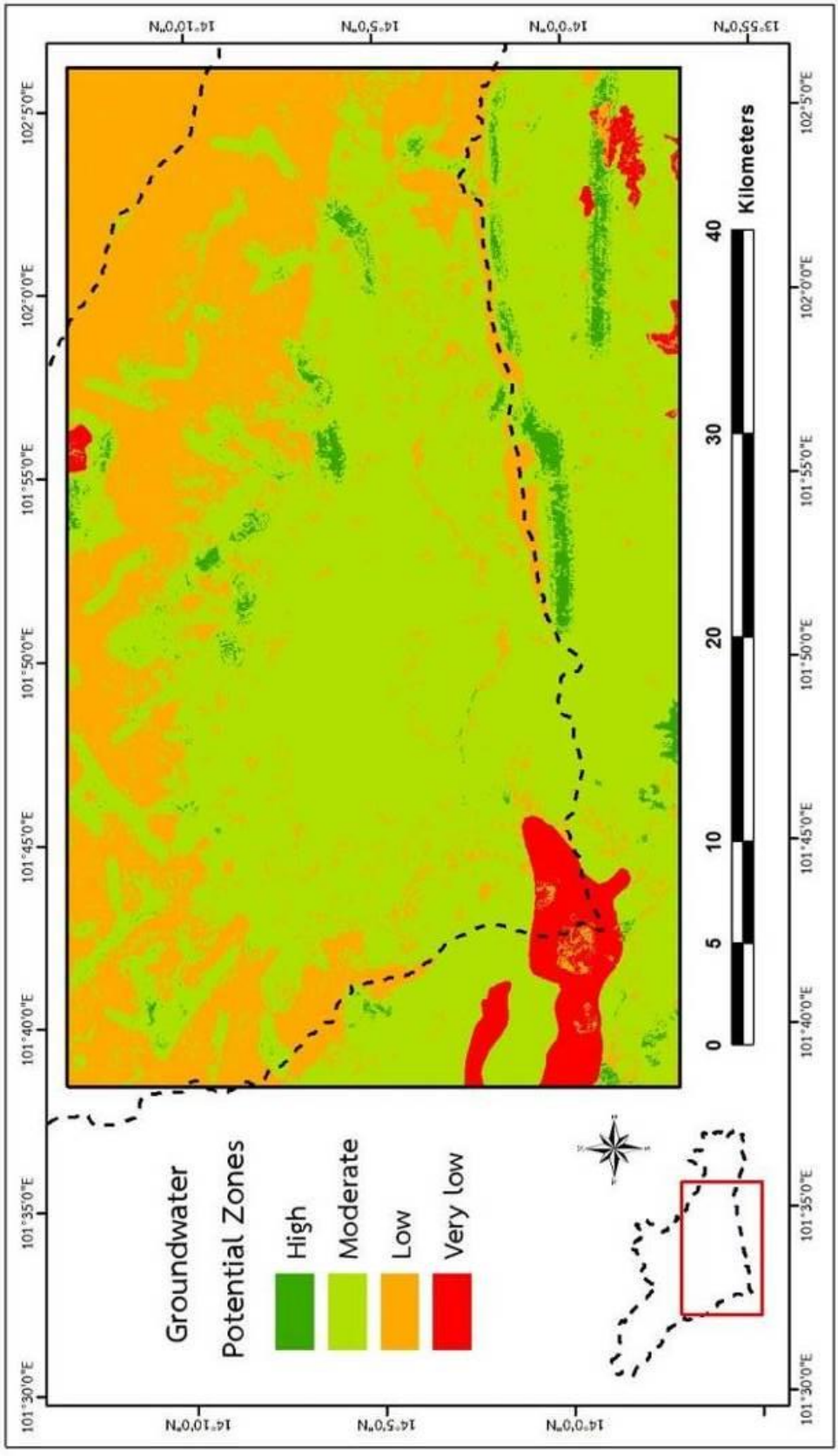

Figure 4. 16 Groundwater recharge potential map of the area

CHAPTER V
GROUNDWATER FLOW MODELING

5.1 Modeling Background

A mathematical model can be used efficiently as a tool in groundwater resources planning and management at all levels, from the primary stage of exploration to those of feasibility study and detailed design. Groundwater system model can be improved when more data are available. All data, either those already existed or newly collected, will be used in installation, verification and improvement of the model, in order to apply in predicting and analyzing hydrogeological conditions, which will be considered in the groundwater development and management.

The mathematical model is a useful tool, which can describe natural phenomena or manmade systems, leading to better understanding the performance of those phenomena or systems. In this study, mathematical models are set up to simulate groundwater system for evaluating the potential of groundwater resources in the study area.

5.2 The hydrogeological conceptual model

The data used in the hydrogeological conceptual model can be divided into 3 types as bellows:

1) Geology consists of stratigraphic formation, structural geology and geomorphology.

2) Hydrology consists of river characteristics, rainfall and evaporation amounts.

3) Hydrogeology consists of characteristics of groundwater aquifers, groundwater level, groundwater recharge, groundwater flow and hydraulic properties (i.e., hydraulic conductivity and storativity, etc.).

These assumption data is used to develop hydrogeological cross-sections. They refer the relationship between surface water and groundwater, corresponding to

aquifer characteristics. The Geographic Information System (GIS) was applied to identify the water balance and characteristics of geology and hydrogeology.

The conceptual model is the conclusion of understanding on physical properties and groundwater flow system. The analysis of data includes geology, geomorphology, hydrogeology, hydrology, topography, groundwater use, soil properties and land use. The result displays in numerical data, map and cross-section of hydrogeology, which were used to explain the hydrogeological conditions and further help to primarily check the calculation result of the groundwater modeling.

In general, the data were analyzed as the form of block diagram. The cross-section shows shape, thickness and hydraulic properties of aquifers (e.g. hydraulic conductivity (K) and storativity (S)), the distribution of water levels in aquifers and the distribution of groundwater recharge. The conceptual model is determined the size and boundary of numerical model and grid design. The authentic model completely cannot be generated, leading to the development of conceptual model in order to analyze systematization of data into an available form to be used. The accuracy of numerical model will increase if the hydrogeological conceptual model is nearly natural condition.

Hydrogeology of aquifers area composes of 2 types of aquifers as follows: confined and unconfined aquifers. The featuring permeable and groundwater storage are different. The flow direction of groundwater is from west to east and north to south in the horizontal due to permeable properties in the horizontal flow better than the vertical. The scopes of groundwater simulation are:

1) Constant density of water

2) Initial head condition at the time of the study on March 1, 2015.

3) The quaternary aquifer is unconsolidated which it is heterogeneous and anisotropy.

4) Hard rock aquifers in the basin area are sustained. Assuming storage properties of water from the fractures and bedding of rocks are unstable. There has a porous in aquifers uniform by a form of homogeneous and anisotropy; however, the thickness of the layer 2 and layer 3 in the model are around 30 m and 40 m respectively.

5) The hydraulic conductivity is based on the study of groundwater investigation and detailed mapping of the Upper Chao Phraya basin at the scale of 1:50,000 (DGR 2011) due to there is not pumping test data in the study area.

6) Recharge rate was estimated following modified of the study of (Selvam, Dar et al. 2016).

The study area covers part of the lower Khwae Hanuman sub-basin. However, the simulation considered the characteristics of the hydrogeology in the whole area.

Groundwater resource is an available resource, with the flow direction from high mountains, acting as recharge areas, locating in the north, east and west parts of the basin. On the other hand, the groundwater flows out in the south side of the study area, which is a low-lying plain. The high mountains and plain of central area are recharged by rainfall and loss of discharged by mainly groundwater pumping in a plain. Surface water flows through the area of Khwae Hanuman River in direction north to south, and east to south in two sub-rivers. The convergence on Khwae Hanuman River is in the middle area which consist of Khwae Kamong River and Huai Yang River. The rivers in the area are qualified to recharge and discharge. No flow boundary set up in the north and south side due to it has geology structure control (fault zones). This study was needed to stratify into four groundwater layers, based on cross-section data. The first layer is quaternary sediment aquifer with an average thickness varing from 20 to 30 m. The second layer is high weathered rock aquifer, composing of sandstone and shale with high fractures with an average thickness ranging from 20 to 40 m. The next layer is weathered rock aquifer, composing of sandstone and low fractured shale with an average thickness ranging from 30 to 40 m. The final layer is the fresh rock, which is set up as the no flow boundary with the thickness of 10 m. All aquifers are heterogeneity and anisotropy as shown the conceptual model in **Figure 5.1**.

5.3 Computer Program Selection

The Visual MODFLOW software was used in groundwater flow modeling in this study, developed by the Waterloo Hydrogeologic, Inc., Canada. The groundwater level change was calculated by the mathematical model. This study applied the

MODFLOW (MODular finite-difference groundwater FLOW model), which model was commonly used to calculate the groundwater flow regime in 3D.

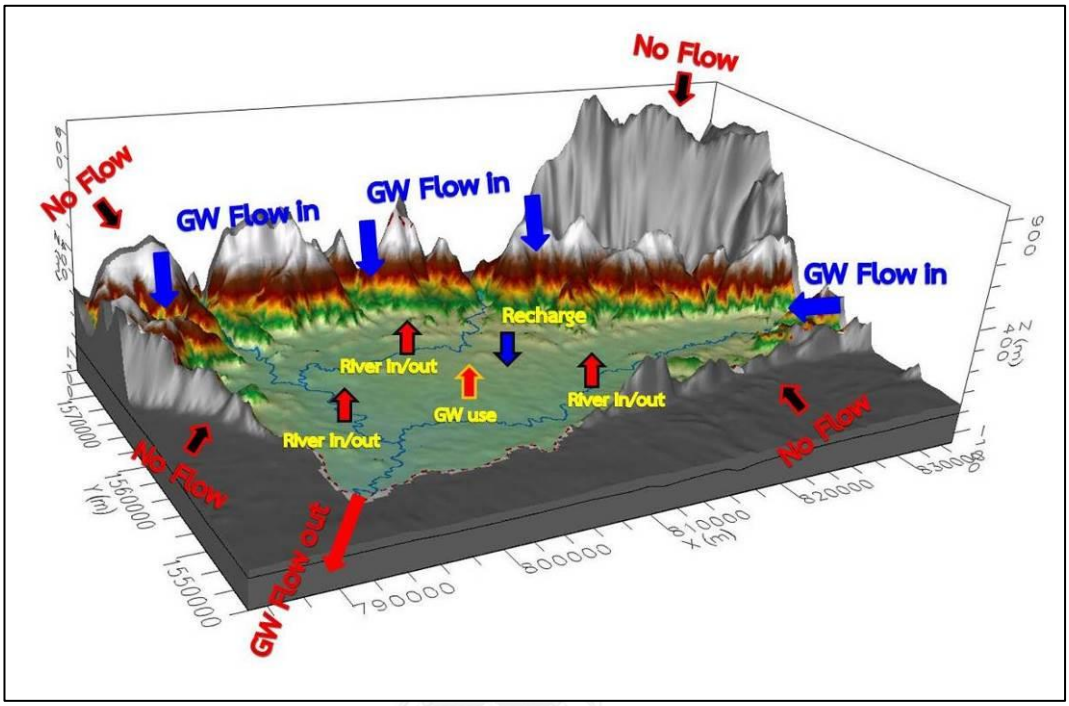

Figure 5. 1 The conceptual model in the lower Khwae Hanuman sub-basin area

5.4 Model Design

In the groundwater model design, the physical features of the aquifers are transformed into the 2 or 3 dimensional numerical model. Each aquifer will be characterized by its width, length, thickness and depth from the ground level. The aquifer data will be classified into groups according to the groundwater database system. The data are also categorized into subdivisions. Some data categories vary with time, such as groundwater extraction rates. In the other hand, some data categories are always constant, such as coverage area and thickness of the aquifers. In this study, the ready-made software is employed, so the step of model design will be emphasized on preparation of data in the formats which described in the software manual. However, the objective of model design is the same. This is to obtain the numerical tool that represents the studied aquifer system.

5.4.1 Grids design

The study of conceptual model cover areas 1,500 square kilometer. The model boundary is a rectangular shape with a width of 50 km in east-west direction, from the coordinate 785,000 to 835,000 m East, and with a length of 24 km in north-south direction, from the coordinate 1,547,000 to 1,574,000 m North. The constant grid size inside the study area is 200 m x 200 m The grid size will be increased with distance from the boundary area of study. The total number of grids in each model layer is 30,000 grids (120 rows x 250 columns), as shown in **Figure 5.2**.

The total number of model layers is 4 layers, which is corresponding to the aquifer characteristics -the first layer is quaternary sediment aquifer, average thickness from 20 to 30 m, the second layer is high weathered rock aquifer, average thickness ranges from 20 to 40 m, next layer is moderate weathered rock aquifer, average thickness ranges from 30 to 40 m, and the final layer is the fresh rock, thickness is 10 m-. Therefore, the total number of grid cells used in this model is 120,000 grid cells, that shown in **Table 5.1**.

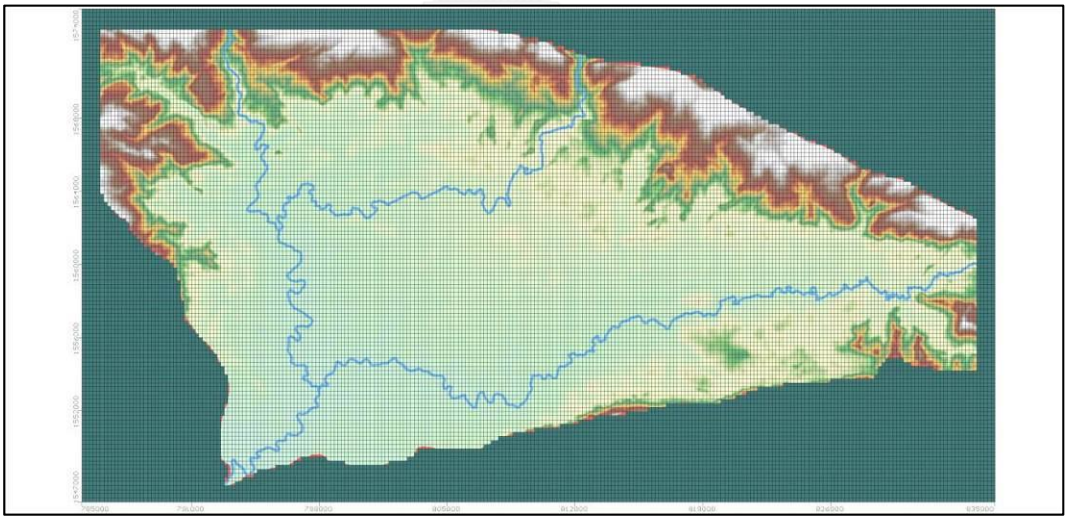

Figure 5. 2 Grid division of the model

5.4.2 Boundary Conditions

The boundary of the model has been assigned by considering the available hydrogeological data. The study area located on the quaternary sediments, which boundaries of sediment reach to the north end of the Khao Yai National Park and

Thap Lan National Park in Nadi district, end Huai Samong Nadi district in the east, and the west end of the Khao Yai National Park in Nadi district, Prachinburi province. The hydrogeology of Aquifers can be divided into three aquifers consist of quaternary sediment aquifer, high weathered rock aquifer and weathered rock aquifer.

The boundary conditions of the model in the study area, determined using boundary character of hydrogeologic unit distribution, groundwater divide and stream lines. The boundary conditions defined by following (**Table 5.2** and **Figure 5.3**):

1) Determine boundaries on the top of model which has groundwater level changed from the parameters of hydrology such as recharge, pumping and surface water changes.

2) Determine boundaries on the lower end models were depth of -60 m amsl. and allowing water to seep up and down.

3) Determine boundaries on the north, east and west of the Khwae Hanuman sub-basin were dividing line watershed groundwater and no water flow boundary conditions on the groundwater divide area.

4) Determine river which can flow on the second layer due to some area river flows on rock layers.

5) Determine vertical hydraulic conductivity of river bed about 6.35 – 5.20 m/d, and river bed thickness about 1 - 2 m.

6) No determine evapotranspiration conditions because the researchers used the groundwater recharge potential data instead of the rainfall data in recharge conditions.

5.4.3 The import data used in the model

1) Top and Bottom: The top and bottom elevations of each aquifer are determined from the topographic maps and cross section of hydrogeology. The ground surface elevation in the study area is topographic contour 1:50,000 map scale derived from the Royal Thai Survey Department. This study uses the highest level of 60 meters above mean sea level (m amsl.) to easily calibrate the model. The maps of the bottom elevations of each aquifer found that cross-section of hydrogeology include layer I is sedimentary aquifer has the bottom elevation of 1 to 30 m amsl., layer II is high weathered aquifer has bottom elevation -9 to -20 m amsl., layer III is

moderately weathered aquifer has bottom elevation constant -50 m amsl. The final is fresh rock has bottom elevation constant -60 m amsl., which it is no flow boundary set up. The maps of the top and bottom elevations of this model are shown in Figure **5.4**

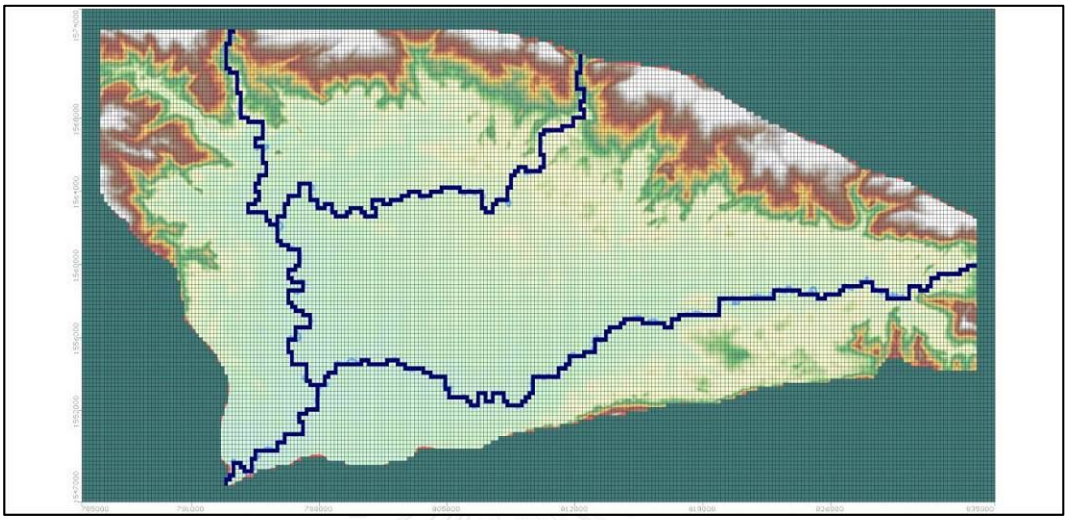

Figure 5. 3 Boundary conditions of the Khwae Hanuman sub-basin model

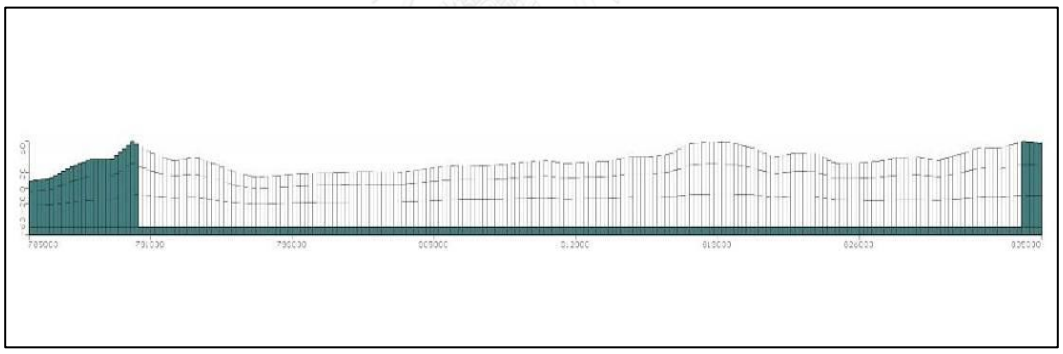

Figure 5. 4 Top and bottom elevation of numerical model

Table 5. 1 The model resolution for determination

Details	Model
1) Size of model	
Coordinates East (UTM)	785,000 - 835,000 m
Coordinates North (UTM)	1,547,000 - 1,574,000 m
Thickness of the mean sea level	-60 m to +60 m
2) Resolution of model	
Grid cell	200 x 200 m^2
Column	250 column
Row	120 row
3) The stratification model	
Quaternary aquifer - Unconfined aquifer	Layer 1 (20-30 m thickness)
The Middle Khorat aquifer (high weathered) - Confined Aquifer	Layer 2 (20-40 m thickness)
The Middle Khorat aquifer (weathered layer) - Confined aquifer	Layer 3 (30-40 m thickness)
No flow layer (fresh rock)	Layer 4 (10 m thickness)
4) layers of grid cell	120,000 grid cell
5) The units used of model (metric system)	
Length	m
Time	day
Conductivity	m/d
Pumping rate	m^3/d
Recharge	m/d
6) Time	
Initial head condition at the time of the study	1 March 2015
Start and End model (1 March 2015)	1 to 458 day
Steady state (1 day)	1 period (1/3/2015)
Transient state (1-153 day)	3 periods (1/3/15 – 31/7/15)
Transient state (154-306 day)	(1/8/15 – 31/12/15)
Transient state (307-458 day)	(1/1/16 – 31/5/16)
7) Wells	
Pumping wells	307 wells
Observation well	14 wells (DGR wells)

Table 5. 2 Boundary conditions

Details	Model
1) River Boundary	
- Vertical hydraulic conductivity of river bed	6.35 – 5.20 m/d (sediment)
- River bed thickness	1 – 2 m
- River width	Khwae Hanuman river width 50 – 120 m Huai Yang river width 50 – 70 m Khwae Kamong river width 50 – 80 m
- River bed bottom	Khwae Hanuman river 52.0 – 5.2 m amsl. Huai Yang river 55.0 – 12.2 m amsl. Khwae Kamong river 52.0 – 7.0 m amsl.
- River stage	Khwae Hanuman river 54.0 – 8.8 m amsl. Huai Yang river 54.0 – 15.1 m amsl. Khwae Kamong river 52.0 – 9.5 m amsl.
2) Recharge	The groundwater recharge potential data (overlay parameters: slope, soil, geology, land use, lineaments and river density multiply the average rainfall of the year 2015-2016, by average rainfall 30 years equal 1,416.15 mm/year, it has recharge rate about 12.8% or 181.27 mm/y or 0.0005 m/d.
- High	0.00028 m/d
- Moderate	0.00013 m/d
- Low	0.000065 m/d
- Very low	0.000025 m/d

2) Aquifer Type: The specific aquifer type can divide into four aquifer layers. The first layer is quaternary sediment aquifer and defined as the unconfined aquifer layer, composed of gravel, sand, silt, and clay. The layer II to IV is composed of sandstone, siltstone, and shale with high to very low fractures, which defined as confined aquifer layer, as shown in **Figure 5.4**.

3) Specific Storage: The specific storage is an important parameter to be filled in each slot of the Visual MODFLOW program due to there is no specific storage

data, no pumping tests. Therefore, the researchers use storativity data from other areas with similar rock properties as the study area, based on the Study of Groundwater Investigation and detailed mapping of the upper Chao Phraya basin 1:50,000 scale (DGR 2011). Then, storativity is used to calculate specific storage (confined aquifer) and specific yield (unconfined aquifer) using the formula in Chapter 2. The layer I is sedimentary aquifer has storativity range 4.33×10^{-6} to 5.43, the middle Khorat aquifer has storativity range 0.002 to 0.119, the Permo-Carboniferous meta-sediments aquifer has storativity range 3.35×10^{-6} to 0.306, and the volcanic aquifer has storativity range 7.45×10^{-7} to 1.13. In calibrating the model, the specific storage and specific yield values are adjusted to the above range.

4) Hydraulic Conductivity: The hydraulic conductivity is the most important parameter in groundwater modeling. Because there is no hydraulic conductivity data and no pumping tests. Therefore, the researchers use hydraulic conductivity data from other areas with similar rock properties as the study area. According to the Study of Groundwater Investigation and detailed mapping of the upper Chao Phraya basin 1:50,000 scale (DGR 2011). The layer I is sedimentary aquifer has hydraulic conductivity range 0.08 to 257 m/d, the middle Khorat aquifer has hydraulic conductivity range 0.065 to 50.0 m/d, the Permo-Carboniferous meta-sediments aquifer has hydraulic conductivity range 5.66×10^{-3} to 30.4 m/d, and the volcanic aquifer has hydraulic conductivity range 5.61×10^{-3} to 14.8 m/d. In calibrating the model, the specific storage and specific yield values are adjusted to the above range.

5) Initial Heads: The piezometric levels of each particular aquifer measured in the field from 14 observation wells in March, 2015 as shown in **Table 5.3**. Whereas, in the areas where there is no observation well, the researchers used hand pump wells, shallow wells and groundwater wells of inactivity instead of observation well. These piezometric head data are used as initial heads of the studied aquifers. Moreover, data is used in the analysis of the model in the steady state condition. For the transient state condition, the initial heads value obtained from the steady state condition of model in calibration process.

6) Recharge Rate: The absorption of rainfall through on top soil downward to lower soil layer and become groundwater is called recharge. The groundwater recharge potential map and the process of studies were shown in Chapter 4. This map

is created from overlay data which consist of the slope, soil, geology, land use, lineaments density and river density. The result indicates potential areas of high, medium, low and very low groundwater recharge, and then multiplied by the average amount of rainfall during the summer and the rainy season of 2015.

The recharge potential from average rainfall on 30 years is equal 1,416.15 mm/y. It has recharge rate in study area about 12.8% or 181.27 mm/y or 0.0005 m/d. In this model, adjust the groundwater recharge in the north of study area (high mountain zone) to the highest recharge zone as shown in **Figure 5.5**. The potential recharge data of the steady and transient state conditions are showed details in **Table 5.4**.

7) River: The river in the model is three rivers include the Khwae Hanuman River, the Huai Yang River, and Khwae kamong River. The data required for the model include locations of gauging stations, elevations of river beds, widths of the rivers, and river stage as shown in **Table 5.2**. The hydraulic conductivity (Kz) of sediments on the river beds about 6.35 – 5.20 m/d. They supposed that the sediments have thickness in the range about 1 - 2 meters.

8) Rate of Groundwater Use (Pumping): The groundwater use data relies on the rates of groundwater pumping from those wells requested for groundwater use, derived from the Department of Groundwater Resources. The rate of groundwater use is one of the most important data in the analysis by the mathematical model. The pumping wells data are considered for the location of wells, top and bottom screen, and pumping rate. This study used pumping well 307 wells **(Figure 5.6)**, which is the 39 private wells and 268 DGR wells. There are 24 wells in the 1st aquifer, 195 wells in the 2nd aquifer, 85 wells in the 3rd aquifer, and 13 wells all three aquifer layer (open hole). The total pumping rates are 12,520.91 m^3/d.

Table 5. 3 Piezometric levels of observation wells

Well name	Coordinate		Screen elevation	Piezometric level (m amsl.)		
	E	N	(m amsl)	Dry season I	Rainy season I	Dry season II
งฆ0209	799535	1565951	2.230	22.58	25.65	20.73
DCD12310	793058	1563837	-18.510	14.16	17.38	13.33
MA148	797932	1556505	-16.190	4.85	6.33	4.16
MF1026	808626	1558456	-3.120	15.23	14.64	13.98
MF1098	800733	1567078	-24.020	25.68	27.30	24.61
MF1174	798190	1565929	0.650	27.35	32.34	24.91
MF151	804505	1568303	1.990	26.09	28.39	25.56
MF688	799607	1566108	-9.670	17.63	24.08	16.39
MF944	792153	1562436	4.100	24.99	27.21	23.53
MW2	797704	1550066	12.160	10.90	10.97	8.99
MW4	800784	1552272	11.260	11.21	12.83	10.37
PB294	798132	1562563	-37.000	12.40	15.80	11.59
PW22955	795674	1559482	-7.890	13.17	14.41	12.29
PW29276	810774	1563532	2.230	29.87	33.05	29.00

Table 5. 4 Groundwater recharges potential data

Periods	Average rainfall		Groundwater Recharge (m/d)			
	mm/y	m/d	high	moderate	low	very low
Mar 15	181.27	$5x10^{-4}$	$2.8x10^{-4}$	$1.3x10^{-4}$	$6.5x10^{-5}$	$2.5x10^{-5}$
Apr 15 - Jul 15	66.90	$1.8x10^{-4}$	$1.x10^{-4}$	$4.8x10^{-5}$	$2.4x10^{-5}$	$8x10^{-6}$
Aug 15 - Dec 15	108.46	$3x10^{-4}$	$1.7x10^{-4}$	$7.8x10^{-5}$	$3.9x10^{-5}$	$1.3x10^{-5}$
Jan 16 - May 16	20.42	$5.6x10^{-5}$	$3.2x10^{-5}$	$1.5x10^{-5}$	$7x10^{-6}$	$2x10^{-6}$

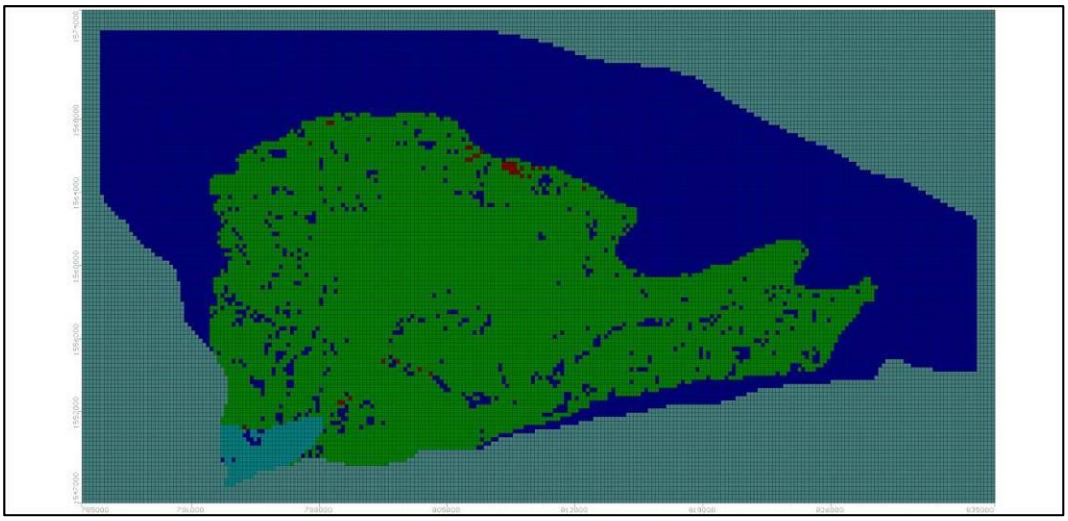

Figure 5. 5 Recharge area in the lower Khwae Hanuman sub-basin

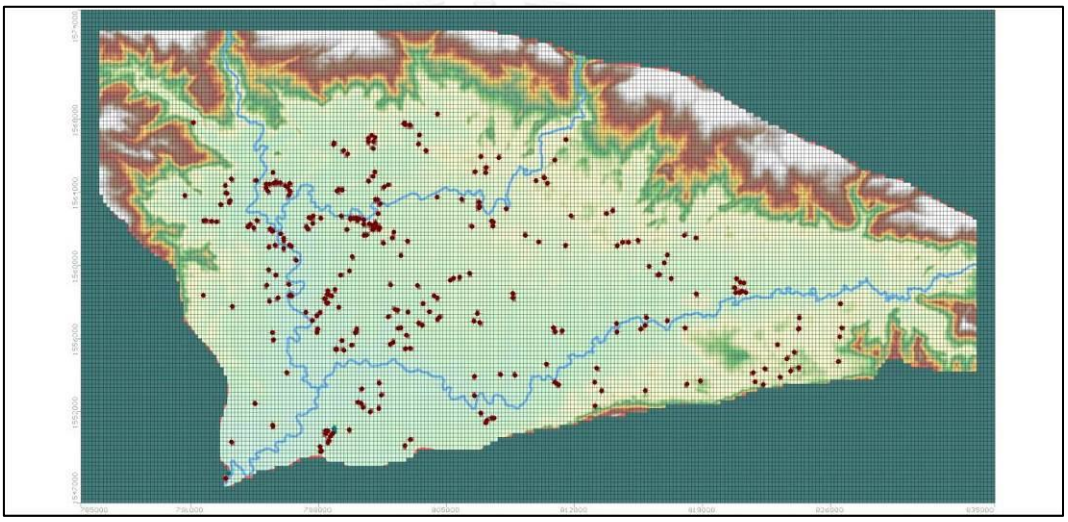

Figure 5. 6 Pumping wells in the lower Khwae Hanuman sub-basin area

5.5 Model Calibration

5.5.1 Processes in Model Calibration

1) Calibration under steady state condition: data received from March 1, 2015 (1 day), as the beginning date for water table data collection and the starting year for transient groundwater flow analysis. The calibration in the steady state case is conducted in order to verify the concept of the model, aquifer classification, and model boundaries. The model parameter which is hydraulic conductivity and recharge were calibrated. The 14 observation wells use for model calibration shows in **Figure 5.7**, and details in **Table 5.3**.

2) Calibration under transient condition uses the available data during the years 2015-2016 which is 1 year duration of modeling, starting from March 1, 2015, as the first day in the model and ends at May 31, 2016 (total 458th days in the model). The time step used in the calculation is season which corresponding to duration of data collection from the observation wells of the Department of Groundwater Resources. This study divides the seasonal time into 3 seasons: 2015, dry season (March to July), rainy season (August to December) and 2016, dry season (January to May), which is show details in **Tables 5.1** and **5.3**. The calibration in the transient condition is conducted in order to determine the values of parameters that vary with time such as the storage, recharge rates and river.

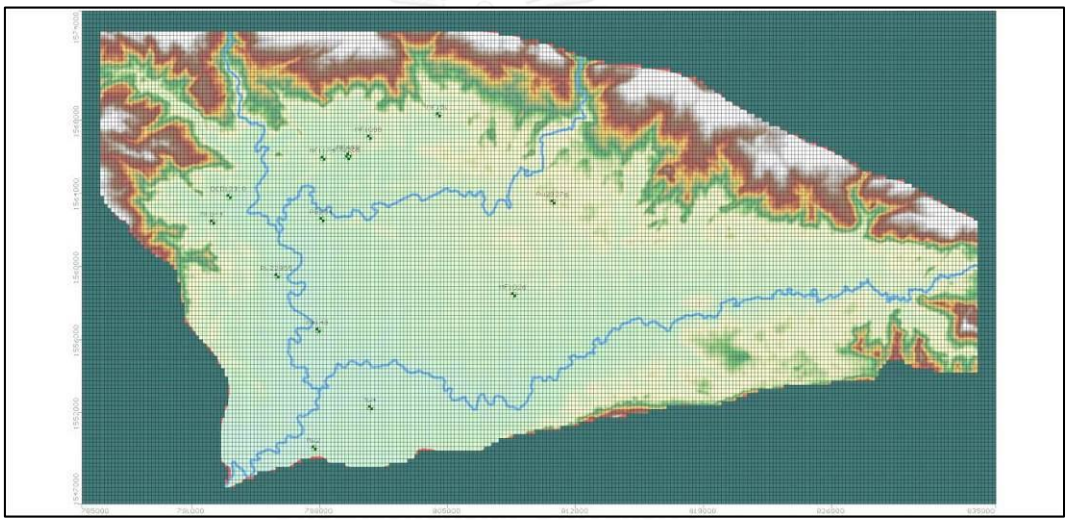

Figure 5. 7 The 14 observation wells in the study area

5.5.2 Results of Model Calibration under Steady State Condition

The simulation of groundwater flow under steady state condition is conducted by using data from March 1, 2015. The model parameters varied until the values of hydraulic heads obtained from the model which close to those obtained from the observation wells from March 1, 2015. **Figure 5.8** shows the results of the simulation compared with the field data. In comparing results from the simulation with those measured in 14 observation wells, there found that the calibrated results have a mean residual as 3.87 m, a mean absolute residual as 4.55 m, the root mean squared as 5.55 m, and the normalized root mean squared is 22.17 %.

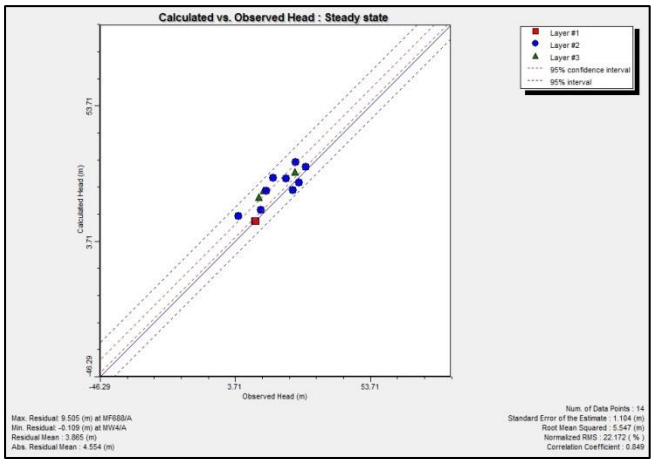

Figure 5. 8 Simulating result model of steady state conditions

5.5.3 Results of Model Calibration under Transient Condition

The simulation of groundwater flow under transient condition is conducted by using data from March 1, 2015 to May 31, 2016. The model parameters are varied until the values of hydraulic heads obtained from the model which close to those obtained from the observation wells during the years 2015-2016. The results of the simulation compared with the field data. In comparing results from the simulation with those measured in 14 observation wells of each period as follow:

Period dry season in year 2015: There found that the calibrated results have a mean residual in the range of 3.75 m, the mean absolute residual as 4.49 m, the root mean squared as 5.47 m, and the normalized root mean squared is 21.87 %, as shown in **Figure 5.9 (a)**.

Period rainy season in year 2015: There found that the calibrated results have a mean residual in the range of 1.81 m, the mean absolute residual as 3.97 m, the root mean squared as 4.65 m, and the normalized root mean squared is 17.39 %, as shown in **Figure 5.9 (b)**.

Period dry season in year 2016: There found that the calibrated results have a mean residual in the range of 4.91 m, the mean absolute residual as 5.11 m, the root mean squared as 6.16 m, and the normalized root mean squared is 24.79 %, as shown in **Figure 5.9 (c)**.

(a)

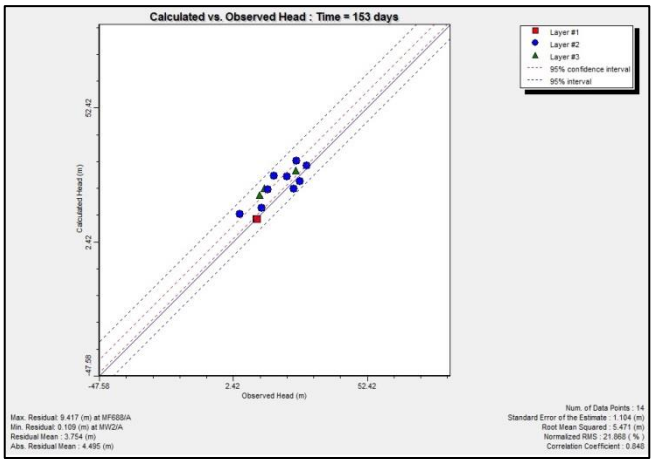

(b)

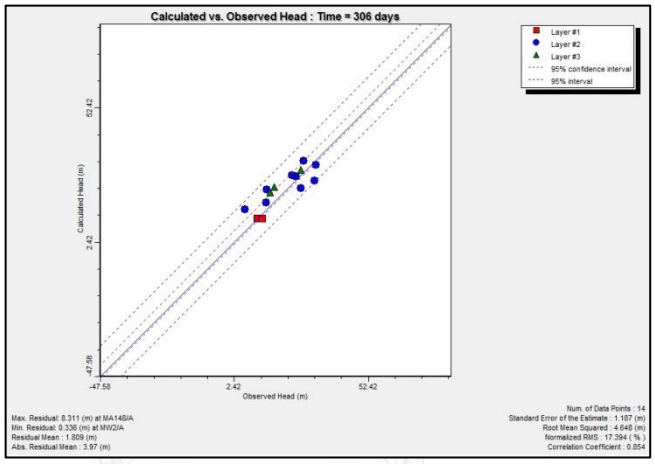

(c)

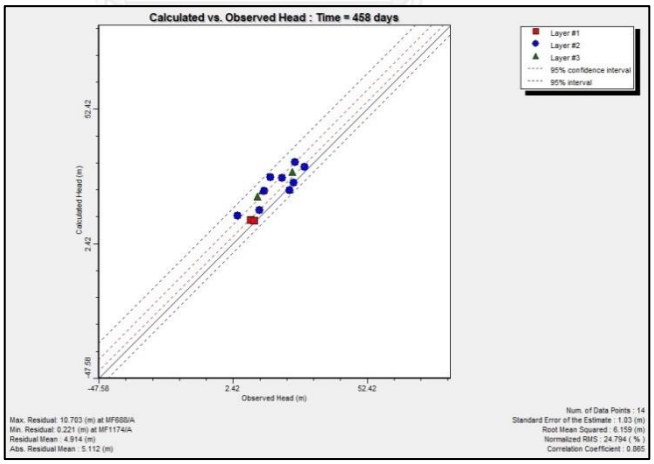

Figure 5. 9 Simulating result model of transient state conditions (a) Dry season in year 2015, (b) Rainy season in year 2015, and (c) Dry season in year 2016

5.6 Groundwater Balance

The balance of groundwater flow can be evaluated from dry season and wet season by applying the model to simulate groundwater flow and hydraulic heads during March 1, 2015 to May 31, 2016 (transient state condition). The water balance in the study area is divided into 4 zones include sedimentary aquifer (Q), middle Khorat aquifer (Jmk), volcanic aquifer (PTrv), and meta-sediment aquifer (PCms), which can be described as follows:

5.6.1 The Dry Season in year 2015

The simulation of groundwater flow in the first period is March 1, 2015 to July 31, 2015. The total amount of water inflow to the groundwater aquifers in the project area is 0.95 Mm^3/d and the total amount of water outflow from these groundwater aquifers is 0.95 Mm^3/d. During the dry season, the water loss from sub-basin is about 40 m^3/d and 0.0 % discrepancy. The details of groundwater balance of dry season I is shown in **Tables 5.5** to **5.8**.

Table 5. 5 The groundwater balance of dry season in year 2015 of Q aquifer

IN	**m^3/d**	**OUT**	**m^3/d**
STORAGE	68,507	STORAGE	0
WELLS	0	WELLS	129
RIVER LEAKAGE	195,840	RIVER LEAKAGE	336,530
RECHARGE	50,397	RECHARGE	0
Jmk to Q aquifer	311,080	Q to Jmk aquifer	290,420
PTrv to Q aquifer	1,459	Q to PTrv aquifer	69
PCms to Q aquifer	23	Q to PCms aquifer	123
Total IN	627,300	Total OUT	627,270

Table 5. 6 The groundwater balance of dry season in year 2015 of Jmk aquifer

IN	m^3/d	OUT	m^3/d
STORAGE	19,714	STORAGE	0
WELLS	0	WELLS	12,347
RIVER LEAKAGE	0	RIVER LEAKAGE	0
RECHARGE	14,620	RECHARGE	0
PTrv to Jmk aquifer	25	Jmk to PTrv aquifer	1,302
PCms to Jmk aquifer	71	Jmk to PCms aquifer	120
Q to Jmk aquifer	290,420	Jmk to Q aquifer	311,080
Total IN	324,850	Total OUT	324,840

Table 5. 7 The groundwater balance of dry season in year 2015 of PTrv aquifer

IN	m^3/d	OUT	m^3/d
STORAGE	4	STORAGE	0
WELLS	0	WELLS	3
RIVER LEAKAGE	0	RIVER LEAKAGE	0
RECHARGE	0	RECHARGE	0
Jmk to PTrv aquifer	1,302	PTrv to Jmk aquifer	25
PCms to PTrv aquifer	120	PTrv to PCms aquifer	8
Q to PTrv aquifer	69	PTrv to Q aquifer	1,459
Total IN	1,494	Total OUT	1,494

Table 5. 8 The groundwater balance of dry season in year 2015 of PCms aquifer

IN	m^3/d	OUT	m^3/d
STORAGE	0	STORAGE	0
WELLS	0	WELLS	38
RIVER LEAKAGE	0	RIVER LEAKAGE	0
RECHARGE	0	RECHARGE	0
Jmk to PCms aquifer	120	PCms aquifer to Jmk	71
PTrv to PCms aquifer	8	PCms to PTrv aquifer	120
Q to PCms aquifer	123	PCms to Q aquifer	23
Total IN	252	Total OUT	252

5.6.2 The Rainy Season in year 2015

The simulation of groundwater flow in the second period is August 1, 2015 to December 31, 2015. The total amount of water inflow to the groundwater aquifers in the project area is 0.98 Mm^3/d and the total amount of water outflow from these groundwater aquifers is 0.98 Mm^3/d. During wet season, the water added to sub-basin is about 50 m^3/d and 0.0 % discrepancy. The details of groundwater balance of rainy season I is shown in **Tables 5.9** to **5.12**.

Table 5. 9 The groundwater balance of rainy season in year 2015 of Q aquifer

IN	**m^3/d**	**OUT**	**m^3/d**
STORAGE	4,886	STORAGE	127,950
WELLS	0	WELLS	129
RIVER LEAKAGE	282,070	RIVER LEAKAGE	244,040
RECHARGE	81,577	RECHARGE	0
Jmk to Q aquifer	294,320	Q to Jmk aquifer	291,460
PTrv to Q aquifer	1,153	Q to PTrv aquifer	639
PCms to Q aquifer	251	Q to PCms aquifer	0
Total IN	664,260	Total OUT	664,210

Table 5. 10 The groundwater balance of rainy season in year 2015 of Jmk aquifer

IN	**m^3/d**	**OUT**	**m^3/d**
STORAGE	1,568	STORAGE	9,150
WELLS	0	WELLS	12,347
RIVER LEAKAGE	0	RIVER LEAKAGE	0
RECHARGE	23,638	RECHARGE	0
PTrv to Jmk aquifer	518	Jmk to PTrv aquifer	1,209
PCms to Jmk aquifer	32	Jmk to PCms aquifer	190
Q to Jmk aquifer	291,460	Jmk to Q aquifer	294,320
Total IN	317,220	Total OUT	317,220

Table 5. 11 The groundwater balance of rainy season in year 2015 of PTrv aquifer

IN	**m^3/d**	**OUT**	**m^3/d**
STORAGE	0	STORAGE	43
WELLS	0	WELLS	3
RIVER LEAKAGE	0	RIVER LEAKAGE	0
RECHARGE	0	RECHARGE	0
Jmk to PTrv aquifer	1,209	PTrv to Jmk aquifer	518
PCms to PTrv aquifer	6	PTrv to PCms aquifer	138
Q to PTrv aquifer	639	PTrv to Q aquifer	1,153
Total IN	1,854	Total OUT	1,854

Table 5. 12 The groundwater balance of rainy season in year 2015 of PCms aquifer

IN	**m^3/d**	**OUT**	**m^3/d**
STORAGE	0	STORAGE	1
WELLS	0	WELLS	38
RIVER LEAKAGE	0	RIVER LEAKAGE	0
RECHARGE	0	RECHARGE	0
Jmk to PCms aquifer	190	PCms to Jmk aquifer	32
PTrv to PCms aquifer	138	PCms to PTrv aquifer	6
Q to PCms aquifer	0	PCms to Q aquifer	251
Total IN	328	Total OUT	328

5.6.3 The Dry Season in year 2016

The simulation of groundwater flow in the final period is January 1, 2016 to May 31, 2016. The total amount of water inflow to the groundwater aquifers in the project area is 1.1 Mm^3/d and the total amount of water outflow from these groundwater aquifers is 1.1 Mm^3/d. During the dry season, the water loss from sub-basin is about -10 m^3/d and 0.0 % discrepancy. The details of groundwater balance of dry season II is shown in **Tables 5.13** to **5.16**.

Table 5. 13 The groundwater balance of dry season in year 2016 of Q aquifer

IN	m^3/d	OUT	m^3/d
STORAGE	188,590	STORAGE	106
WELLS	0	WELLS	129
RIVER LEAKAGE	179,870	RIVER LEAKAGE	412,490
RECHARGE	15,470	RECHARGE	0
Jmk to Q aquifer	368,290	Q to Jmk aquifer	340,860
PTrv to Q aquifer	2,237	Q to PTrv aquifer	671
PCms to Q aquifer	2	Q to PCms aquifer	201
Total IN	754,450	Total OUT	754,460

Table 5. 14 The groundwater balance of dry season in year 2016 of Jmk aquifer

IN	m^3/d	OUT	m^3/d
STORAGE	36,525	STORAGE	0
WELLS	0	WELLS	12,347
RIVER LEAKAGE	0	RIVER LEAKAGE	0
RECHARGE	4,622	RECHARGE	0
PTrv to Jmk aquifer	194	Jmk to PTrv aquifer	1,628
PCms to Jmk aquifer	98	Jmk to PCms aquifer	39
Q to Jmk aquifer	340,860	Jmk to Q aquifer	368,290
Total IN	382,300	Total OUT	382,300

Table 5. 15 The groundwater balance of dry season in year 2016 of PTrv aquifer

IN	m^3/d	OUT	m^3/d
STORAGE	34	STORAGE	0
WELLS	0	WELLS	3
RIVER LEAKAGE	0	RIVER LEAKAGE	0
RECHARGE	0	RECHARGE	0
Jmk to PTrv aquifer	1,628	PTrv to Jmk aquifer	194
PCms to PTrv aquifer	105	PTrv to PCms aquifer	3
Q to PTrv aquifer	671	PTrv to Q aquifer	2,237
Total IN	2,437	Total OUT	2,437

Table 5. 16 The groundwater balance of dry season in year 2016 of PCms aquifer

IN	**m^3/d**	**OUT**	**m^3/d**
STORAGE	1	STORAGE	0
WELLS	0	WELLS	38
RIVER LEAKAGE	0	RIVER LEAKAGE	0
RECHARGE	0	RECHARGE	0
Jmk to PCms aquifer	39	PCms to Jmk aquifer	98
PTrv to PCms aquifer	3	PCms to PTrv aquifer	105
Q to PCms aquifer	201	PCms to Q aquifer	2
Total IN	244	Total OUT	244

5.7 Model prediction

From the study of Department of Groundwater Resources (2008), found that the groundwater demand of Prachinburi province is gradually increased 2% per year. The groundwater prediction in the future is done by simulation to estimate the groundwater level under various scenarios.

5.7.1 Scenarios of groundwater pumping

There are four scenarios of various groundwater pumping and groundwater recharge as follows:

1) The 1st scenario: The present groundwater pumping rate in 2016 with the cumulative increase of 2 percent per year at 20 years, with the minimum amount of precipitation of 1,302.6 mm/y in 1979 (TMD, 2016), which is equivalent to 167 mm/y of groundwater recharge rate (12.8% of precipitation) was simulated.

2) The 2nd scenario: The present groundwater pumping rate in 2016, with the cumulative increase of 2 percent per year 20 years, with the maximum amount of precipitation to 2,652.4 mm/y in 1966 (TMD, 2016), which is equivalent to 339 mm/y of groundwater recharge rate (12.8% of precipitation) was simulated.

3) The 3rd scenario: The present groundwater pumping rate in 2016, with the cumulative increase of 4 percent per year at 20 years, with the maximum amount of precipitation to 1,302.6 mm/y in 1979 (TMD, 2016), which is equivalent to 167 mm/y of groundwater recharge rate (12.8% of precipitation) was simulated.

4) The 4th scenario: Groundwater pumping data in 2016, with the cumulative increase of 4 percent per year at 20 years, with the maximum amount of precipitation to 2,652.4 mm/y in 1966 (TMD, 2016), which is equivalent to 339 mm/y of groundwater recharge rate (12.8% of precipitation) was simulated.

5.7.2 The results of scenarios

1. Groundwater level

Groundwater level of all cases seem to be not changed much and are described as follows (**Figure 5.10**). The 1st groundwater aquifer has the groundwater level between 5 to 60 meters above mean sea level (m amsl.) and groundwater levels in the 2nd and 3rd aquifers ranges between 5 to 50 m amsl.. The groundwater level of these three aquifers appears to be not decreased.

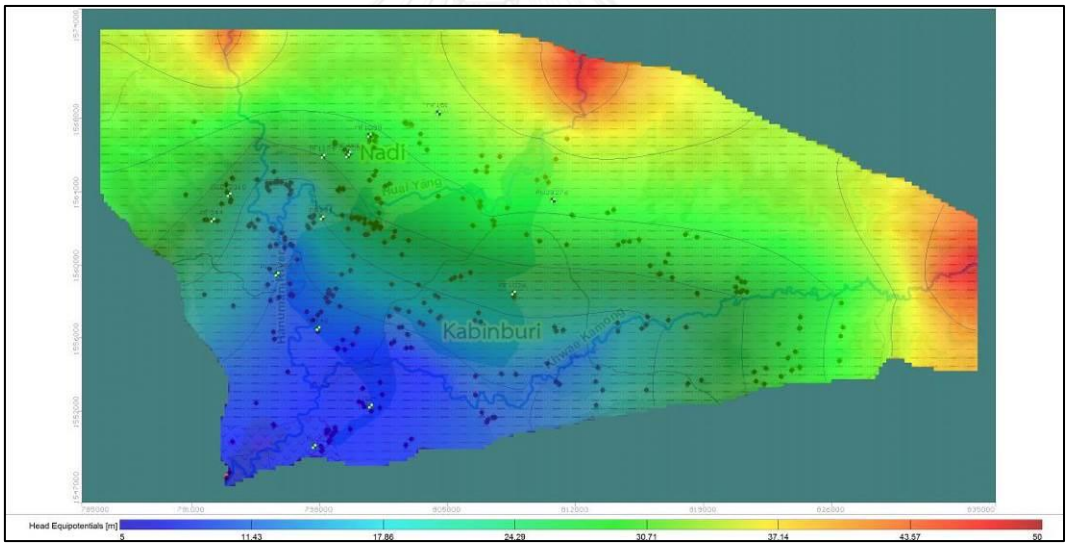

Figure 5. 10 The map showing groundwater level under various scenarios

2. Groundwater drawdown

1) According to the 1st scenario simulation, the drawdown of the 1st layer in the Q aquifer as well as the 2nd and 3rd layers of the Jmk aquifer were ranged between 0.10-0.40, 0.10-0.40, and 0.10-0.50 m, respectively (**Figure 5.11**).

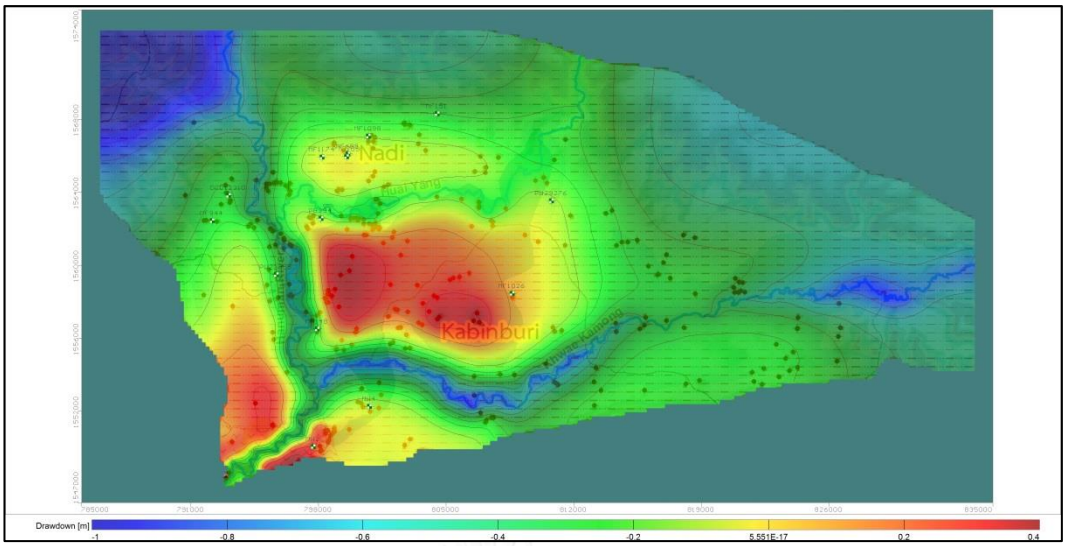

Figure 5. 11 The map showing drawdown of the 2nd aquifer due to 2 percent cumulative pumping in 20 years with the minimum groundwater recharge rate

2) According to the 2st scenario simulation, there are no drawdown inducing from the pumping under this scenario in the 1st layer in Q aquifer as well as the 2nd and 3rd layers of the Jmk aquifer.

3) According to the 3st scenario simulation, , the drawdown found in the 1st layer of Q aquifer as well as the 2nd and 3rd layers of Jmk aquifer were ranged between 0.10-1.0, 0.10-1.0, and 0.10-1.40 m, respectively (**Figure 5.12**).

4) According to the 4th scenario simulation, the drawdown of all layers were ranged between 0.10-0.30 m (**Figure 5.13**).

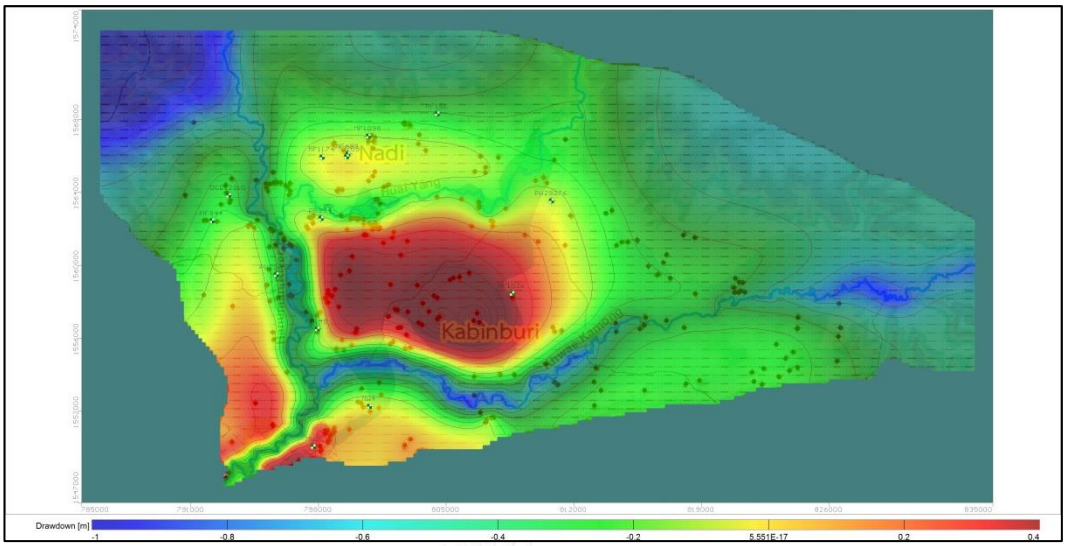

Figure 5. 12 The map showing drawdown of the 2nd aquifer due to 4 percent cumulative pumping in 20 years with the minimum groundwater recharge rate

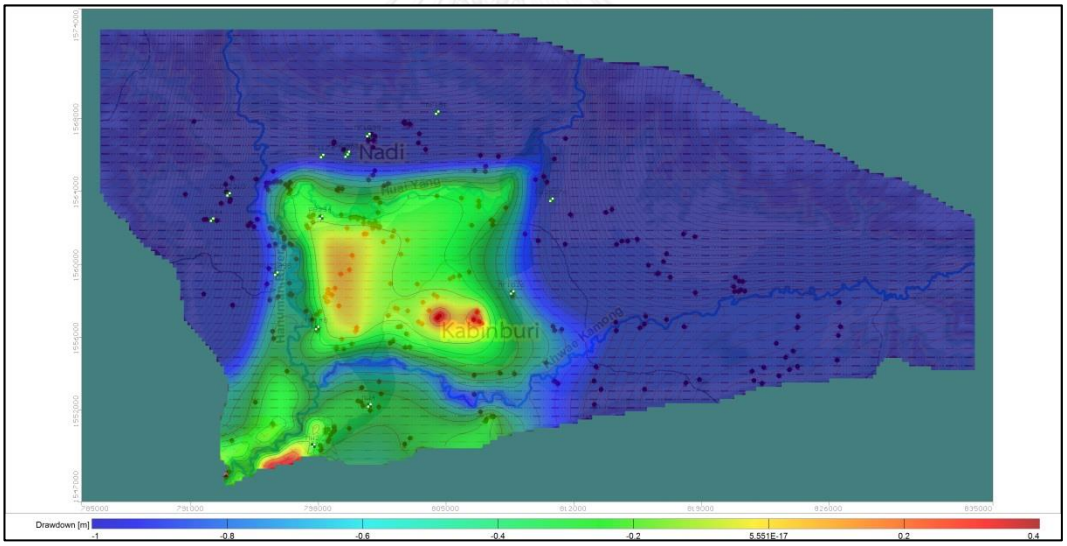

Figure 5. 13 The map showing drawdown of the 2nd aquifer due to 4 percent cumulative pumping in 20 years with the maximum groundwater recharge rate

5.8 Safe yield in the lower Khwae Hanuman sub-basin area

Simulation of groundwater safe yield aims to identify the potential of groundwater and to conduct the suitable groundwater management plan. Factors considered for the reduction of groundwater level such as water consumption and groundwater recharge have to be taken into account. Initially, the criteria for

determining the maximum water consumption can be safely used, by simulating groundwater for a period of 20 consecutive years.

Since the difference in groundwater level measured from the field during the dry season and the rainy season is about 2 m, therefore groundwater levels of all aquifers allow to be decreased not more than 2 m as compared those levels before pumping , implying the groundwater level can rebound in each year.

Simulation of the groundwater safe yield in the study area is conducted using a modified groundwater model from the calibration and verification stages. The safe yield estimation is based on the trial and error method by various pumping rate with the same locations of groundwater wells and groundwater pumping rate in 2016.

5.8.1 Result of safe yield

By 10%, 50%, 100%, and 200% increasing of groundwater pumping over 20 years, the total pumping rates of all wells are approx. 13,579, 18,516, 24,688, and 37,033 m^3/d, respectively. According to previous pumping rates, it was found that groundwater level of the 1^{st} aquifer range between 5 to 60 m amsl. and groundwater levels of the 2^{nd} and 3^{rd} aquifers range between 5 to 50 m amsl.. Drawdown was decreased 2.50, 2.50, 3.00, and 4.00 m (**Figures 5.14** to **5.17**), when increasing pumping rate 10%, 50%, 100%, and 200%, respectively.

The result of 200% increasing of groundwater pumping over 20 years resulted in the cone of depression covering area of 90 km^2 which appeared in the industrial area located in Nong ki Sub-district. Moreover, groundwater balance of 12 sub-district areas was shown in **Tables 5.17** to **5.28.**

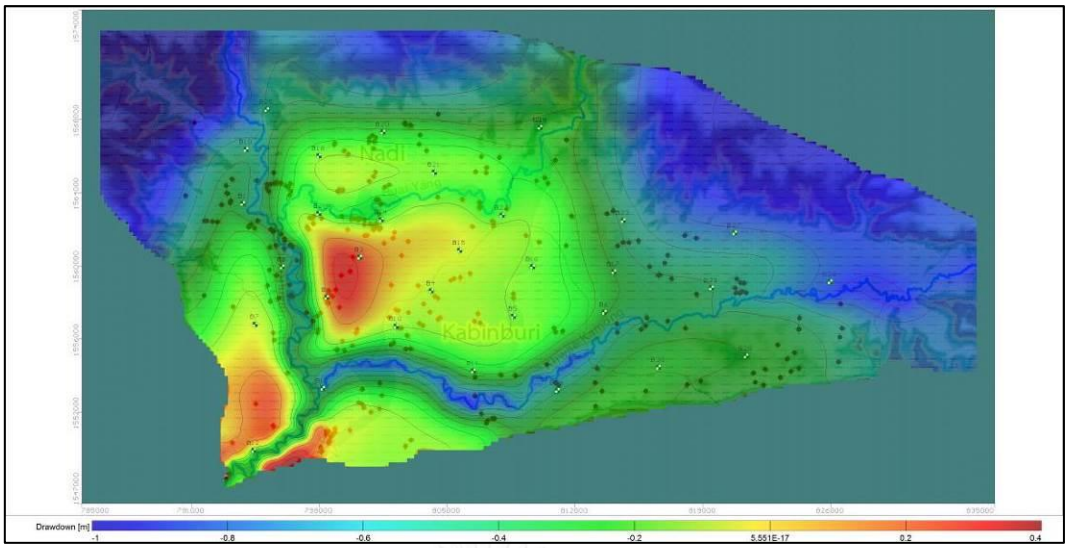

Figure 5. 14 The map showing drawdown of 10% increasing of pumping rate in 20 years

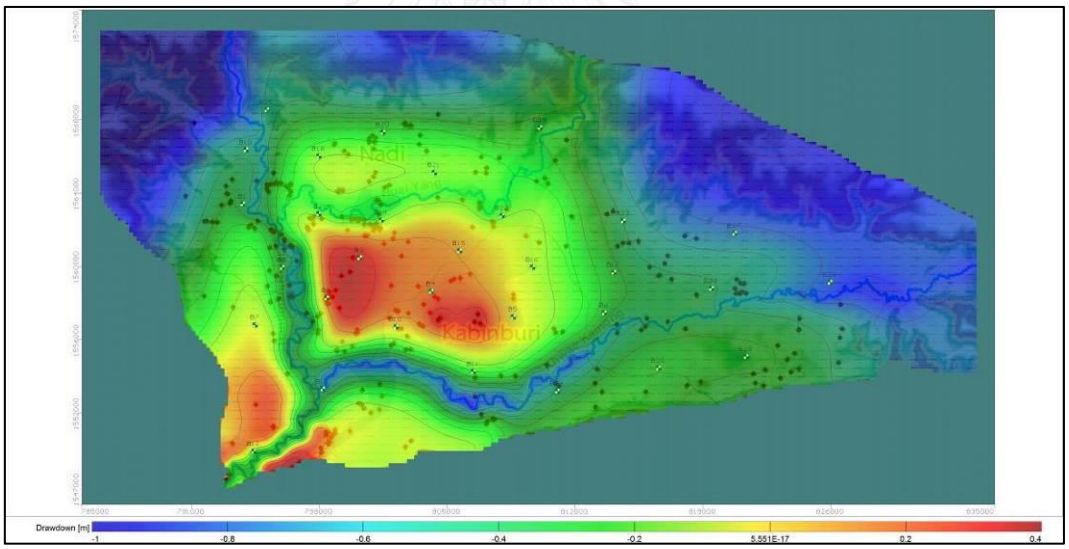

Figure 5. 15 The drawdown of cumulative pumping 50 percent in 20 years

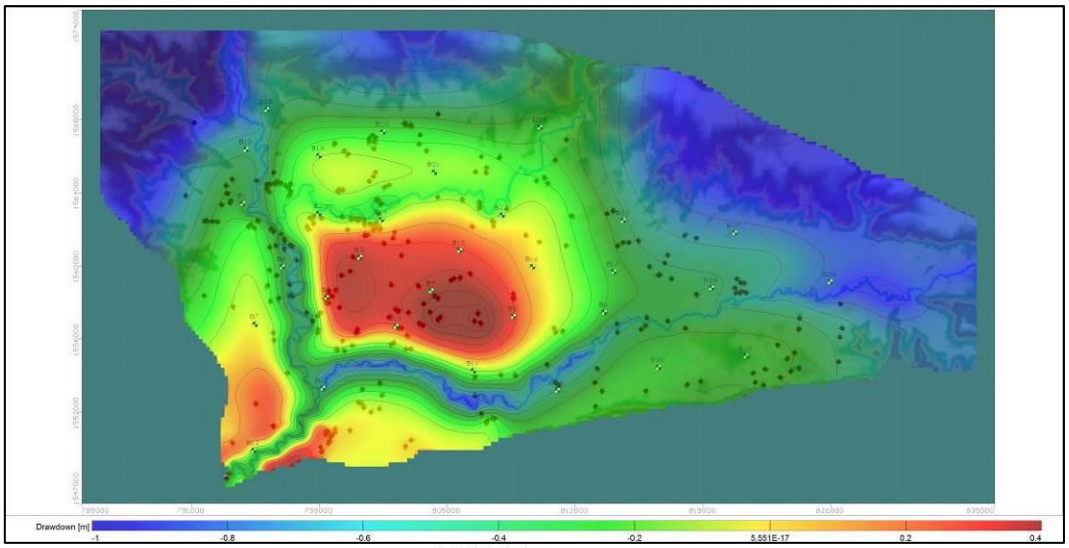

Figure 5. 16 The drawdown of cumulative pumping 100 percent in 20 years

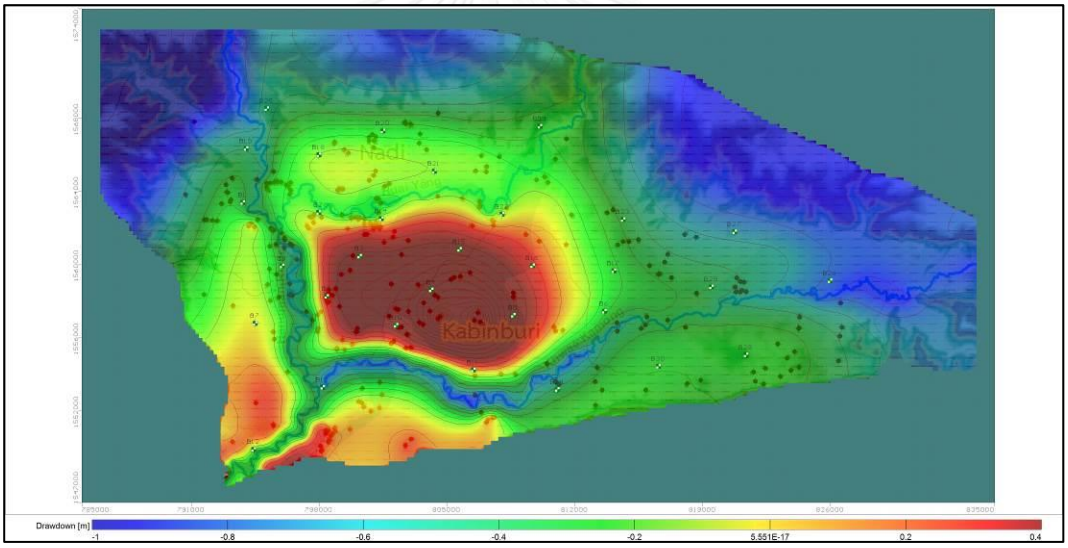

Figure 5. 17 The drawdown of cumulative pumping 200 percent in 20 years

Table 5. 17 The groundwater balance of Kham Tanod sub-district area

IN	**m^3/d**	**OUT**	**m^3/d**
STORAGE	0	STORAGE	0
RECHARGE	2,419	RECHARGE	0
Saphan Hin to Kham Tanod	2,627	Kham Tanod to Saphan Hin	5,045
Total IN	5,046	Total OUT	5,045

Table 5. 18 The groundwater balance of Sam Pan Ta sub-district area

IN	**m^3/d**	**OUT**	**m^3/d**
STORAGE	0	STORAGE	2
WELLS	0	WELLS	4,328
RIVER LEAKAGE	35,916	RIVER LEAKAGE	84,999
RECHARGE	17,138	RECHARGE	0
Saphan Hin to Sam Pan Ta	41,859	Sam Pan Ta to Saphan Hin	44,140
Nadi to Sam Pan Ta	50,938	Sam Pan Ta to Nadi	11,531
Nong Ki to Sam Pan Ta	3,089	Sam Pan Ta to Nong Ki	4,625
Muang Khao to Sam Pan Ta	4,176	Sam Pan Ta to Muang Khao	7,967
Na Kheam to Sam Pan Ta	10,759	Sam Pan Ta to Na Kheam	6,279
Total IN	163,880	Total OUT	163,870

Table 5. 19 The groundwater balance of Saphan Hin sub-district area

IN	**m^3/d**	**OUT**	**m^3/d**
STORAGE	0	STORAGE	5
WELLS	0	WELLS	2,564
RIVER LEAKAGE	19,409	RIVER LEAKAGE	35,123
RECHARGE	24,391	RECHARGE	0
Kham Tanod to Saphan Hin	5,045	Saphan Hin to Kham Tanod	2,627
Sam Pan Ta to Saphan Hin	44,140	Saphan Hin to Sam Pan Ta	41,859
Na Kheam to Saphan Hin	6,052	Saphan Hin to Na Kheam	16,854
Total IN	99,037	Total OUT	99,033

Table 5. 20 The groundwater balance of Kabin sub-district area

IN	**m^3/d**	**OUT**	**m^3/d**
STORAGE	0	STORAGE	0
WELLS	0	WELLS	8
RIVER LEAKAGE	92	RIVER LEAKAGE	1,289
RECHARGE	256	RECHARGE	0
Muang Khao to Kabin	133	Kabin to Muang Khao	0
Na Kheam to Kabin	917	Kabin to Na Kheam	101
Total IN	1,398	Total OUT	1,398

Table 5. 21 The groundwater balance of Nadi sub-district area

IN	**m^3/d**	**OUT**	**m^3/d**
STORAGE	0	STORAGE	7
WELLS	0	WELLS	2,870
RIVER LEAKAGE	72,771	RIVER LEAKAGE	17,417
RECHARGE	28,203	RECHARGE	0
Sam Pan Ta to Nadi	11,531	Nadi to Sam Pan Ta	50,938
Thung Pho to Nadi	17,385	Nadi to Thung Pho	33,621
Nong Ki to Nadi	6,379	Nadi to Nong Ki	31,402
Total IN	136,270	Total OUT	136,250

Table 5. 22 The groundwater balance of Thung Pho sub-district area

IN	**m^3/d**	**OUT**	**m^3/d**
STORAGE	0	STORAGE	9
WELLS	0	WELLS	347
RIVER LEAKAGE	24,905	RIVER LEAKAGE	15,968
RECHARGE	14,388	RECHARGE	0
Nadi to Thung Pho	33,621	Thung Pho to Nadi	17,385
Kaeng Dinso to Thung Pho	16,685	Thung Pho to Kaeng Dinso	27,938
Ban Na to Thung Pho	483	Thung Pho to Ban Na	0
Nong Ki to Thung Pho	2,561	Thung Pho to Nong Ki	30,993
Total IN	92,643	Total OUT	92,640

Table 5. 23 The groundwater balance of Kaeng Dinso sub-district area

IN	**m^3/d**	**OUT**	**m^3/d**
STORAGE	0	STORAGE	37
WELLS	0	WELLS	1,066
RIVER LEAKAGE	6,433	RIVER LEAKAGE	91,459
RECHARGE	52,366	RECHARGE	0
Thung Pho to Kaeng Dinso	27,938	Kaeng Dinso to Thung Pho	16,685
Khok Pi Kong to Kaeng Dinso	37,567	Kaeng Dinso to Khok Pi Kong	10,482
Ban Na to Kaeng Dinso	2,240	Kaeng Dinso to Ban Na	6,814
Total IN	126,540	Total OUT	126,540

Table 5. 24 The groundwater balance of Ban Na sub-district area

IN	**m^3/d**	**OUT**	**m^3/d**
STORAGE	0	STORAGE	1
WELLS	0	WELLS	3,968
RIVER LEAKAGE	4,207	RIVER LEAKAGE	21,813
RECHARGE	6,964	RECHARGE	0
Thung Pho to Ban Na	0	Ban Na to Thung Pho	483
Kaeng Dinso to Ban Na	6,814	Ban Na to Kaeng Dinso	2,240
Nong Ki to Ban Na	18,515	Ban Na to Nong Ki	4,120
Muang Khao to Ban Na	1,407	Ban Na to Muang Khao	5,282
Total IN	37,907	Total OUT	37,907

Table 5. 25 The groundwater balance of Nong Ki sub-district area

IN	**m^3/d**	**OUT**	**m^3/d**
STORAGE	0	STORAGE	5
WELLS	0	WELLS	20,907
RIVER LEAKAGE	901	RIVER LEAKAGE	22,692
RECHARGE	10,113	RECHARGE	0
Sam Pan Ta to Nong Ki	4,625	Nong Ki to Sam Pan Ta	3,089
Nadi to Nong Ki	31,402	Nong Ki to Nadi	6,379
Thung Pho to Nong Ki	30,993	Nong Ki to Thung Pho	2,561
Ban Na to Nong Ki	4,120	Nong Ki to Ban Na	18,515
Muang Khao to Nong Ki	28	Nong Ki to Muang Khao	8,035
Total IN	82,182	Total OUT	82,183

Table 5. 26 The groundwater balance of Khok Pi Kong sub-district area

IN	**m^3/d**	**OUT**	**m^3/d**
STORAGE	0	STORAGE	1
RIVER LEAKAGE	26,276	RIVER LEAKAGE	5,939
RECHARGE	6,754	RECHARGE	0
Kaeng Dinso to Khok Pi Kong	10,482	Khok Pi Kong to Kaeng Dinso	37,567
Total IN	43,511	Total OUT	43,507

Table 5. 27 The groundwater balance of Muang Khao sub-district area

IN	m^3/d	OUT	m^3/d
STORAGE	0	STORAGE	0
WELLS	0	WELLS	1,296
RIVER LEAKAGE	1,595	RIVER LEAKAGE	23,685
RECHARGE	4,622	RECHARGE	0
Sam Pan Ta to Muang Khao	7,967	Muang Khao to Sam Pan Ta	4,176
Ban Na to Muang Khao	5,282	Muang Khao to Ban Na	1,407
Nong Ki to Muang Khao	8,035	Muang Khao to Nong Ki	28
Na Kheam to Muang Khao	3,650	Muang Khao to Na Kheam	426
Kabin to Muang Khao	0	Muang Khao to Kabin	133
Total IN	31,151	Total OUT	31,150

Table 5. 28 The groundwater balance of Na Kheam sub-district area

IN	m^3/d	OUT	m^3/d
STORAGE	0	STORAGE	1
WELLS	0	WELLS	198
RIVER LEAKAGE	3,192	RIVER LEAKAGE	13,019
RECHARGE	7,744	RECHARGE	0
Saphan Hin to Na Kheam	16,854	Na Kheam to Saphan Hin	6,052
Sam Pan Ta to Na Kheam	6,279	Na Kheam to Sam Pan Ta	10,759
Muang Khao to Na Kheam	426	Na Kheam to Muang Khao	3,650
Kabin to Na Kheam	101	Na Kheam to Kabin	917
Total IN	34,596	Total OUT	34,596

5.9 Sensitivity Analysis

Sensitivity analysis of each parameters is a comparison of the effects of each variables which is shown by various percentages (x-axis), onto the output or percentage of groundwater level change (y-axis). This study revealed that the rate of groundwater recharge had the greatest effect on the change of groundwater level. The second sensitive variable is the hydraulic conductivity in the X- and Y- directions because the groundwater flow in the study area has better horizontal flow than vertical flow, as shown in **Figure 5.18**.

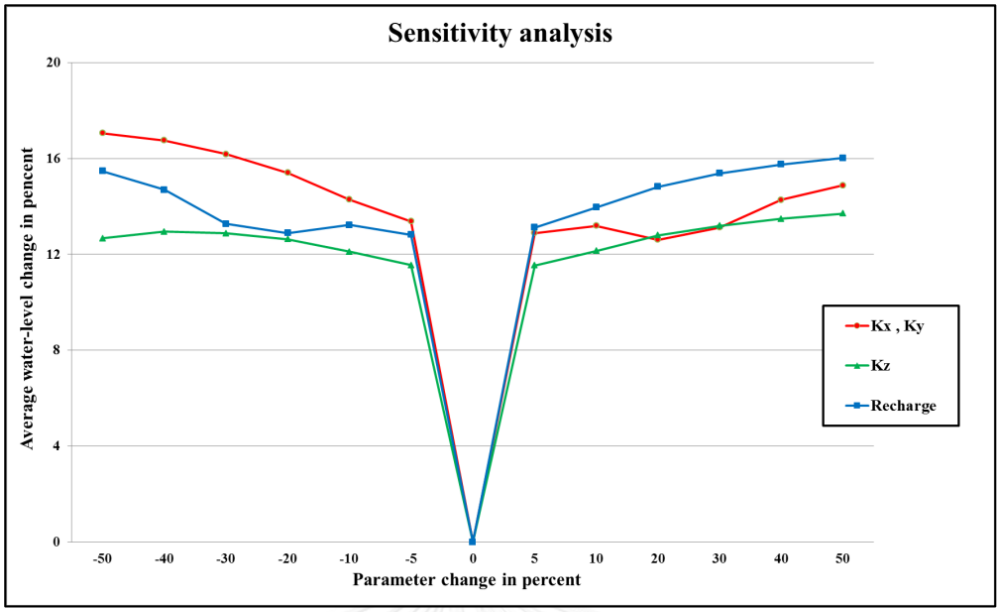

Figure 5. 18 Sensitivity analysis of Kx, Ky and recharge in groundwater modeling

5.10 Uncertainty Analysis

Uncertainty analysis results based on the 95 percentile of the mean difference obtained from the model and the mean error value. Based on the standard deviation (SD) distribution of each data compared to mean, the upper and the lower boundary values of MODFLOW data can be estimated. The results of the analysis of groundwater level uncertainty in each season are as follows:

1) Observation well no. งฒ0209 was found that the groundwater level from the actual measurements tended to be close to the values obtained from the model and the mean error, which showed that the model performed well. The mean difference between the calculated value of the model and the measured value, SD, the upper and the lower boundary values were -3.85, 2.41, 0.88 m and -8.58 m, respectively, as shown in **Figure 5.19**.

2) Observation well no. DCD12310 was found that the groundwater level from the actual measurements tended to be close to the values obtained from the model and the mean error, which showed that the model was performing well. The mean difference between the calculated value of the model and the measured value,

SD, the upper and the lower boundary values were -7.67, 1.71, -4.32 m and -11.01 m, respectively, as shown in **Figure 5.20**.

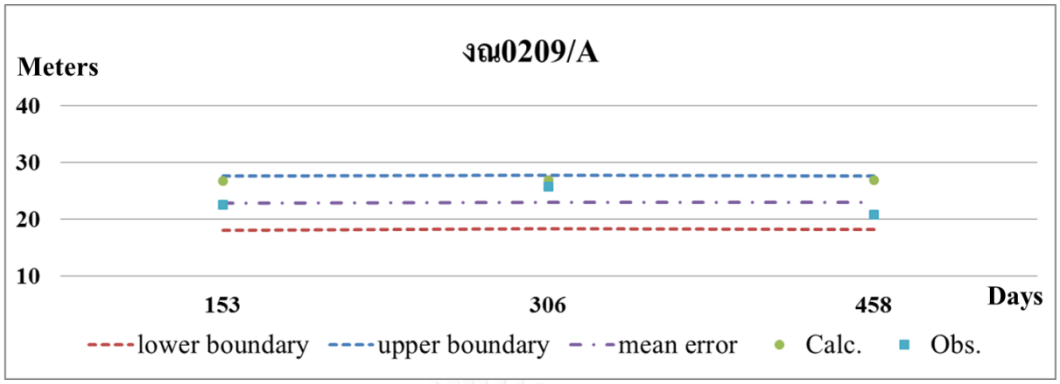

Figure 5. 19 Uncertainty analysis of observation well no. งฉ0209

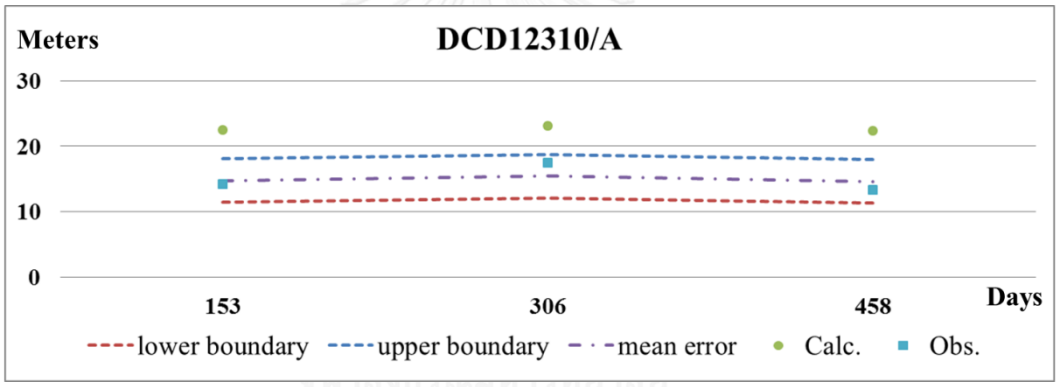

Figure 5. 20 Uncertainty analysis of observation well no. DCD12310

3) Observation well no. MA148 was found that the groundwater level from the actual measurements tended to be close to the values obtained from the model and the mean error, which showed that the model was performing well. The mean difference between the calculated value of the model and the measured value, SD, the upper and the lower boundary values were -8.35, 0.31, -7.75 m and -8.95 m, respectively, as shown in **Figure 5.21**.

4) Observation well no. MF1026: found that the groundwater level from the actual measurements tended to be close to the values obtained from the model and the mean error, which showed that the model was performing well. The mean difference between the calculated value of the model and the measured value,

SD, the upper and the lower boundary values were -7.44, 0.60, -6.26 m and -8.63 m, respectively, as shown in **Figure 5.22**.

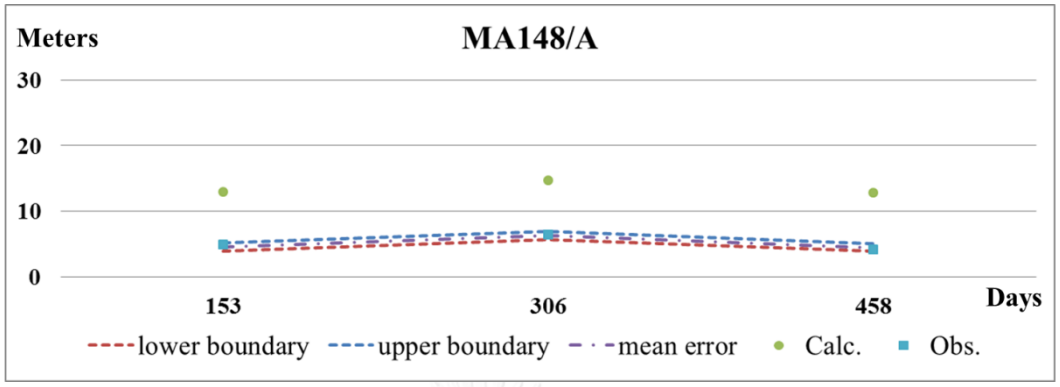

Figure 5. 21 Uncertainty analysis of observation well no. MA148

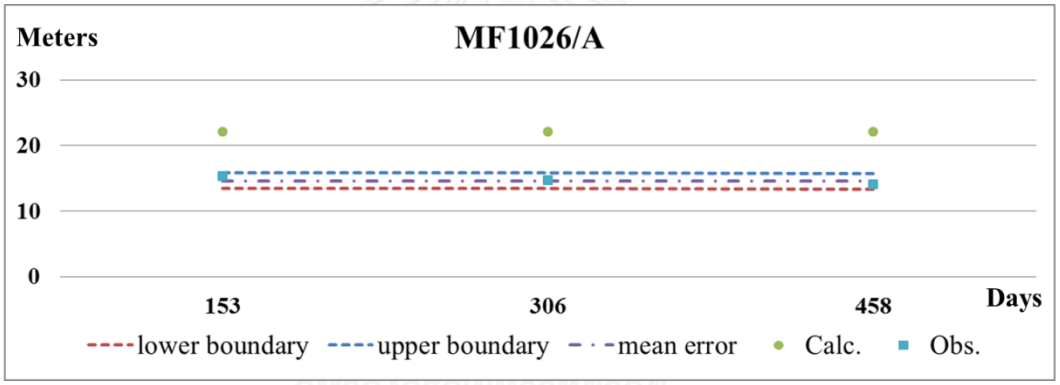

Figure 5. 22 Uncertainty analysis of observation well no. MF1026

5) Observation well no. MF1098 was found that the groundwater level from the actual measurements tended to be close to the values obtained from the model and the mean error, which showed that the model was performing well. The mean difference between the calculated value of the model and the measured value, SD, the upper and the lower boundary values were -3.34, 1.32, -0.76 m and -5.93 m, respectively, as shown in **Figure 5.23**.

6) Observation well no. MF1174 was found that the groundwater level from the actual measurements tended to be close to the values obtained from the model and the mean error, which showed that the model was performing well. The mean difference between the calculated value of the model and the measured value,

SD, the upper and the lower boundary values were 3.00, 3.65, 10.15 m and -4.14 m, respectively, as shown in **Figure 5.24**.

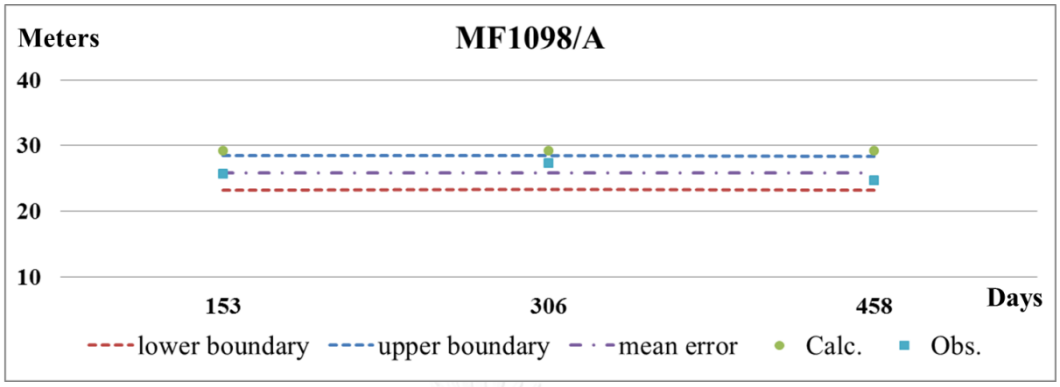

Figure 5. 23 Uncertainty analysis of observation well no. MF1098

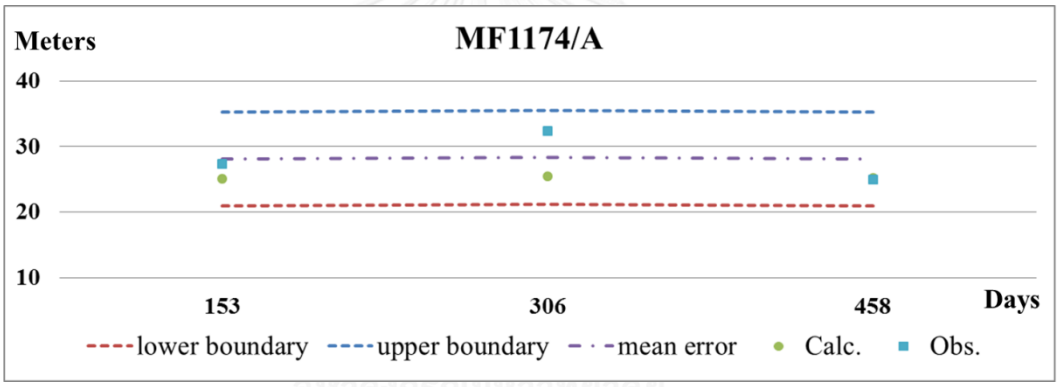

Figure 5. 24 Uncertainty analysis of observation well no. MF1174

7) Observation well no. MF151 was found that the groundwater level from the actual measurements tended to be close to the values obtained from the model and the mean error, which showed that the model was performing well. The mean difference between the calculated value of the model and the measured value, SD, the upper and the lower boundary values were -6.03, 1.45, -3.19 m and -8.88 m, respectively, as shown in **Figure 5.25**.

8) Observation well no. MF688 was found that the groundwater level from the actual measurements tended to be close to the values obtained from the model and the mean error, which showed that the model was performing well. The mean difference between the calculated value of the model and the measured value,

SD, the upper and the lower boundary values were -7.75, 4.06, 0.20 m and -15.70 m, respectively, as shown in **Figure 5.26**.

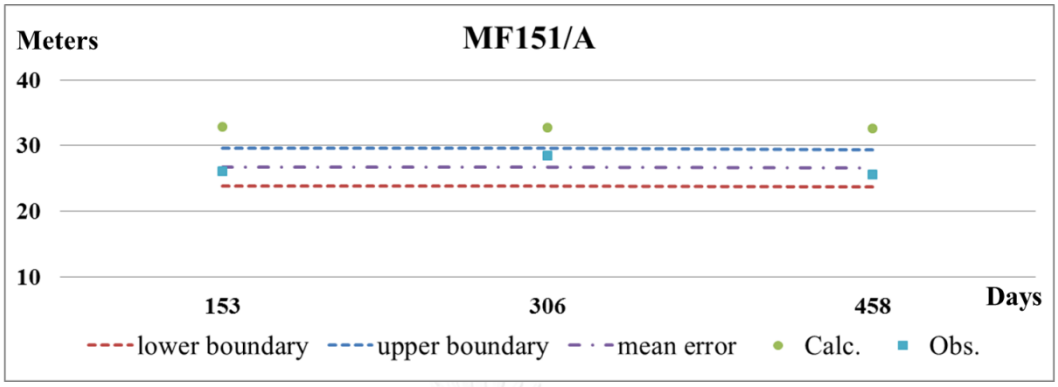

Figure 5. 25 Uncertainty analysis of observation well no. MF151

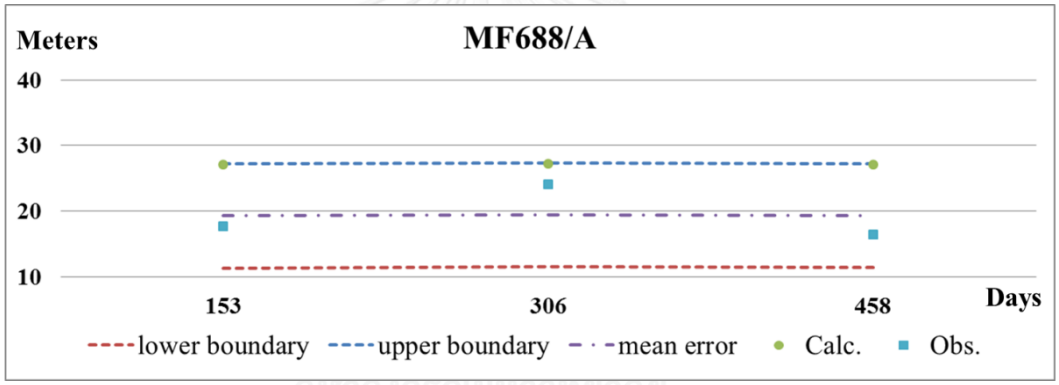

Figure 5. 26 Uncertainty analysis of observation well no. MF688

9) Observation well no. MF944 was found that the groundwater level from the actual measurements tended to be close to the values obtained from the model and the mean error, which showed that the model was performing well. The mean difference between the calculated value of the model and the measured value, SD, the upper and the lower boundary values were 2.94, 1.66, 6.19 m and -0.31 m, respectively, as shown in **Figure 5.27**.

10) Observation well no. MW2 was found that the groundwater level from the actual measurements tended to be close to the values obtained from the model and the mean error, which showed that the model was performing well. The mean difference between the calculated value of the model and the measured value,

SD, the upper and the lower boundary values were -0.90, 1.18, 1.42 m and -3.22 m, respectively, as shown in **Figure 5.28**.

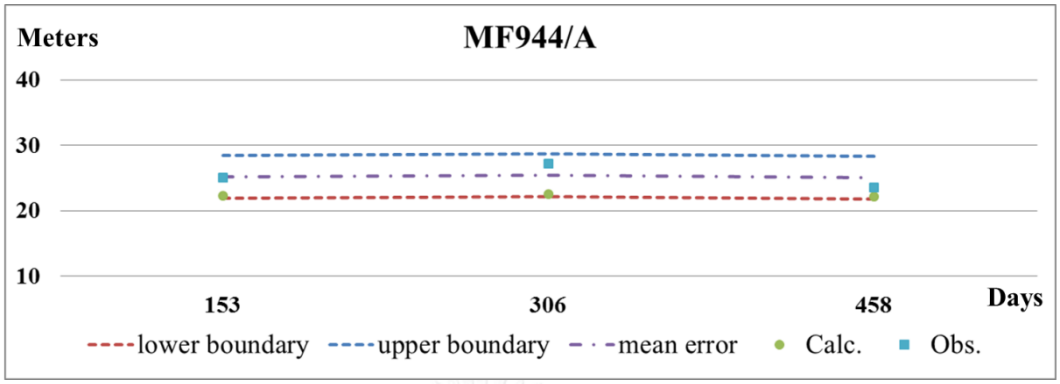

Figure 5. 27 Uncertainty analysis of observation well no. MF944

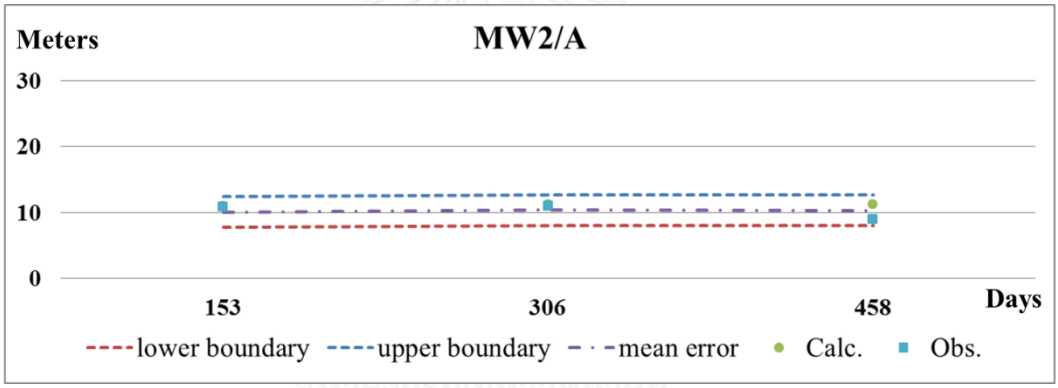

Figure 5. 28 Uncertainty analysis of observation well no. MW2

11) Observation well no. MW4 was found that the groundwater level from the actual measurements tended to be close to the values obtained from the model and the mean error, which showed that the model was performing well. The mean difference between the calculated value of the model and the measured value, SD, the upper and the lower boundary values were 0.38, 1.14, 2.61 m and -1.86 m, respectively, as shown in **Figure 5.29**.

12) Observation well no. PB294 was found that the groundwater level from the actual measurements tended to be close to the values obtained from the model and the mean error, which showed that the model was performing well. The mean difference between the calculated value of the model and the measured value,

SD, the upper and the lower boundary values were -7.06, 1.65, -3.81 m and -10.30 m, respectively, as shown in **Figure 5.30**.

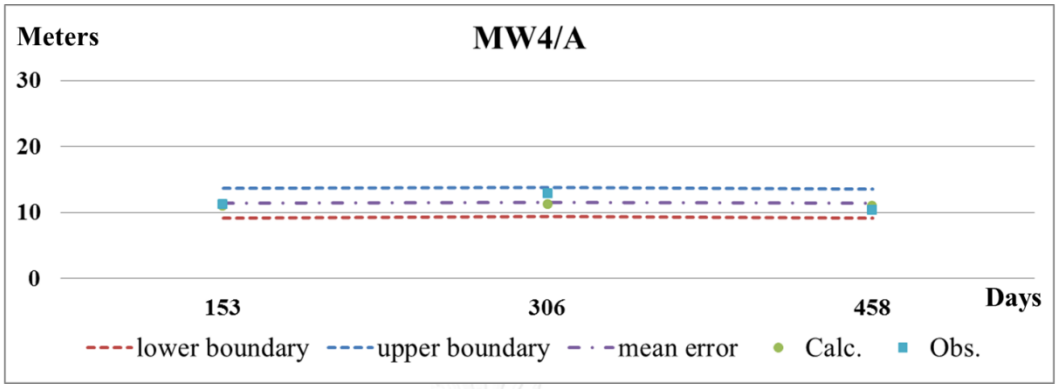

Figure 5. 29 Uncertainty analysis of observation well no. MW4

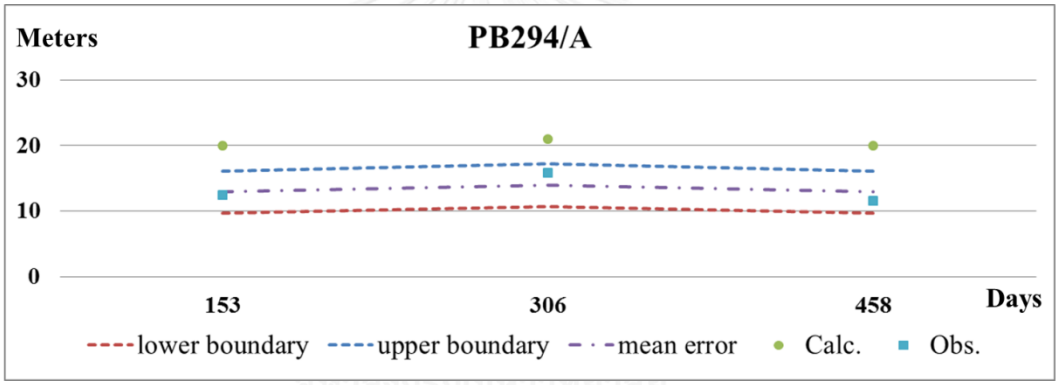

Figure 5. 30 Uncertainty analysis of observation well no. PB294

13) Observation well no. PW22955was found that the groundwater level from the actual measurements tended to be close to the values obtained from the model and the mean error, which showed that the model was performing well. The mean difference between the calculated value of the model and the measured value, SD, the upper and the lower boundary values were -2.44, 0.43, -1.60 m and -3.29 m, respectively, as shown in **Figure 5.31**.

14) Observation well no. PW29276: found that the groundwater level from the actual measurements tended to be close to the values obtained from the model and the mean error, which showed that the model was performing well. The mean difference between the calculated value of the model and the measured value,

SD, the upper and the lower boundary values were -0.39, 2.00, 3.54 m and -4.31 m, respectively, as shown in **Figure 5.32**.

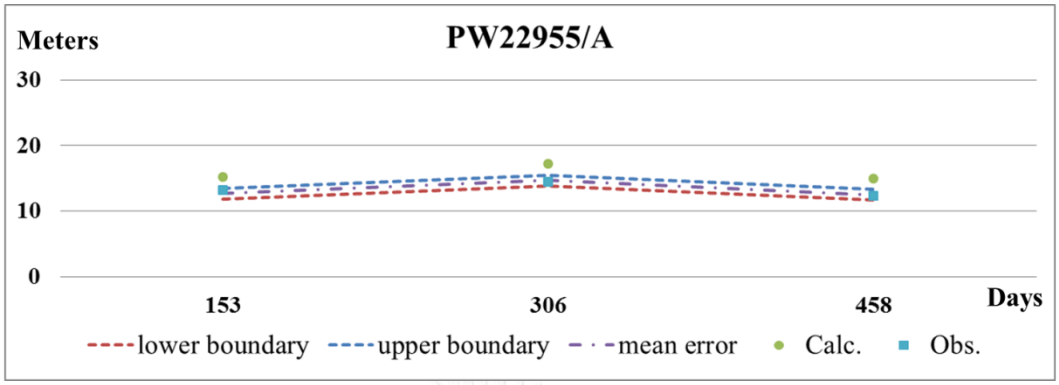

Figure 5. 31 Uncertainty analysis of observation well no. PW22955

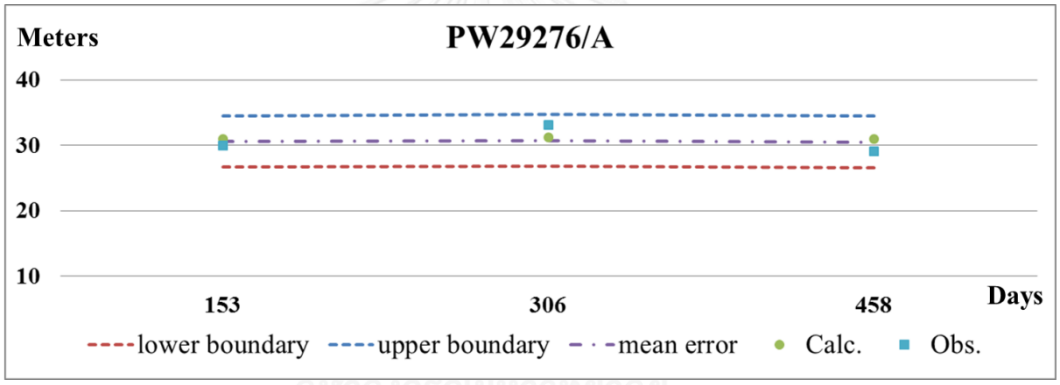

Figure 5. 32 Uncertainty analysis of observation well no. PW29276

5.11 Model Constraints

Groundwater mathematical model is created to assess groundwater balance and safe yield. It can represent the hydrological system of the study area as well. However, this groundwater model would not be able to simulate the hydrological condition of the area accurately and like all natural conditions since there are many model constraints, including:

- Conceptual modeling provides a lesser complex condition as compared to the real world condition, which is hardly to simulate and fit to the observed groundwater level.

- Uncertainty of external factor, such as the groundwater use, is not constant, which affect simulation results. Uncertainty of internal factors such as hydraulic conductivity and storativity is one of the constraints because these factors are derived from specific studies. Therefore, discrepancies in simulation results were found.
- A short period of monitoring during 14 month (March, 2015 to May, 2016) can not be used to completely represent all water level changes in the study area.
- The grid distribution of the model is 40,000 square meters and the thickness of the groundwater layer is about 30-50 m, which may lead to inaccurate results due to the groundwater flow in cracks, fractures, and bed rock, which is smaller than the grid on each cell. This groundwater model would not be able to simulate the hydrological condition of the area accurately and like all natural conditions. In practice, it is not possible to divide the grid into a higher resolution because it makes the model larger and model error in the running process.

CHAPTER VI
DISCUSSION AND CONCLUSION

6.1 Discussion

6.1.1 Geology and Hydrogeology Fieldwork

1) Geology in the area is the middle Khorat formation include white sandstone and white, purplish red siltstone. The orientation of main bedding is the northwest - southeast (NW-SE), and multi-directional joints as consists of 350/72E, 250/70NW, 40/70SE, 320/90, and 350/70E. Based on the results of the field study, there is a high fracture rock compared to the groundwater yield map of the Department of Groundwater Resources (DGR), it is found that the area has high groundwater quantity, which is consistent with field data, since groundwater is storage in the fracture.

2) Beheaded stream characteristics may be influenced by the impact of the Khao Yai fault zone, which passes through the north of the study area, implying that it may cause very fracture. The high fracture rock results in the higher groundwater potential, which can be verified from the field data of the Klong Sai area. It was found that fracture in the sandstone layer and groundwater flowed from the cracks at coordinates 1568306 N and 804536 E.

3) Based on the field data, groundwater flows from the north to the south and the groundwater aquifer is a confined aquifer. Observation of the field data found that in the rainy season, the groundwater flows out of the well. It appears in the area of Ban Khlong Din Daeng (well no.MF823), at 1561266 N and 818457 E.

6.1.2 Simulation process

1) Mapping of potential groundwater recharge zones using the overlay method by GIS program, the potential for groundwater addition was 12.8 percent of the average annual rainfall. This corresponds to the groundwater recharge by Somchai Wongsawat (2001) who found that the groundwater recharge into the underground

around the country is in the range of 7-15 percent of the average annual rainfall (DMR 2007).

2) According to mapping of potential groundwater recharge zones using the overlay method by GIS program, the results can be used to initially set up the model. The adjustment of the recharge parameter in calibration process is much easier and more saving-time due to the groundwater recharge from overlay technique is close to the calibrated recharge water. This finding can be further used in groundwater modeling step both in steady and transient states.

3) As a result of the calibrate model, the hydraulic conductivity values (K) obtained from the model calibration were within the range of the hydraulic conductivity value from the pumping test in the same rock in the vicinity, indicating a good calibration. In other words, the hydraulic conductivity value obtained from steady state is close to hydraulic conductivity of pumping test data.

4) As a result of the calibrate model, the specific storage and specific yield value obtained from the model calibration were fallen in the range of the specific storage and specific yield value from the pumping test on the same rock in the vicinity.

5) The observation wells used in the calibration model have a total of 14 wells found in the western and central study areas. The observation well data are relatively well dispersed and can be used to calibrate the model, but there is no data for the eastern observation wells because the area is high mountainous areas and the groundwater well can not be measured the groundwater level. Although there is no eastern observation well, but the information available covers the all aquifers in most study areas.

6) From the simulation results, the direction of the groundwater flows from the north to the south of the area, corresponding to the mapping of the groundwater flow direction from the field observation data,.

7) For grid design in top of the first groundwater aquifer model (top layer 1), the topography should be constructed from the topographic map scale 1: 50,000 of the Royal Thai Survey Department (RTSD) because the resolution and error are lower than the terrain mapping from the digital elevation model or DEM, at 90x90 resolution of the USGS, which is considered low resolution.

8) The hydraulic conductivity of the simulation is high in the middle Khorat aquifer, located in the central of the study area, corresponding to the potential zone of high specific capacity and groundwater yield derived from DGR. It may imply that this area has high fractures, leading high hydraulic conductivity of the hard rock aquifer. Therefore, the hydraulic conductivity of the groundwater simulation is reliable.

9) According to sensitivity analysis, this study found that the rate of groundwater recharge had the greatest effect on the change of groundwater level. The second impact is the horizontal hydraulic conductivity (Kx) in the 1st aquifer because this layer receives water directly from infiltrated rainwater.

10) The hydraulic conductivity values are very different even in the same groundwater aquifer due to the varying amounts of fractures and joint of rocks. It can conclude that the volume of fractures affects the amount and groundwater level.

11) According to water balance and safe yield of the lower Khwae Hanuman watershed, the limitation of the model is hydraulic parameters used for calibrating, such as hydraulic conductivity and storage coefficient, which are derived from other areas. Furthermore, geology in the study area is complex, making it difficult to identify zones of aquifer and groundwater yield. As a result, the simulation results in some wells are not close to the observed groundwater levels.

6.1.3 Safe yield

The safe yield is relatively high since the area is the downstream area, contacting with Khao Yai mountainous areas, which is the main groundwater recharge of the lower Khwae Hanuman sub-basin area. The study of (DGR 2008) found that the groundwater demand in Prachinburi province will increase at a rate of 2% per year, corresponding pumping rate of approx. 24,688 m^3/d (or 100% increase pumping rate in 2016) for 20 years. The simulation result reveals that the groundwater level was not significantly changed. Thus, it can conclude that the groundwater quantity in the lower Khwae Hanuman sub-basin has enough potential for the future needs.

6.2 Conclusion

6.2.1 Research background

The objectives of this study is delineating the zones of groundwater recharge, infiltrating into the hard rock aquifer, namely the middle Khorat aquifer, located in Nadi and Kabinburi districts. The other is to assess groundwater balance and safe yield of the middle Khorat aquifer in the lower Khwae Hanuman sub-basin, Prachinburi Province.

The study area is the lower Khwae Hanuman sub-basin, part of the Prachinburi basin, which covers the Nadi and Kabinburi Districts, Prachinburi province. The area is about 900 square kilometers, and its elevation ranges from 1-548 m amsl.. The main drainage of this area is Khwae Hanuman River with 38.3 km long and flows into the Bang Pakong River at the southern part of the study area.

The major geological features are sandstone, siltstone and conglomeratic sandstone, which have a medium-thick bedded and cross-bedding, as part of the middle Khorat group. The hydrogeological feature is the middle Khorat aquifer.

The groundwater levels were collected from 14 wells, which were measured in 2 dry seasons (2015, March and 2016, May) and rainy season (2015, November). The shallow groundwater levels were in the ranges of 6-12 m, and 1-18 m of deep groundwater levels. The directions of deep groundwater flow in both dry seasons and rainy season flow toward the central parts of the study area.

6.2.2 Groundwater recharge

The present study provided an approach for the qualitative assessment of the groundwater recharge potential with the help of remote sensing and GIS in the Khwae Hanuman sub-basin areas, Prachinburi province. An integrated groundwater recharge potential map was prepared and categorized on the basis of six weighted factors (lithology, lineaments density, drainage density, slope, land use and soil). The groundwater recharge potential zones were derived from the calculated weights and rates of each factor. The main influencing factor were the lithology (10.0 relative rating) and land use (8.0 relative rating). The study area was found to have a high potential groundwater recharge located at the south region. Specifically, about 33.9

km^2 (2.3% of the study area) had high recharge potentiality but about 1,466.1 km^2 (97.7% of the area) had a very low to moderate recharge potential zone, with 971.7 km^2 (64.8% of the area) having a moderate recharge potential zone. Only 12.8% of the total precipitated water (180.5×10^6 m^3/y) infiltrated into the groundwater aquifer, while the rest was lost from either surface runoff or evapotranspiration. The first-hand groundwater recharge potential map in this area should be useful for the water management in the future since it provides groundwater recharge information for an effective groundwater exploration for agricultural purposes, and can also recommend suitable pumping rates in order to obtain a long-term sustainable groundwater utilization without affecting the environment.

The qualitative assessment approach for evaluating the groundwater recharge potential using remote sensing and GIS in this study should be applied in other areas with the similar physical characteristics. But the geological characteristics of the selected area should be less complicated to allow easy setting of the score of the corresponding recharge potential factors. For testing the accuracy of the predicted recharge potential map, secondary data should be checked in conjunction with the field data, where the factors affecting the groundwater recharge potential should be integrated with other information, such as the geomorphology, evapotranspiration, specific yield of groundwater and transmissivity. However, the study should be performed together with a numerical model. Finally, the information used in this study was not the latest (2016) due to the non-continuity of recent data. Therefore, a reliable and current recharge map should be derived using more current information when available.

6.2.3 Groundwater balance

The numerical model was created by the physical hydrogeological data and hydraulic properties. This model can be characterized into four aquifers. The first layer is a quaternary sediment aquifer with an average thickness of 20 to 30 m. The second layer is a high weathered rock aquifer, composing of sandstone and shale high fractures with an average thickness of 20 to 40 m. The next layer is a weathered rock aquifer, composing of sandstone and shale with moderately fracture with an average thickness ranging from 30 to 40 m, and the final layer is a fresh rock layer, which is

no flow boundary setup because it has structural geology control (fault zone). All aquifers are heterogeneity and anisotropic. The horizontal hydraulic conductivity (Kx) from model were follows: the sedimentary aquifer of 0.97 and 29.97 m/d, the middle Khorat aquifer of 26.01, 38.12, and 41.53 m/d, the Permo-Carboniferous meta-sediments aquifer of 4.75 m/d, and the volcanic aquifer of 1.58 m/d. The specific yield of the sedimentary aquifer is 0.218 and 0.1. The specific storage from the model were follows: the middle Khorat aquifer of $2x10^{-5}$, $4x10^{-5}$, and $8x10^{-5}$ m^{-1}, the Permo-Carboniferous meta-sediments aquifer of $3.3x10^{-6}$ m^{-1}, and the volcanic aquifer of $2.7x10^{-5}$ m^{-1}. The directions of deep groundwater flow in both dry seasons and rainy season flow toward the central parts of the study area.

The groundwater flow model was proceeded by the Visual MODFLOW software, developed by the Waterloo Hydrogeologic, Inc., Canada. It was used to simulate 3 dimensional groundwater flows for aquifer systems under steady and transient states. The construction of hydrogeological conceptual model has categorized into four groundwater layers based on cross-section data. Groundwater direction flow into the margin of sub-basin including north, east and west, which are high mountains. On the other hand, the water flows out in the south side of the study area, which is low-lying plain. The high mountains and plain of central area are recharge by rainwater. In contrast, plain in the center sub-basin area water mostly are loss from groundwater pumping. Surface water that flows through the area is Khwae Hanuman River and flow from north to south. The rivers are qualified to both recharge and discharge zones.

The study of numerical model cover areas 1,200 square kilometer. The model boundary is width and length of 50 km x 24 km, and grid size of study area 200 m x 200 m^2. The total number of grid is 120,000 grid cells (120 rows x 250 columns x 4 layers).

The boundary conditions in the study area, determined by using boundary character of hydrogeology units, groundwater divide and stream lines. This area is determined boundaries on the northern, eastern and western were divided line watershed groundwater and no water flow boundary conditions beyond the groundwater divide area. Vertical hydraulic conductivity of river bed is about 6.35 to 5.20 m/d, and river bed thickness is about 1 to 2 m.

The model calibration conducted in this study can be divided calibration under steady state condition, and under transient condition. The calibration under steady state condition uses the March 1, 2015 data, the parameters calibration were hydraulic conductivity. Calibration under transient condition uses the available data during the years 2015-2016 that is the duration of modeling is 1 year, starting from March 1, 2015, as the first day in the model and ends at May 31, 2016, which is the 458^{th} day in the model. The calibration in the transient condition is conducted in order to determine the values of parameters that vary with time such as the storage and recharge rates

In steady state condition, with h those measured in 14 observation wells, the results revealed the residual mean of 3.87 m, the absolute residual mean of 4.55 m, the root mean squared of 5.55 m, and the normalized root mean squared of 22.17 %.

In transient state condition, the results from the dry season in 2015 revealed that the residual mean in the range of 3.75 m, the absolute residual mean of 4.49 m, the root mean squared of 5.47 m, and the normalized root mean squared of 21.87 %. Next, the rainy season in 2015 period is the residual mean in the range of 1.81 m, the absolute residual mean of 3.97 m, the root mean squared of 4.65 m, and the normalized root mean squared of 17.39 %. Finally, the dry season in 2016 is the residual mean in the range of 4.91 m, the absolute residual mean of 5.11 m, the root mean squared of 6.16 m, and the normalized root mean squared of 24.79 %.

The groundwater balance in the dry season (2015), the groundwater balance in the study area is 0.95 Mm^3/d while the middle Khorat aquifer is 0.33 Mm^3/d. Rainy season in year 2015, the groundwater balance is 0.98 Mm^3/d and the middle Khorat aquifer is 0.32 Mm^3/d. The dry season in year 2016, the groundwater balance is 1.1 Mm^3/d and the middle Khorat aquifer is 0.38 Mm^3/d.

During 20 years ago, when pumping increased by 200% from the pumping rate in 2016, found that the Nong Ki sub-district does affect water balance because of the amount of water recharge is lower than pumping, causing the cone of depression covering areas about 90 square kilometers.

6.2.4 Groundwater safe yield

Groundwater potential in the study area is assessed by the current groundwater use and groundwater development that cannot be mitigated by a decrease in groundwater level, based on the criteria in Chapter 5. The simulation results show that there is no change in groundwater level, but drawdown changes in the vicinity areas, under various pumping rates. The result of groundwater drawdown found that drawdown is decreased 2.50, 2.50, 3.00, and 4.00 m when groundwater pumping more than the recent as 10%, 50%, 100%, and 200%, respectively. The water level did not change due to the recharge rate of the area over the pumping rate, such as the total pumping rate is 37,033 m^3/d (200% more than the recent) but, the recharge rate was 40,224 m^3/d, which was higher than the pumping rate. It is possible that when the water is pumped, the groundwater level will not decrease or decrease very little and/or the groundwater level can recover quickly.

Therefore, the safe yield in this area can be concluded that the safe yield is the rate groundwater recharge due to the recharge of groundwater from the outside, if no water is used, the groundwater will flow out of the system. Based on the current groundwater pumping rate is 12,938 m^3/d, and the recharge rate was 40,224 m^3/d so the lower Khwae Hanuman sub-basin area can pump groundwater up to 27,286 m^3/d or about 2 times the current pumping rate.

Based on this study, it is possible to conclude the definition of safe yield that the pumping rate in the area is equal to the rate of groundwater recharge in the area, without affecting the water balance in the area.

In case groundwater pumping more than the recent as 200% found that the area of the Nong ki Industrial Estate was a drawdown more than 2 meters and a cone of depression covering areas approx. 90 square kilometers, which exceeds safe yield. So, this area is prone to imbalance groundwater.

From the definition of safe yield in the Nong ki Industrial Estate area found that the safe yield of 1st in Q aquifer as well as 2nd and 3rd layers in Jmk aquifer were pump no more than 6.2%, 6.2%, and 6.0% of current pumping rate, respectively.

6.3 Recommendations

1) The information used in this study was not the latest (2016) due to the non-continuity of recent data. Therefore, a reliable and current recharge map should be derived using more current information when available.

2) Pumping tests should be done in the study area to obtain the actual hydraulic conductivity and storativity values of the study area. It will make the calibrate model closest to the natural state of the area and the result will be reliable.

3) Groundwater level data should be kept monthly to monitor changes in groundwater level and construction of observation wells in areas . When modeling, simulations will be made that are close to reality and are credible.

4) This study of safe yield uses a trial and error method that may not be appropriate for use in geologically complex studies, but with the limitations of the data, the researchers chose to use this method. If anyone is interested in using this model for further study, researchers recommend using the method with the optimization method to achieve more similar results.

5) Based on the study results, it was found that the area of Kabinburi Industrial Estate has a very high water level and the cone of depression is about 90 square kilometers. It should be built around the observation wells to monitor the groundwater level for estimation on groundwater balance and safe yield in industrial areas.

REFERENCES

Adham, M., et al. (2010). "Study on groundwater recharge potentiality of Barind tract, Rajshahi district, Bangladesh using GIS and remote sensing technique." Journal of the Geological Society of India **75**(2): 432-438.

Alley, W. M., et al. (1999). Sustainability of ground-water resources, US Department of the Interior, US Geological Survey.

Anderson, M. and H. Wang (1982). "introduction to Groundwater Modeling." Finite Differentiates and Finite Element Methods.

Anderson, M. P., et al. (2015). Applied groundwater modeling: simulation of flow and advective transport, Academic press.

Arlai, P., et al. (2012). "Numerical Investigation of the Groundwater Balance in the Mae Sai Aquifer, Northern Thailand." Procedia Engineering **32**: 1214-1220.

Baghapour, M. A., et al. (2014). "Assessment of Groundwater Nitrate Pollution and Determination of Groundwater Protection Zones Using DRASTIC and Composite DRASTIC (CD) Models: The Case of Shiraz Unconfined Aquifer." Journal of health sciences and surveillance system **2**(2): 54-65.

Bear, J. (1979). Hydraulics of Groundwater, 569, McGraw-Hill, New York.

Beven, K. and A. Binley (1992). "The future of distributed models: model calibration and uncertainty prediction." Hydrological Processes **6**(3): 279-298.

Bunopas, S. and P. Vella (1983). Tectonic and geologic evolution of Thailand. Proceedings of a workshop on stratigraphic correlation of Thailand and Malaysia.

Chotpantarat, S., et al. (2015). "Groundwater Recharge Potential Using GIS around the Land Development Facilities of Chulalongkorn University at Kaeng Khoi District, Saraburi Province, Thailand." Applied Environmental Research **37**(2): 75-83.

Deepa, S., et al. (2016). "Groundwater recharge potential zones mapping in upper Manimuktha Sub basin Vellar river Tamil Nadu India using GIS and remote sensing techniques." Modeling Earth Systems and Environment **2**(3): 1-13.

DGR (2008). Improvement of groundwater map at provincial project, scale 1: 4,000, Prachin Buri province (In Thai). Jirangrat Company Limited

DGR (2009). Geographic Information System for Groundwater Management in the groundwater crisis zone project (In Thai).

DGR (2011). Pilot study and experiment on managed aquifer recharge using ponding system in the Lower North Region River Basin, Phitsanulok, Sukhothai, and Pichit provinces (In Thai). Khon Kean University.

Dinesh Kumar, P., et al. (2007). "Application of remote sensing and GIS for the demarcation of groundwater potential zones of a river basin in Kerala, southwest coast of India." International Journal of Remote Sensing **28**(24): 5583-5601.

DMR (2007). Geology of Thailand, Department of Mineral Resources.

Domenico, P. A. and F. W. Schwartz (1998). Physical and chemical hydrogeology, Wiley New York.

Dupuit, J. É. J. (1863). Études théoriques et pratiques sur le mouvement des eaux dans les canaux découverts et à travers les terrains perméables: avec des considérations relatives au régime des grandes eaux, au débouché à leur donner, et à la marche des alluvions dans les rivières à fond mobile, Dunod.

DWR (2004). Integrated Plan for Water Resources Management in Bang Pakong-Prachin Buri Basins (In Thai)

El-Baz, F., et al. (1995). "Groundwater potential of the Sinai Peninsula, Egypt." Project Summery.

Freeze, R. A. (1979). "GROUNXDWATER."

Greenbaum, D. (1985). "Review of remote sensing applications to groundwater exploration in basement and regolith."

Helton, J. C. (1993). "Uncertainty and sensitivity analysis techniques for use in performance assessment for radioactive waste disposal." Reliability Engineering & System Safety **42**(2-3): 327-367.

Hugman, R., et al. (2013). "The importance of temporal scale when optimising abstraction volumes for sustainable aquifer exploitation: a case study in semi-arid South Portugal." Journal of hydrology **490**: 1-10.

Karuchit, S. (2002). "Assessment of cumulative risk from pesticides with the scenario-model-parameter uncertainty analysis."

Khawlie, M. (1986). "Land-use planning for the development of a disrupted urban center: Beirut, Lebanon." Int. Jour. Dev. Technol **4**: 267-281.

Koch, M., et al. (2012). Modeling Investigation of the future permissible Yield in the upper Chiang Rai Aquifer System, Procedia Engineering, 32, 69–76. Proceedings of the 3 rd International Sci ence, Social-Science, Engineering and Energy Conference (ISEEC), Nakhon Pathom University, Thailand, Febru-ary.

Leduc, C., et al. (2001). "Long-term rise in a Sahelian water-table: The Continental Terminal in south-west Niger." Journal of hydrology **243**(1): 43-54.

Lee, C. H. (1915). "The Determination of Safe Yields of Underground Reservoirs of the Closed-basin Type." Transactions of the American Society of Civil Engineers **79**(1): 148-218.

Lillesand, T., et al. (2014). Remote sensing and image interpretation, John Wiley & Sons.

Lohman, S. W. (1972). Ground-water hydraulics, US Government Printing Office.

McDonald, M. G. and A. W. Harbaugh (1988). "A modular three-dimensional finite-difference ground-water flow model."

Morgan, M. G., et al. (1992). Uncertainty: a guide to dealing with uncertainty in quantitative risk and policy analysis, Cambridge university press.

Murthy, K. (2000). "Ground water potential in a semi-arid region of Andhra Pradesh-a geographical information system approach." International Journal of Remote Sensing **21**(9): 1867-1884.

Nebraska–Lincoln, U. o. Retrieved 2017-05-14, from http://snr.unl.edu/data/water/groundwater/realtime/satuate.aspx.

Nettasana, T., et al. (2012). "Conceptual and numerical models for sustainable groundwater management in the Thaphra area, Chi River Basin, Thailand." Hydrogeology Journal **20**(7): 1355-1374.

O'leary, D., et al. (1976). "Lineament, linear, lineation: some proposed new standards for old terms." Geological Society of America Bulletin **87**(10): 1463-1469.

Patil, S. G. and N. M. Mohite (2014). "Identification of groundwater recharge potential zones for a watershed using remote sensing and GIS." International Journal of Geomatics and Geosciences **4**(3): 485.

Ponce, V. M. (2007). "Sustainable yield of groundwater." California Department of Water Resources.

Resources, A. "Overlay analysis." Retrieved 2017-02-19, from http://resources.esri.com/help/9.3/arcgisdesktop/com/gp_toolref/geoprocessing/overlay_analysis.htm.

Ridd, M. F., et al. (2011). The geology of Thailand, Geological Society of London.

Selvam, S., et al. (2016). "Application of remote sensing and GIS for delineating groundwater recharge potential zones of Kovilpatti Municipality, Tamil Nadu using IF technique." Earth Science Informatics **9**(2): 137-150.

Selvam, S., et al. (2014). "Deciphering of groundwater potential zones in Tuticorin, Tamil Nadu, using remote sensing and GIS techniques." Journal of the Geological Society of India **84**(5): 597-608.

Shaban, A. (2003). Studying the hydrogeology of Occidental Lebanon: utilization of remote sensing. Etude de phydrogeologie du Liban occidental: utilization of de la deledection, These de doctorates, University Bordeaux 1, 202p.

Shaban, A., et al. (2006). "Use of remote sensing and GIS to determine recharge potential zones: the case of Occidental Lebanon." Hydrogeology Journal **14**(4): 433-443.

Shi, F., et al. (2012). "Identifying the sustainable groundwater yield in a Chinese semi-humid basin." Journal of hydrology **452**: 14-24.

Society, C. G. Retrieved 2017-05-14, from http://www.douglas.co.us/water/water-supply/what-is-an-aquifer/.

Su, Z. (2000). "Remote sensing of land use and vegetation for mesoscale hydrological studies." International Journal of Remote Sensing **21**(2): 213-233.

Todd, D. K. (1959). Annotated bibliography on artificial recharge of ground water through 1954, Citeseer.

Todd, D. K. (1980). Groundwater hydrology 2ed, John Wiley.

Toth, J. (1963). "A theoretical analysis of groundwater flow in small drainage basins." Journal of geophysical research **68**(16): 4795-4812.

Verruijt, A. (1982). The Finite Element Method. Theory of Groundwater Flow, Springer**:** 105-121.

Winter, T. C. (1998). Ground water and surface water: a single resource, DIANE Publishing Inc.

Yeh, H.-F., et al. (2009). "GIS for the assessment of the groundwater recharge potential zone." Environmental geology **58**(1): 185-195.

Zhou, Y., et al. (2012). "Options of sustainable groundwater development in Beijing Plain, China." Physics and Chemistry of the Earth, Parts A/B/C **47**: 99-113.

APPENDIX A
GROUNDWATER PUMPING WELLS

Pumping wells of Department of Groundwater Resources (2016)

No	Name	World coordinate		Top screen	Bottom screen	Pumping Rate
		X	Y	m AMSL.		m^3/d
1	5203D001	823826.00	1554229.00	4.00	-2.00	-15.00
				-14.00	-20.00	
				-44.00	-50.00	
2	5203D003	793112.00	1563441.00	-36.57	-42.57	-15.00
3	5303D003	826565.10	1557913.00	-11.99	-17.99	-5.00
				-23.99	-29.99	
				-35.99	-41.99	
4	5303L002	798128.00	1562591.00	-27.90	-33.90	-8.00
5	5503D023	814956.00	1561275.00	38.67	-40.33	-8.00
6	5503E029	798358.00	1558192.00	-1.66	-7.66	-15.00
				-19.66	-25.66	
7	5503H005	802989.00	1567697.00	18.60	-29.40	-20.00
8	5503H006	814621.00	1561275.00	31.40	-50.00	-5.00
9	5503H007	810359.00	1564806.00	34.99	-9.01	-20.00
10	5503H046	805828.00	1563640.00	9.90	-26.10	-12.00
11	5703D035	797304.70	1557435.00	-3.87	-6.87	-10.00
				-36.87	-39.87	
12	5703D045	795546.00	1564518.00	-16.99	-50.00	-8.00
13	5703H046	801943.00	1558937.00	3.00	-1.00	-20.00
				-17.00	-21.00	
14	5703H047	799098.00	1564155.00	5.48	-2.52	-20.00
				-18.52	-22.52	
15	5703H050	802033.00	1561516.00	-16.80	-22.80	-8.00
16	5703H051	802121.00	1561841.00	-16.56	-22.56	-10.00
				-26.56	-30.56	
17	5703H052	802863.00	1561336.00	-7.00	-13.00	-15.00
				-19.00	-27.00	
18	5703H053	801552.00	1561223.00	-17.40	-23.40	-15.00
				-27.40	-35.40	
19	5703H054	822407.00	1554353.00	-1.64	-7.64	-15.00
				-13.64	-21.64	
20	5703L011	823111.00	1555678.00	-20.00	-26.00	-15.00
21	5703L012	823613.00	1554900.00	-17.00	-23.00	-15.00
22	5803D052	824295.00	1557139.00	1.82	-1.18	-10.00
				-10.18	-43.18	
23	5803D053	826519.10	1556108.00	21.47	-30.53	-12.00
24	5803D054	826612.70	1556594.00	29.71	26.71	-15.00
				23.71	20.71	
				17.71	-36.29	
25	5803D055	821789.00	1554143.00	18.80	15.80	-10.00
				6.80	-34.20	
				-26.80	-30.80	

Pumping wells of Department of Groundwater Resources, 2016 (continue)

No	Name	World coordinate		Top screen	Bottom screen	Pumping Rate
		X	Y	m AMSL.		m^3/d
26	5803H001	822330.00	1553479.00	4.17	-1.83	-15.00
				-31.83	-35.83	
				-39.83	-43.83	
27	5803H002	821882.00	1553637.00	10.37	4.37	-10.00
				-9.63	-17.63	
28	5803H003	823244.00	1553895.00	14.00	8.00	-15.00
				-2.00	-10.00	
29	5803H005	824028.00	1555257.00	12.28	-5.72	-10.00
30	5803H006	824263.40	1554415.00	29.91	17.91	-10.00
31	5803H007	826427.60	1554748.00	1.76	-4.24	-15.00
32	5803H008	824264.90	1556557.00	2.95	-9.05	-15.00
				-31.05	-35.05	
				-43.05	-47.05	
33	5803H009	824255.80	1556521.00	3.14	-2.86	-10.00
				-14.86	-22.86	
34	5903F017	800742.00	1564618.00	-3.88	-7.88	-20.00
35	C792	793082.40	1548643.00	-1.27	-7.27	-1.59
36	C793	798843.00	1551076.00	7.71	1.71	-1.59
37	C794	798878.00	1550895.00	7.97	-4.53	-1.14
38	DCD12236	795787.00	1558239.00	-18.93	-28.93	-8.00
39	DCD12239	794526.00	1552442.00	-12.00	-22.00	-12.00
40	DCD12246	801421.00	1552909.00	-13.46	-16.46	-5.00
41	DCD12247	798503.00	1550960.00	2.50	-0.50	-4.00
42	DCD12248	798400.00	1550972.00	-1.25	-4.25	-2.00
43	DCD12252	800336.00	1552440.00	-5.97	-8.97	-2.60
44	DCD12253	798075.00	1550085.00	-22.00	-25.00	-4.70
45	DCD12255	798571.00	1550410.00	-15.17	-23.17	-3.00
46	DCD12292	807965.00	1554032.00	-41.80	-50.00	-15.00
47	DCD12296	821268.00	1559052.00	-4.97	-7.97	-6.50
48	DCD12297	813485.00	1553141.00	18.00	15.00	-2.30
49	DCD12299	818048.00	1556591.00	8.60	0.60	-3.20
50	DCD12300	816589.00	1559491.00	-30.06	-50.00	-15.00
51	DCD12301	811544.00	1566885.00	23.23	20.23	-5.20
52	DCD12302	800904.00	1567131.00	11.63	8.63	-2.20
53	DCD12303	803466.00	1566644.00	17.42	14.42	-8.20
54	DCD12309	796388.00	1563868.00	-22.08	-25.08	-2.09
55	DCD12310	792987.00	1563943.00	-8.00	-16.00	-5.60
56	DCD12311	791826.00	1562473.00	-11.32	-19.32	-3.10
57	DCD12312	794624.00	1562470.00	-19.17	-27.17	-4.40
58	DCD12313	796514.00	1561055.00	-3.00	-6.00	-2.00
59	DH267	799753.70	1562587.00	19.23	7.23	-2.00
60	DH268	804480.00	1563756.00	1.00	-5.00	-2.00

Pumping wells of Department of Groundwater Resources, 2016 (continue)

No	Name	World coordinate		Top screen	Bottom screen	Pumping Rate
		X	Y	m AMSL.		m^3/d
61	DH270	797702.00	1562721.00	-4.95	-10.95	-1.00
62	DH271	797469.00	1562627.00	10.60	-7.40	-2.00
63	DH272	797565.00	1562586.00	-0.03	-6.03	-2.00
64	DH315	798985.00	1555443.00	-7.62	-11.62	-2.00
65	DH316	798979.00	1555398.00	-9.00	-17.00	-4.00
66	DH329	796259.00	1554144.00	-12.81	-26.81	-4.00
67	DH331	792156.00	1562432.00	26.90	-10.10	-3.00
68	DH342	792924.00	1548353.00	-4.40	-17.40	-3.00
69	DH397	809897.00	1564643.00	27.60	21.60	-2.00
				19.60	-44.40	
70	DH433	795544.00	1555943.00	7.56	1.56	-5.00
71	DH438	795500.00	1551214.00	-7.00	-13.00	-2.00
72	DJ308	796430.00	1564087.00	14.90	-3.10	-2.50
73	DJ309	796422.00	1564509.00	17.00	5.00	-2.50
74	DJ310	798904.00	1558693.00	10.29	-10.71	-3.00
75	DJ311	798510.00	1558610.00	-18.00	-24.00	-3.00
76	DJ312	799690.00	1559704.00	-12.00	-18.00	-3.00
77	DJ313	796407.00	1561130.00	-7.50	-13.50	-3.00
78	DJ314	796098.00	1561372.00	-15.00	-21.00	-2.50
79	DJ315	798502.00	1557963.00	-1.99	-7.99	-2.50
80	MA132	800158.00	1552516.00	-4.73	-16.73	-17.97
81	MA143	808261.40	1563114.00	15.03	9.03	-1.14
82	MA145	810926.00	1565783.00	42.20	36.20	-6.58
83	MA147	799392.00	1555356.00	-5.03	-11.03	-57.06
84	MA148	797957.00	1556517.00	-5.83	-11.83	-7.98
85	MA149	802500.00	1560550.00	22.19	16.19	-4.24
				4.19	-1.81	
86	MA150	810847.00	1556606.00	2.98	-3.02	-7.98
87	MF1025	806533.00	1552873.00	-2.46	-8.46	-2.00
88	MF1026	808621.00	1558473.00	0.06	-5.94	-2.00
89	MF1027	807543.00	1562161.00	2.00	-4.00	-5.00
90	MF1029	800465.00	1562506.00	6.63	0.63	-2.00
91	MF1030	799290.00	1564130.00	0.08	-5.92	-5.00
92	MF1093	801111.00	1562316.00	-8.03	-14.03	-4.00
93	MF1094	801248.00	1562836.00	1.47	-4.53	-1.00
94	MF1097	800730.00	1566968.00	-4.00	-7.00	-2.00
95	MF1098	800732.00	1566782.00	-21.00	-24.00	-2.00
96	MF1101	806873.00	1565966.00	16.12	13.12	-1.00
97	MF1117	798390.00	1550800.00	-12.19	-18.19	-2.00
98	MF1120	801325.00	1553565.00	-18.00	-24.00	-4.00
99	MF1121	798638.00	1550656.00	-15.53	-21.53	-4.00
100	MF1122	798111.00	1549813.00	-18.81	-24.81	-3.00

Pumping wells of Department of Groundwater Resources, 2016 (continue)

No	Name	World coordinate		Top screen	Bottom screen	Pumping Rate
		X	Y	m AMSL.		m^3/d
101	MF1123	801002.00	1566792.00	8.79	2.79	-2.00
102	MF1124	802733.00	1567711.00	3.61	-2.39	-2.00
103	MF1149	798504.00	1558633.00	-20.73	-26.73	-4.00
104	MF1151	799112.00	1557723.00	-4.90	-10.90	-5.00
105	MF1152	796451.40	1558393.00	4.95	-16.05	-5.00
106	MF1153	799204.00	1559469.00	10.00	-12.50	-6.00
107	MF1154	797916.00	1556348.00	-8.84	-14.84	-4.00
108	MF1155	798728.00	1558326.00	-14.07	-20.07	-2.00
109	MF1156	798566.00	1558409.00	4.00	-2.00	-3.00
110	MF1172	803013.00	1567686.00	-5.03	-11.03	-2.00
111	MF1173	798841.00	1566720.00	19.83	-10.17	-2.00
112	MF1175	791161.00	1567830.00	27.14	21.14	-2.00
113	MF1177	795638.00	1564564.00	-11.97	-15.97	-2.00
114	MF1178	797352.00	1562121.00	-8.00	-12.00	-2.00
115	MF1180	821030.00	1558513.00	8.13	4.13	-3.00
116	MF1181	816918.00	1560145.00	-2.09	-6.09	-3.00
117	MF1201	801108.80	1563622.00	6.00	0.00	-2.00
118	MF1202	800139.00	1562492.00	-13.22	-19.22	-2.00
119	MF1203	796189.00	1564366.00	-34.10	-40.10	-2.00
120	MF1204	800983.00	1564890.00	1.61	-4.39	-2.00
121	MF1206	803874.00	1566301.00	-13.63	-19.63	-2.00
122	MF1208	807858.00	1565909.00	-2.65	-8.65	-3.00
123	MF1209	799801.00	1555637.00	-18.00	-24.00	-3.00
124	MF1210	796541.00	1558322.00	-18.18	-24.18	-3.00
125	MF1211	792642.00	1563348.00	-13.33	-19.33	-3.00
126	MF1230	796321.00	1564298.00	-15.90	-19.90	-2.00
127	MF125	798159.00	1549857.00	1.06	-4.94	-5.68
128	MF1283	795168.00	1558925.00	-10.00	-18.00	-3.00
129	MF1285	798435.00	1557953.00	-22.07	-25.07	-3.00
130	MF1287	813126.00	1552319.00	16.61	4.61	-1.00
131	MF1288	815881.00	1553151.00	10.93	2.93	-3.00
132	MF1312	791718.00	1562462.00	14.10	-20.90	-5.00
133	MF1313	794590.00	1564665.00	0.28	-35.72	-3.00
134	MF1316	802073.00	1555790.00	-0.10	-31.10	-5.00
135	MF1328	811810.00	1562736.00	3.30	-2.70	-1.50
136	MF135	790681.00	1563838.00	7.00	1.00	-9.56
137	MF1415	796096.00	1561492.00	-5.64	-37.64	-5.00
138	MF1416	795321.00	1558036.00	4.66	-34.34	-5.00
139	MF1419	795486.00	1551268.00	7.07	-31.93	-3.00
140	MF151	804508.00	1568304.00	10.53	4.53	-13.32
141	MF152	810948.00	1556380.00	7.49	-4.51	-14.03
142	MF155	791695.00	1558368.00	12.00	6.00	-10.39

Pumping wells of Department of Groundwater Resources, 2016 (continue)

No	Name	World coordinate		Top screen	Bottom screen	Pumping Rate
		X	Y	m AMSL.		m^3/d
143	MF199	793162.00	1563563.00	-1.91	-7.91	-4.24
144	MF200	795466.00	1561873.00	-4.66	-10.66	-8.00
145	MF201	796778.70	1560291.00	-0.50	-6.50	-6.36
146	MF264	816087.00	1559966.00	5.57	-0.43	-12.55
147	MF270	799002.00	1564081.00	3.47	-2.53	-2.27
148	MF271	799745.00	1562536.00	17.00	11.00	-2.27
149	MF303	800925.00	1562204.00	-7.67	-13.67	-11.74
150	MF305	799371.00	1566298.00	10.42	4.42	-11.54
151	MF307	800462.00	1562267.00	-3.60	-9.60	-3.41
152	MF308	814304.00	1556830.00	3.83	-2.17	-11.74
153	MF311	807462.00	1562442.00	10.00	4.00	-11.32
154	MF312	810518.00	1564521.00	34.53	28.53	-7.20
155	MF313	813766.00	1562845.00	26.14	20.14	-1.59
156	MF386	797908.00	1557257.00	-6.00	-12.00	-7.20
157	MF387	795309.00	1564469.00	12.00	6.00	-3.41
158	MF419	810927.00	1553607.00	-5.07	-11.07	-9.92
159	MF422	818653.00	1558460.00	-18.37	-24.37	-2.27
160	MF423	817290.00	1559300.00	9.17	3.17	-1.59
161	MF458	800611.00	1561668.00	-9.00	-15.00	-7.20
162	MF505	802889.00	1557442.00	0.89	-5.11	-7.20
163	MF507	807173.00	1565371.00	24.99	18.99	-3.60
164	MF509	800371.00	1553251.00	-3.02	-9.02	-7.20
165	MF510	816632.00	1559519.00	0.02	-5.98	-7.20
166	MF529	818163.00	1553522.00	14.71	8.71	-1.59
167	MF554	802714.00	1567803.00	11.90	5.90	-3.41
168	MF642	801362.00	1562068.00	16.00	10.00	-7.20
169	MF643	801215.00	1562100.00	12.00	6.00	-4.80
170	MF645	800065.00	1562589.00	17.24	11.24	-1.59
171	MF647	806786.00	1563165.00	12.23	6.23	-4.80
172	MF678	795618.00	1561117.00	1.90	-4.10	-2.27
173	MF679	795265.00	1559780.00	-4.67	-10.67	-7.20
174	MF680	792892.00	1564373.00	6.17	0.17	-2.27
175	MF682	806790.00	1563475.00	15.00	9.00	-6.00
176	MF685	801089.00	1567023.00	5.61	-0.39	-2.27
177	MF688	799595.00	1566109.00	2.47	-3.53	-4.55
178	MF689	806576.00	1565144.00	25.79	19.79	-4.80
179	MF690	820777.00	1558774.00	14.00	8.00	-2.27
180	MF691	821385.00	1558520.00	15.50	9.50	-2.27
181	MF692	817081.00	1560573.00	12.93	6.93	-2.27
182	MF693	815862.00	1556713.00	5.27	-0.73	-3.41
183	MF694	813208.00	1554385.00	11.39	5.39	-7.20
184	MF702	800997.00	1566401.00	15.00	9.00	-2.40

Pumping wells of Department of Groundwater Resources, 2016 (continue)

No	Name	World coordinate		Top screen	Bottom screen	Pumping Rate
		X	Y	m AMSL.		m^3/d
185	MF704	799834.00	1560499.00	-4.00	-10.00	-4.80
				-16.00	-22.00	
186	MF705	797409.00	1562000.00	1.50	-4.50	-7.20
187	MF706	792942.00	1563965.00	3.00	-3.00	-1.80
188	MF767	800821.00	1551992.00	-16.17	-22.17	-4.80
189	MF779	814352.00	1561101.00	-10.47	-16.47	-2.42
190	MF780	801022.00	1562047.00	6.00	0.00	-7.20
191	MF81	798510.00	1550311.00	1.11	-4.89	-3.60
				-16.89	-22.89	
192	MF82	798771.00	1550815.00	11.82	5.82	-4.55
193	MF823	818014.00	1561651.00	20.00	14.00	-1.59
194	MF825	814094.00	1563000.00	15.00	9.00	-4.80
195	MF828	810339.00	1564801.00	-13.00	-19.00	-6.82
196	MF829	799274.00	1555889.00	-2.36	-8.36	-4.80
197	MF830	795938.00	1561744.00	-2.00	-8.00	-7.20
198	MF831	795905.00	1564533.00	9.93	3.93	-7.20
199	MF832	807551.00	1562384.00	21.36	15.36	-7.20
200	MF834	817078.00	1556972.00	-18.72	-24.72	-7.20
201	MF836	798337.00	1558196.00	0.96	-5.04	-7.20
202	MF837	795503.00	1565098.00	1.77	-4.23	-3.60
203	MF839	801082.00	1565130.00	11.81	5.81	-2.88
204	MF84	800775.00	1562296.00	12.63	6.63	-11.38
205	MF840	798818.00	1566621.00	5.90	-0.10	-2.88
206	MF841	801810.00	1564425.00	9.72	3.72	-7.20
207	MF842	801310.00	1561989.00	10.00	4.00	-3.60
208	MF844	809312.00	1561657.00	13.25	7.25	-7.20
209	MF85	806799.00	1563245.00	9.00	3.00	-11.48
210	MF852	799927.00	1562583.00	16.93	10.93	-1.80
211	MF86	821161.00	1558603.00	13.50	7.50	-11.70
212	MF882	793230.00	1550342.00	-12.98	-36.98	-1.14
213	MF883	793283.00	1557772.00	9.34	3.34	-7.20
214	MF884	807145.00	1565081.00	14.20	8.20	-4.80
215	MF908	796379.80	1558965.00	2.12	-3.88	-2.27
216	MF909	796080.50	1560946.00	-17.00	-23.00	-3.41
217	MF912	808621.00	1558237.00	7.06	1.06	-7.20
218	MF914	818629.00	1561518.00	18.74	12.74	-1.59
219	MF915	818891.00	1553689.00	18.37	12.37	-2.88
220	MF916	815616.00	1556525.00	0.00	-6.00	-7.20
221	MF917	811140.00	1553475.00	-3.50	-9.50	-3.60
222	MF944	792411.00	1562399.00	3.21	-2.79	-4.55
223	MF95	815940.00	1557144.00	1.00	-5.00	-10.57
224	MF96	820818.00	1558510.00	3.06	-2.94	-9.02

Pumping wells of Department of Groundwater Resources, 2016 (continue)

No	Name	World coordinate		Top screen	Bottom screen	Pumping Rate
		X	Y	m AMSL.		m^3/d
225	MF97	814327.70	1556367.00	14.00	11.00	-12.53
				5.00	-1.00	
226	PB209	798783.00	1550822.00	-3.09	-7.09	-6.00
227	PB213	801923.00	1555696.00	-10.10	-16.10	-20.00
				-22.10	-28.10	
228	PB25	802376.00	1556582.00	-10.00	-36.00	-20.00
229	PB255	802199.00	1557600.00	1.93	-2.07	-10.00
				-14.07	-18.07	
230	PB256	798073.00	1557422.00	10.00	-50.00	-5.00
231	PB26	808755.00	1553998.00	1.00	-19.00	-20.00
232	PB27	811524.00	1561114.00	10.37	-21.63	-15.00
233	PB272	800964.00	1561967.00	-9.33	-13.33	-10.00
				-21.33	-25.33	
				-29.33	-49.33	
234	PB278	801382.20	1563375.00	-14.47	-18.47	-5.00
				-22.47	-26.47	
235	PB28	802803.00	1556192.00	-5.17	-43.17	-20.00
236	PB29	803674.00	1556724.00	-3.00	-47.00	-20.00
237	PB30	813110.00	1553606.00	4.60	-27.40	-10.00
238	PB32	796413.90	1558342.00	-11.23	-35.23	-18.00
239	PB33	803407.00	1558915.00	-0.33	-20.33	-18.00
240	PB34	798958.00	1555394.00	-4.84	-30.84	-12.00
241	PW10184	815466.00	1561392.00	42.53	36.41	-1.00
242	PW10385	802663.00	1567769.00	23.49	17.34	-1.00
243	PW22863	795470.00	1556337.00	3.97	-2.23	-7.00
244	PW22910	811329.00	1556443.00	9.34	3.24	-2.00
245	PW22911	806539.00	1553930.00	3.27	-2.83	-5.00
246	PW22913	810463.00	1554605.00	13.53	7.43	-2.00
247	PW22914	811520.00	1561114.00	6.95	0.85	-6.00
248	PW22915	810034.00	1561288.00	12.73	6.63	-5.00
249	PW22955	795650.00	1559478.00	-6.62	-12.72	-7.00
250	PW22957	806398.00	1562135.00	12.75	6.70	-3.00
251	PW23286	795359.00	1562014.00	1.85	-4.20	-3.00
252	PW23287	795727.00	1564538.00	9.75	3.70	-3.00
253	PW4577	821067.00	1559090.00	19.51	13.41	-0.50
254	PW4578	820855.00	1559287.00	7.44	1.35	-1.00
255	PW4614	803527.00	1567156.00	23.83	17.73	-1.50
256	PW4615	795288.00	1561006.00	7.53	1.46	-1.00
257	PW4616	793220.00	1564751.00	-4.75	-7.80	-2.00
258	PW4617	795499.00	1561890.00	5.21	2.16	-10.00
259	Q100	797684.00	1562301.00	-6.63	-24.63	-3.64
260	Q101	800219.00	1562555.00	11.20	-6.80	-10.57

Pumping wells of Department of Groundwater Resources, 2016 (continue)

No	Name	World coordinate		Top screen	Bottom screen	Pumping Rate
		X	Y	m AMSL.		m^3/d
261	Q102	801214.70	1563619.00	-15.58	-33.58	-10.93
262	Q103	802508.00	1556600.00	9.55	-8.45	-10.35
263	Q95	801590.00	1564305.00	22.67	4.67	-12.01
264	Q96	801105.00	1562298.00	4.57	-19.43	-14.41
265	Q99	798482.00	1558428.00	8.43	-9.57	-14.41
266	TN193	800432.00	1552231.00	2.12	-50.00	-3.00
267	TN196	811000.00	1553560.00	17.69	-50.00	-4.00
268	X72	801299.00	1552176.00	7.97	1.97	-22.10
				-4.03	-10.03	

Pumping wells of private agencies, 2016

No	Name	World coordinate		Top screen	Bottom screen	Pumping Rate
		X	Y	m AMSL		m^3/d
1	2107-0003	804502.00	1558235.00	-26.57	-32.57	-15.00
2	2107-0009	799564.00	1561980.00	-8.99	-14.99	-15.00
3	2107-0010	799234.00	1562714.00	-9.01	-15.01	-15.00
4	2107-0014	801808.00	1557192.00	-22.00	-31.00	-80.00
5	2109-0006	799675.00	1551013.00	-16.29	-22.29	-20.00
6	2109-0066	806877.00	1551933.00	-22.93	-31.93	-80.00
7	2110-0003	804613.00	1557163.00	-39.93	-50.00	-1,100.00
8	2110-0005	806818.00	1556882.00	-40.08	-50.00	-1,100.00
9	2110-0006	806500.00	1556955.00	-36.00	-50.00	-1,100.00
10	2110-0007	804507.00	1557059.00	-38.12	-50.00	-1,100.00
11	2110-0008	806686.00	1557382.00	-36.73	-50.00	-1,100.00
12	2112-0001	800015.00	1556322.00	-17.00	-29.00	-200.00
13	2112-0004	800038.00	1556363.00	-17.60	-29.60	-200.00
14	2112-0005	800083.00	1556524.00	-17.47	-29.47	-200.00
15	2112-0006	803001.00	1555480.00	-15.93	-27.93	-200.00
16	2112-0007	802764.00	1555448.00	-14.37	-26.37	-200.00
17	2112-0019	795222.00	1564071.00	5.64	-6.36	-200.00
18	215004-0019	804323.00	1558344.00	-46.18	-50.00	-36.00
19	215106-0003	807483.00	1551666.00	-27.06	-39.06	-300.00
20	215402-0003	800484.00	1561652.00	-12.76	-24.76	-500.00
21	4604-0002	805726.00	1559369.00	-25.37	-34.37	-150.00
22	4704-0003	797643.00	1556986.00	-17.07	-26.07	-95.00
23	4706-0002	795137.00	1564261.00	-35.21	-44.21	-120.00
24	4706-0004	795131.00	1564473.00	-28.73	-37.73	-120.00
25	4707-0001	805390.00	1559313.00	-32.00	-41.00	-120.00
26	4802-0004	806253.00	1559584.00	-20.97	-29.97	-60.00
27	4802-0005	803480.00	1556860.00	-7.00	-13.00	-36.00

Pumping wells of private agencies, 2016 (continue)

No	Name	World coordinate		Top screen	Bottom screen	Pumping Rate
		X	Y	m AMSL.		m^3/d
28	4802-0006	804054.00	1557464.00	-11.92	-17.92	-30.00
29	4804-0017	803717.00	1557919.00	-13.00	-22.00	-80.00
30	4906-0003	802722.00	1550142.00	-29.23	-38.23	-150.00
31	4906-0005	803008.00	1550475.00	-24.00	-33.00	-150.00
32	4906-0008	807599.00	1551654.00	-22.37	-34.37	-300.00
33	4906-0009	807162.00	1551397.00	-48.98	-50.00	-300.00
34	4906-0010	807207.00	1551522.00	-47.80	-50.00	-300.00
35	5002-0015	805201.00	1559198.00	-29.09	-38.09	-100.00
36	5002-0016	802333.00	1557557.00	-8.76	-17.76	-160.00
37	5006-0001	794451.00	1562073.00	-28.00	-40.00	-245.00
38	5006-0002	794260.00	1562271.00	-29.39	-41.39	-245.00
39	5006-0003	794135.00	1562121.00	-34.00	-46.00	-245.00

VITA

Mr. Narongsak Kaewdum was born in Chiang Rai, Thailand on July 13, 1988. In 2011 he received a Bachelor of Science degree in Geoscience from Department of Physic, Faculty of Sciences, Mahidol University. After then he entered the Geology program, Department of Geology, Faculty of Science, Chulalongkorn University for a Master of Science degree study.